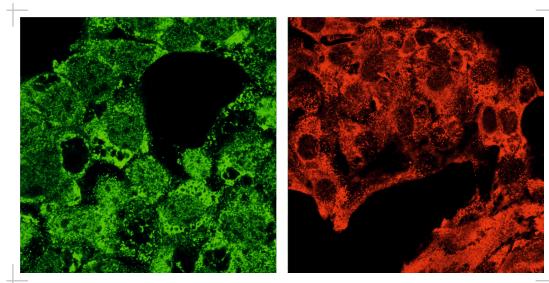


LILIT KAMALYAN

Role of peroxisomes in steroid synthesis in Leydig cells and their influence on male fertility



INAUGURAL DISSERTATION

submitted to the Faculty of Medicine
in partial fulfilment of the requirements
for the PhD degree
of the Faculties of Veterinary Medicine and Medicine
of the Justus Liebig University Giessen



edition scientifique
VVB LAUFERSWEILER VERLAG

Das Werk ist in allen seinen Teilen urheberrechtlich geschützt.

Die rechtliche Verantwortung für den gesamten Inhalt dieses Buches liegt ausschließlich bei dem Autor dieses Werkes.

Jede Verwertung ist ohne schriftliche Zustimmung des Autors oder des Verlages unzulässig. Das gilt insbesondere für Vervielfältigungen, Übersetzungen, Mikroverfilmungen und die Einspeicherung in und Verarbeitung durch elektronische Systeme.

1. Auflage 2018

All rights reserved. No part of this publication may be reproduced, stored in a retrieval system, or transmitted, in any form or by any means, electronic, mechanical, photocopying, recording, or otherwise, without the prior written permission of the Author or the Publishers.

1st Edition 2018

© 2018 by VVB LAUFERSWEILER VERLAG, Giessen
Printed in Germany



édition linguistique
VVB LAUFERSWEILER VERLAG

STAUFENBERGRING 15, D-35396 GIESSEN
Tel: 0641-5599888 Fax: 0641-5599890
email: redaktion@doktorverlag.de

www.doktorverlag.de

Institute for Anatomy and Cell Biology II
Faculty of Medicine of the Justus Liebig University Giessen

**Role of peroxisomes in steroid synthesis in Leydig cells
and their influence on male fertility**

Inaugural Dissertation
submitted to
the Faculty of Medicine
in partial fulfillment of the requirements
for the PhD-degree
of the Faculties of Veterinary Medicine and Medicine
of the Justus Liebig University Giessen

by

Lilit Kamalyan

of
Yerevan, Armenia

Giessen, 2017

From the Institute for Anatomy and Cell Biology II
of the Faculty of Medicine of the Justus Liebig University of Giessen
Director/Chairperson: Prof. Dr. Eveline Baumgart-Vogt

First Supervisor and Committee Member: Prof. Dr. Eveline Baumgart-Vogt

Second Supervisor and Committee Member: Prof. Dr. Martin Bergmann

Examination Chair and Committee Members: Prof. Dr. Friedemann Weber

Date of Doctoral Defense: 18nd April 2018

Declaration

“I declare that I have completed this dissertation single-handedly without the unauthorized help of a second party and only with the assistance acknowledged therein. I have appropriately acknowledged and referenced all text passages that are derived literally from or are based on the content of published or unpublished work of others, and all information that relates to verbal communications. I have abided by the principles of good scientific conduct laid down in the charter of the Justus Liebig University of Giessen in carrying out the investigations described in the dissertation.”

Giessen, June 28th 2017

Lilit Kamalyan

Table of contents

1. Introduction	9
1.1. Overview on the male reproduction system.....	9
1.1.1. Structure of the testis	9
1.1.2. Regulation of testicular function.....	9
1.1.2.1. Endocrine regulation of the testicular function	9
1.1.2.2. Local, paracrine and autocrine regulation of testicular function.....	11
1.1.3. Overview on structure and function of Leydig cells in testis.....	11
1.1.3.1. Morphology and development of Leydig cell	11
1.1.4. Steroidogenesis	13
I. Signal Transduction.....	13
II. Cholesterol Synthesis, Uptake and Transport.....	13
III. Steroidogenic acute regulatory protein (StAR).....	15
IV. Enzymatic conversions for steroid synthesis	17
1.1.5. Function of testosterone	20
1.2. Peroxisomes.....	21
1.2.1. Peroxisome biogenesis	21
1.2.2. Metabolic functions of peroxisomes.....	22
1.2.2.1. Peroxisomal fatty acid β -oxidation	22
1.2.2.2. The role of peroxisomes in cholesterol synthesis.....	24
1.2.3. Oxidative stress in the cells	25
1.2.3.1. Mitochondria and oxidative stress.....	26
1.2.3.2. Peroxisomes and oxidative stress	27
1.2.4. Peroxisomal disorders.....	28
1.2.4.1. Peroxisome biogenesis disorders	28
1.2.4.2. Single Peroxisomal enzyme deficiencies	29
1.2.5. Peroxisomes and testis	30

1.2.6. Peroxisomal dysfunction and testicular impairment	30
2. Materials and Methods	34
2.1. Materials.....	34
2.1.1. Laboratory Instruments	34
2.1.2. General materials, culture media, buffers and solutions.....	35
2.1.3. Chemicals	39
2.1.4. Antibodies.....	42
2.1.5. Primers.....	46
2.2. Cell Culture	49
2.2.1 Mouse Leydig Tumor cells (MLTC-1 and MA-10 cells).....	49
2.2.1.1. Culture of MLTC-1 cells	49
2.2.1.2. Culture of MA-10 cells	49
2.2.2. Isolation and primary culture of mouse Leydig cells.....	50
2.3. Transformation of E.coli and preparation of plasmid DNA	51
2.3.1. Endotoxin-free, midi preparation of plasmid DNA	52
2.4. Transfection.....	53
2.4.1. Transfection via microporation with <i>Pex13</i> shRNA in MLTC-1 cells	53
2.4.2. Transfection of MLTC-1 cells via lipofection using shRNA.....	55
2.4.3. <i>Pex13</i> or <i>Mfp2</i> (<i>Hsd17b4</i>) silencing by RNA interference technology (RNAi) in MLTC-1 and in primary Leydig cells	56
2.5. RNA expression analysis by semi-quantitative RT-PCR	59
2.6. Western Blot analysis	60
2.7. Immunofluorescence for MLTC-1 and mouse primary Leydig cells	61
2.8. ROS detection by staining with dihydroethidium (DHE)	61
2.9. Detection of glutathione using GSH-Glo™ Glutathione Assay	62
2.10. Determination of catalase activity.....	62
2.11. Detection of the Mitochondrial Membrane Potential ($\Delta\Psi_m$)	63

2.12. Enzyme-linked immunosorbent assays (ELISA) and radioimmunoassays (RIA).....	64
2.13. Experiments with different treatments of MLTC-1 cells and primary Leydig cells.....	65
2.13.1. Treatment with human chorionic gonadotropin (hCG).....	65
2.13.2. Treatment with 22 (R)-Hydroxycholesterol.....	66
2.13.3. Treatment of MLTC-1 cells with trilostan and abiraterone acetate	66
2.13.4. Treatment of MLTC-1 cells with antimycin A.....	67
3. Aims of the study.....	68
4. Results	70
4.1. Comparison of genes involved in steroidogenesis in MA-10 and MLTC-1 cells.....	70
4.2. MLTC-1 cells respond to human chorionic gonadotropin (hCG) treatment	72
4.2.1. Hormone production in MLTC-1 cells.	74
4.3. Peroxisomal genes and proteins are differently expressed in MLTC-1 cells.....	76
4.4. shRNA mediated knock-down of <i>Pex13</i> in MLTC-1 cells.....	78
4.4.1. Establishing the <i>Pex13</i> knockdown in MLTC1 cells	78
4.4.2. shRNA mediated knock-down of <i>Pex13</i> leads to mistargeting of catalase into the cytoplasm in MLTC-1 cells	80
4.5. hCG-induced up-regulation of StAR is strongly inhibited in Leydig cells with <i>Pex13</i> knockdown in MLTC-1 cells	81
4.6. Mouse primary Leydig cell isolation, culture and treatment with hCG	83
4.6.1. Isolation of primary Leydig cells.....	83
4.6.2. Treatment of primary Leydig cells with hCG.	85
4.6.3. Hormone production in primary mouse Leydig cells and comparison with hormone secretion in MLTC-1 cells.	86
4.6.4. Establishing a <i>Pex13</i> knockdown in mouse primary Leydig cells via a siRNA approach.....	88
4.6.4.1. Establishment of a siRNA-mediated RNAi-analysis of the functionality of different <i>Pex13</i> siRNAs for the knockdown of the <i>Pex13</i> gene in MLTC-1 cells and	

establishing a <i>Pex13</i> knockdown in mouse primary Leydig cells via siRNA approach in primary Leydig cells.....	88
4.6.5. hCG-induced up-regulation of StAR is inhibited in primary Leydig cells with <i>Pex13</i> knockdown	91
4.7. <i>Pex13</i> knockdown reduces progesterone secretion in response to hCG treatment in MLTC-1 and in primary Leydig cells	92
4.7.1. Effects of peroxisome deficiency on the activity of P450scc in Leydig cells. .	93
4.7.2. Effects of peroxisomal deficiency on 22R-HC-stimulated progesterone synthesis.....	95
4.8. <i>Pex13</i> knockdown leads to inhibition of testosterone synthesis in MLTC-1 cells and in primary Leydig cells	96
4.9. A down regulation of <i>Pex13</i> leads to an inhibition of DHEA production in Leydig cells.....	98
4.10. Detection of reactive oxygen species in MLTC-1 cells	99
4.10.1. Decrease of reduced glutathione levels in MLTC-1 cells with <i>Pex13</i> knock down.....	99
4.10.2. Detection of increased ROS production by DHE staining in MLTC-1 cells with <i>Pex13</i> knockdown	100
4.11. <i>Pex13</i> knockdown leads to alterations in antioxidative enzymes levels as well as catalase activity in MLTC-1 cells.....	102
4.12. Knockdown of <i>Pex13</i> induces mitochondrial dysfunction in MLTC-1 cells....	104
4.13. Mitochondrial dysfunction impairs hCG-induced as well as 22R-HC-mediated steroid synthesis in MLTC-1 cells.....	107
4.14. <i>Mfp2</i> siRNA transfection in primary Leydig cells.....	108
4.14.1. <i>Mfp2</i> knock down in Leydig cells leads to an inhibition of DHEA production.....	109
5. Discussion.....	110
5.1. Mouse Leydig tumor cells (MLTC-1 cells) produce steroids, including testosterone.....	111
5.2. Primary Leydig cell culture.....	113

5.3. Comparison of MLTC-1 and primary mouse Leydig cells in their ability to produce steroid hormones	114
5.4. Peroxisomal abundance in murine Leydig cells	116
5.4.1. Peroxisomal deficiency in Leydig cells and alteration of peroxisomal marker proteins.....	116
5.5. Disturbed ROS homeostasis and disturbed mitochondrial function in <i>Pex13</i> knockdown Leydig cells	118
5.6. Functional significance of peroxisomes in steroid synthesis in Leydig cells ..	119
5.7. Functional peroxisomes and mitochondria are required for steroidogenesis in Leydig cells.....	121
5.8. Biological potency of androgens and estrogens in Leydig cells with <i>Mfp2</i> knockdown.....	124
6. Summary.....	126
7. Zusammenfassung	128
8. References.....	130
9. List of Abbreviations	145

1. Introduction

1.1. Overview on the male reproduction system

1.1.1. Structure of the testis

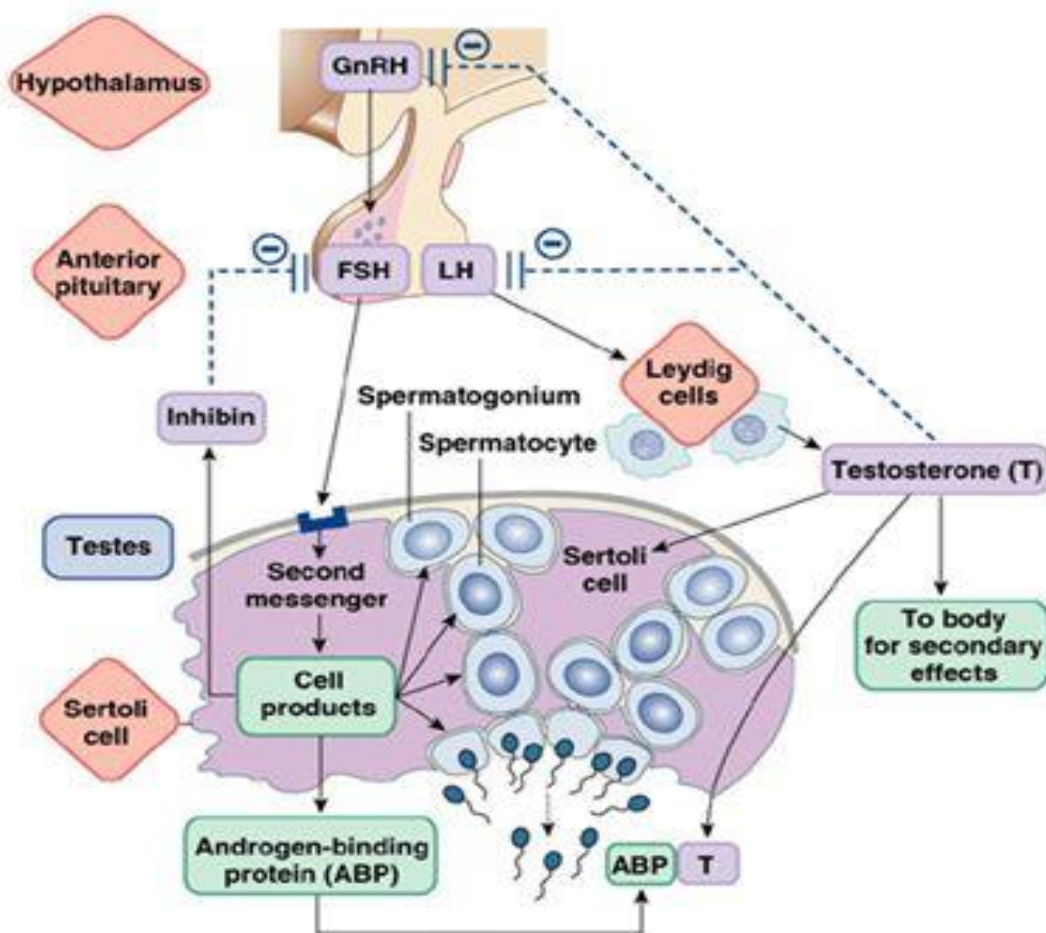
The testes (testicles) are the primary male reproductive organs, which serve two key functions: spermatogenesis and steroid synthesis, particularly the male hormone testosterone. Each testis is covered by a multi-layered tunica of connective tissue called the tunica albuginea, from which partitions of fibrous tissue subdivide the testis into approximately 300 small sections or lobes. Each lobule contains three to four tightly coiled seminiferous tubules, in which spermatogenesis takes place. Tubules are enclosed by a basal lamina, which are surrounded by 3-4 layers of peritubular myoid cells, also called peritubular cells. Tubules are covered with seminiferous epithelium, which is formed of two general types of cells: germ cells and Sertoli cells. Spermatogonia and Sertoli cells reside at the basal part of the seminiferous tubules, whereas spermatocytes, spermatids and spermatozoa are in the adluminal compartment. Sertoli cells within the seminiferous tubules are attached with the neighboring Sertoli cell through a tight junction. They possess a significant role in spermatogenesis, providing support for germ cells to grow and to develop into mature spermatozoa. Leydig cells also called interstitial cells and are located in the interstitial spaces between the seminiferous tubules, which also contain blood vessels, lymphatic elements, fibroblasts and macrophages. They occur in clusters and constitute to the endocrine component of the testis, responsible for hormone secretion.

1.1.2. Regulation of testicular function

1.1.2.1. Endocrine regulation of the testicular function

The hypothalamic–pituitary–testis axis (HPT) plays a crucial role in reproduction and steroid hormone secretion. Gonadotropin-releasing hormone (GnRH), which is synthesized in the hypothalamus by neurons, is transported via the pituitary portal veins to the anterior pituitary gland to facilitate the production of gonadotropic hormones: luteinizing hormone (LH) and follicle stimulating hormone (FSH) (Matsumoto and Bremner 1987). Development and maintenance of testis depends

on the concerted action of the two gonadotropins: FSH and LH. LH activates the receptors expressed on Leydig cells to stimulate testosterone secretion, whereas FSH supports the function of Sertoli cells for spermatogenesis. Sertoli cells produce a protein called androgen-binding protein, binding the active form of testosterone (DHT) as well as inhibin and activin, which act as paracrine factors in testis. The combination of FSH and testosterone are essential for induction and maintenance of a qualitatively and quantitatively normal sperm production. Increased levels of testosterone, its aromatized product estradiol and inhibin cause a negative feedback on the pituitary gland and hypothalamus, inhibiting the production of the LH and thus testosterone production. A reduced testosterone level leads to the GnRH and secretion, thus acting as classic feedback regulator of hypothalamic and pituitary output (Dunkel, et al. 1993; Ellis, et al. 1983; Matsumoto and Bremner 1989; O'Shaughnessy, et al. 2005; Roser 2008).



Copyright © 2007 Pearson Education, Inc., publishing as Benjamin Cummings.

Figure 1. Hypothalamic-pituitary- testicular axis ((Chase 2007).

GnRH is synthesized from the hypothalamus, which stimulates the secretion of LH and FSH by the pituitary gland. LH through LH-receptor stimulates mainly the production of testosterone by Leydig cells in the testis. FSH through FSH receptor supports the function of Sertoli cells for spermatogenesis, stimulates Sertoli cells to produce ABP, inhibin, DHT. Testosterone, its aromatized product estradiol, inhibin and other local products of the somatic cells of testis are acting as classic negative feedback regulator of hypothalamic and pituitary glands.

1.1.2.2. Local, paracrine and autocrine regulation of testicular function

In addition to the endocrine regulation of testicular function and spermatogenesis, there are paracrine and autocrine factors that regulate testicular cell differentiation and function locally in the testis depending on their concentration and overall composition (Saez 1994; Sharpe 1990; Skinner, et al. 1991; Spiteri-Grech and Nieschlag 1993). Paracrine factors are produced by one cell and act on a neighboring cell type, whereas autocrine factors are produced by a specific cell and act on the same cell type. There are different paracrine and autocrine regulators with proven significant influence on testicular function and spermatogenesis, including testosterone, estrogen, inhibin, activin, growth factors like transforming growth factor, α and β ($TGF\alpha$ and β), insulin-like growth factor 1 (IGF-1), cytokines ($IL-1\alpha$ and $IL-1\beta$), GnRH-like peptides, prostaglandins, oxytocin, vasopressin, insulin like peptide 3 (INSL3) and PmodS, a paracrine factor secreted from peritubular myoid cells that modulates Sertoli cell function.

The endocrine-paracrine-autocrine system modulates cell to cell communication within testis. For normal testicular function interactions of Leydig-Leydig cell, Sertoli-Leydig cell, Sertoli-germ cell, Sertoli-peritubular cell are necessary (Roser 2008).

1.1.3. Overview on structure and function of Leydig cells in testis

1.1.3.1. Morphology and development of Leydig cell

The interstitial testicular cells were first described by Franz Leydig born in 1821, in Rothenburg ob der Tauber, Germany. His article in 1850 was mainly about the male

reproductive tract and its accessory glands (Leydig 1850). His remarks on the testis referred to clusters of what appeared to be cells, found between the seminiferous tubules. Thereafter, they were characterized as round cells with enriched smooth endoplasmatic reticulum (ER), mitochondria, different numbers of lipid droplets and a large centrally located nucleus (Christensen 1965; Christensen and Fawcett 1966). Over decades, researchers discovered that Leydig cells have endocrine function producing androgens essential for the correct function of the male reproductive tract, spermatogenesis as well as for the development of male secondary sexual characteristics. In all mammals, during the normal testicular development, two different populations are identified in the testis: fetal Leydig cells and adult Leydig cells. (Lejeune, et al. 1998; Saez 1994). Fetal Leydig cells appear immediately after the formation of testicular cords (embryonic day 12.5 or E12.5 in mice) originating from mesenchymal fibroblasts. In comparison to adult Leydig cells they contain larger lipid droplets and a less-developed Golgi apparatus (Haider, et al. 1995; Kuopio, et al. 1989). Fetal Leydig cells secrete androgens and insulin-like factor 3 (INSL3 or relaxin-like factor), regulating differentiation of the Wolffian duct, external genitalia and the testis descent. A decline of fetal Leydig cells is noted after birth, which suggested that they undergo degeneration (Kuopio et al. 1989; Lording and De Kretser 1972). However, some of them persist in testis together with adult Leydig cells or transform into adult Leydig cell population (Kerr and Knell 1988; Siril Ariyaratne, et al. 2000).

Adult Leydig cells are formed during pubertal development from the stem Leydig cells, which ultimate origin remains a topic of active research. Most investigators inclined to think that they originate from mesenchymal cells derived from the primitive kidney (mesonephros), but others support the idea that sources can include the neural crest and coelomic epithelium (Davidoff, et al. 2002; Davidoff, et al. 2009). It is known that LH, growth factors produced locally by Sertoli as well as androgens, produced by fetal Leydig cells are playing an important role for stimulation of the transition from stem to later stage Leydig cells and for initial development of adult Leydig cells. The cytoplasm of mouse Leydig cells contain a large amount of smooth endoplasmatic reticulum (sER) and tubulovesicular mitochondria, a well-differentiated Golgi apparatus and small lipid droplets. Abundant peroxisomes are also present in steroid producing cells, which are often tubular, elongated and

sometimes are larger than dilated segments of SER (Mendis-Handagama, et al. 1990b; Nenicu 2010; Nenicu, et al. 2007; Reddy and Svoboda 1972a, b). Like mitochondria and lipids, peroxisomes are often closely related to sER (Russel and Burguet 1977; Schulze 1984).

1.1.4. Steroidogenesis

I. Signal Transduction

As stated above, LH is a key regulator of the development, maintenance and proper function of Leydig cells. Steroid hormone biosynthesis is initiated in the testis after stimulation of the LH-receptor by LH or human chorionic gonadotropin (hCG). The LH-receptor is coupled with a G-protein, which stimulates adenylate cyclase activity to form the main second messenger of its signal transduction; cyclic adenosine 3',5'-cyclic monophosphate (cAMP). An increased intracellular level of cAMP stimulates protein kinase A (PKA), which initiates cholesterol biosynthesis and cholesterol transport protein synthesis (Ascoli, et al. 2002; Cooke, et al. 1992; Dufau 1988; Saez 1994; Stocco 1999a; Stocco, et al. 2005). It is well known, that the cAMP/PKA pathway is the major signaling cascade necessary for LH-stimulated steroid synthesis. However, there are less than 1% of cAMP/PKA-independent pathways not involving cAMP for the steroidogenesis, e.g. protein kinase B (PKB), protein kinase C (PKC), mitogen-activated protein kinases (MAPKs), and intracellular Ca^{2+} signaling proteins (Cooke 1999; Manna, et al. 2006). A number of factors including, transforming growth factor (TGF), insulin-like growth factor-I (IGF-I), epidermal growth factor (EGF), fibroblast growth factor, interleukin-1 (IL-1), macrophage-derived factors, chloride ions, and calcium (Ca^{2+}) stimulate steroidogenesis through the cAMP-independent signaling.

II. Cholesterol Synthesis, Uptake and Transport

Cholesterol is the common substrate for the formation of all steroid hormones. There are two potential sources of cholesterol for steroidogenesis in steroidogenic cells. Cellular cholesterol can be synthesized de novo from acetate or can be imported via lipoprotein receptors and receptor-mediated endocytosis from the circulating lipoprotein particles in the blood. Cholesterol synthesis takes place primarily in the smooth ER through a series of enzymatic reactions involving five phases. The first

chain of reactions of intracellular biosynthesis of cholesterol from acetyl-CoA to the HMG-CoA and can take place in the cytosol, mitochondria or peroxisomes (Kovacs, et al. 2002). As mentioned above, steroid producing cells contain a high number of peroxisomes and they are also involved in the biosynthesis and metabolism of cholesterol.

Two mechanisms were described for cholesterol import: uptake of circulating low-density lipoproteins (LDL) by the LDL receptors on the cell surface and uptake of high density lipoproteins (HDL) via scavenger receptor B1 (SR-B1). Human steroidogenic cells mostly take up cholesterol through receptor mediated endocytosis of LDL, whereas rodent cells mostly get through SR-B1. Free cholesterol can be utilized directly for steroid synthesis or can be esterified by acetyl-CoA transferase for storage in lipid droplets. Further, cholesterol esters can be broken down by activation of cholesterol esterase. It has been shown in cell culture models, for example in MLTC-1(mouse Leydig tumor cells) free cholesterol necessary for steroid synthesis can also be derived from the plasma membrane as well (Epstein and Orme-Johnson 1991b).

Under LH stimulation through the LH receptor rapid utilization of newly synthesized or stored cholesterol (ester hydrolysis) takes place in lipid droplets. The transport of intracellular cholesterol to the inner mitochondrial membrane can be divided into two important steps: mobilization of intracellular cholesterol to the outer mitochondrial membrane (OMM) and the transfer of cholesterol from OMM to the inner mitochondrial membrane (IMM) (Jefcoate, et al. 1992; Stocco 2000).

Factors and mechanisms directing the transport of cholesterol to OMM are not yet clearly understood. It may involve vesicular transport, where cholesterol can be incorporated into vesicular membranes such as lysosomes, endosomes, peroxisomes which may act as an intracellular delivery system. Cholesterol can be also delivered through passive aqueous diffusion, nonvesicular carrier-mediated transfer, cytoskeletal elements and transport proteins (Feuilloley and Vaudry 1996; Prinz 2002). There are number of studies revealing the role of sterol carrier protein 2 (SCP2) in cholesterol intracellular transfer. It was shown that SCP-2 is able to bind different lipids (cholesterol, fatty acids, fatty acyl-CoA) (Frolov, et al. 1996; Murphy 1998). SCP-2 has a peroxisomal targeting signal at the C terminus, suggesting its peroxisomal localization (Gallegos, et al. 2001), which might transfer the fatty acids

across the peroxisomal membrane (Stolowich, et al. 1997). Nevertheless, different studies also showed its extraperoxisomal localization in ER, mitochondrial or cytosolic fractions. Moreover, the study with LH treatment in the rat revealed an increase in the volume of peroxisomes and intraperoxisomal content of SCP2 in Leydig cells (Mendis-Handagama, et al. 1992, 1998; Mendis-Handagama, et al. 1990a; Nussdorfer, et al. 1980), suggesting their role in steroid synthesis.

III. Steroidogenic acute regulatory protein (StAR)

Acute steroidogenic responses are regulated by cholesterol transport from the OMM to IMM, which is the rate limiting step for steroidogenesis triggered by the steroidogenic acute regulatory protein (StAR). Cholesterol, being hydrophobic, is not able to pass through the aqueous intermembrane space of the mitochondria, requiring the help of cholesterol transfer proteins (Jefcoate et al. 1992; Stocco 2000). Moreover, mitochondrial membranes, particularly IMM, in comparison to other subcellular membranes are cholesterol-poor, which enables steroidogenic cells to control the steroid synthesis via the rate of cholesterol transport to IMM rather than via enzyme activities.

After the cholesterol transfer via StAR to the inner mitochondrial membrane, cytochrome P450 enzyme converts cholesterol to pregnenolone. StAR mediates a rapid stimulation of steroid synthesis induced by LH in the testis, adrenal and ovary. Mutation in the PKA phosphorylation sites of StAR resulted in the inhibition of steroid synthesis by 85% (Fleury, et al. 2004), consequently only 10-15% of steroid synthesis is regulated by StAR-independent mechanisms (Clark, et al. 1997; Lin, et al. 1995; Manna et al. 2006; Manna, et al. 2001). The significant role of StAR was verified by when mutation in the StAR gene leads to the development of the lipoid congenital adrenal hyperplasia; an autosomal recessive disorder, where steroid synthesis is dramatically impaired (Miller 1997).

The StAR protein involved in cholesterol intramitochondrial movement was initially discovered by Orme-Johnson and colleagues in rat and mouse adrenocortical cells and Leydig cells (Alberta, et al. 1989; Epstein and Orme-Johnson 1991a, b; Krueger and Orme-Johnson 1983; Pon, et al. 1986). Later the cDNA was cloned and this protein was named steroidogenic acute regulatory protein described by Stocco and colleagues in hormone stimulated MA-10 mouse Leydig tumor cells and in human

cells (Clark, et al. 1994; Lin et al. 1995; Stocco and Clark 1996b; Sugawara, et al. 1995). StAR is synthesized as cytoplasmic 37kDa protein containing a N-terminal mitochondrial targeting sequence and the C-terminal StAR-related lipid transfer domain and is cleaved during mitochondrial import into an intramitochondrial 30 kDa form. The mechanisms of StAR-mediated cholesterol transport from the OMM to the IMM are still not completely understood. Initially it has been shown that mitochondrial import of StAR generates “contact sites” between the OMM and IMM, thus permitting cholesterol to flow down from OMM to IMM via a chemical concentration gradient (Stocco and Clark 1996a; Stocco and Sodeman 1991). The rapid cleavage of the 37-kDa cytoplasmic form of StAR to the 30kDa intramitochondrial form suggests that the 37 kDa form is a precursor whereas the 30 kDa protein is the mature form (King and Stocco 1996) and the role of the mature 30-kDa protein in transferring cholesterol to IMM is considered (Stocco and Clark 1996a).

After discovering a cholesterol binding pocket in the structure of StAR it was suggested, that StAR in the mitochondrial intramembranous space (IMS) could shuttle cholesterol one molecule at a time from the OMM to the IMM (Tsujishita and Hurley 2000). The accuracy of these models was questioned, since the deletion of mitochondrial leader N-terminal of the StAR protein had no effect on Star’s activity on cholesterol transfer or steroid production in transfected MA-10 or COS-1 cells (Arakane, et al. 1996). On the contrary, by deletion of 28 C-terminal residues, the capacity to induce the steroid production was lost, indicating that a region in the C terminus is important for cholesterol transfer (Arakane et al. 1996). It was shown that cholesterol was imported when StAR acts only on the OMM but not at the IMM or intermembrane space (IMS) and its activity depends on how long it remains on the OMM (Arakane et al. 1996; Bose, et al. 2002).

It was also shown that StAR undergoes pH-induced conformational changes when interacts with charged phospholipids on the OMM, thus allowing cholesterol access (Baker, et al. 2005; Bose, et al. 1999; Bose, et al. 2009a; Bose, et al. 2009b; Song, et al. 2001).

A multi-protein complex has been described to interact with StAR on the OMM for cholesterol transport to the IMM for pregnenolone synthesis (Bose, et al. 2008; Papadopoulos and Miller 2012; Rone, et al., 2012), which involves the TSPO, voltage-dependent anion channel (VDAC-1), acyl coenzyme A-binding domain

containing A or TSPO-associated protein 7 (PAP7, ACBD3) and protein kinase A regulatory subunit 1 α (PKARalpha)(Liu, et al. 2006; Martin, et al. 2016; Miller 2013; Miller and Bose 2011; Rone, et al. 2009). Nevertheless, the exact composition and the function of this complex is still controversial.

IV. Enzymatic conversions for steroid synthesis

Leydig cells express all enzymes necessary for the synthesis of testosterone: the major sexual hormone produced in the testis. The enzymes involved in steroid synthesis can be divided into two main groups: Cytochrome P450 enzymes such as P450scc, P450 17 α -hydroxylase/C17 - 20 lyase (P450c17 or Cyp17) and P450 aromatase (P450arom), and the hydroxysteroid dehydrogenases such as 3 β -hydroxysteroid dehydrogenase (3 β -HSD) and 17 β -hydroxysteroid dehydrogenases (17 β -HSD).

Cholesterol is converted to pregnenolone by P450scc, which is located in the inner mitochondrial membrane. Thereafter, pregnenolone diffuses through the mitochondrial membrane to the smooth endoplasmic reticulum for further conversion into different hormones. Pregnenolone can be metabolized to 17 α -hydroxypregnenolone by cytochrome P450c17 or it may be converted by 3 β -HSD to the first biologically significant hormone: progesterone.

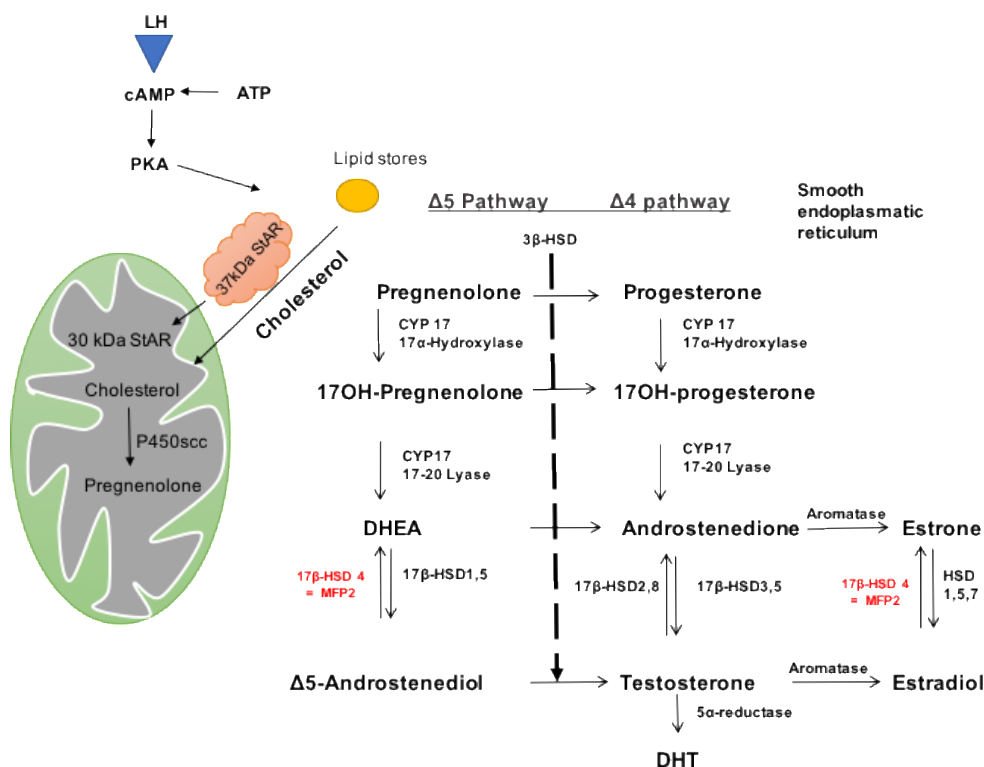


Figure 2: Steroidogenesis in testis.

Steroidogenesis is initiated in the Leydig cells after stimulation of the LH-receptor by LH, which stimulates the synthesis of cAMP from ATP. cAMP induces the activity of protein kinase A (PKA), which initiates cholesterol biosynthesis and cholesterol transport protein synthesis for the transfer of intracellular cholesterol to the OMM and from OMM to the IMM. StAR interacts with a multi-protein complex for transferring cholesterol to IMM, where the P450_{scc} enzyme converts cholesterol into pregnenolone. Thereafter, pregnenolone is transferred to the sER, where next enzymatic reactions take place. 2. reaction: 3 β -HSD: 3 β -hydroxysteroid dehydrogenase, 3. reaction: CYP17 17-20 lyase: cytochrome P450 17 α -hydroxylase; 4. reaction: 17 β -HSD: family of 17 β -hydroxysteroid dehydrogenase 5. reaction: aromatase: cytochrome P450 aromatase, 6. reaction: 5 α -reductase, DHT (dihydrotestosterone). Modified from (Haider 2004; Stocco 1999b).

Thus, the steroidogenic pathway bifurcates into a Δ 5-hydroxysteroid pathway starting with pregnenolone and a Δ 4-ketosteroid pathway starting with progesterone. 3 β -HSD converts the Δ 5-hydroxysteroid pathway substrates into their respective Δ 4-ketosteroids, thus pregnenolone to progesterone, 17 α -hydroxypregnenolone to 17 α -hydroxyprogesterone (17-OHP), dehydroepiandrosterone (DHEA) to androstenedione, androstenedione to testosterone (Lorence, et al. 1990; Miller 2008).

P450_{c17} has both 17 α -hydroxylase as well as 17,20 -lyase activity and catalyzes the conversion of pregnenolone to 17 α -hydroxypregnenolone, which is then converted to DHEA for the Δ 5-hydroxysteroid pathway. Likewise, for the Δ 4-ketosteroids, P450_{c17} converts progesterone to 17OHP, which is then converted to androstenedione (Fan, et al. 1992; Zuber, et al. 1986).

17 β -HSDs catalyze the last step in steroidogenesis, participating in the formation and inactivation of steroid hormones by modulating biological potency of estrogens and androgens by conversion at position 17. There have been up to 12 types of 17 β -HSD described of which 10 are also found in humans. The most important enzyme for the testosterone synthesis from androstenedione is 17 β -hydroxysteroid dehydrogenase 3 (17 β -HSD3) (Geissler, et al. 1994), which is expressed in both human and rodent Leydig cells (Andersson 1995; Sha, et al. 1997). It was documented, that androstenediol is converted from DHEA by 17 β -HSD1 and 5 and

the reverse reaction is catalyzed by 17 β -HSD2 and 4 (Adamski, et al. 1995; Labrie, et al. 2000; Peltoketo, et al. 1999).

As mentioned above the biological potency of estrogens is regulated by 17 β -HSDs, where estrone is converted to the biological active estradiol by 17 β -HSD1, 5 and 7, whereas the reverse reaction of estradiol inactivation is performed by 17 β -HSD2,4,8,10 (Adamski et al. 1995; Fomitcheva, et al. 1998; Peltoketo et al. 1999).

Leydig cells contain a high level of 17 β -HSD4 also known as peroxisomal multifunctional protein 2 (MFP-2) (Carstensen, et al. 1996; Normand, et al. 1995). The localization of the 17 β -HSD4 is exceptional since it is the only 17 β -HSD found in peroxisomes (Markus, et al. 1995). MFP-2 is involved in the peroxisomal β -oxidation of branched fatty acids like pristanic acid, C27-bile acid intermediates, very long chain fatty acids, and in the synthesis of certain polyunsaturated fatty acids (PUFA) (Novikov, et al. 1997). Other 17 β -HSDs are localized either in cytosol, mitochondria or associated with the endoplasmic reticulum (Adamski and Jakob 2001; Peltoketo et al. 1999).

In the testis androgens are irreversibly converted into estrogens by P450 arom (Simpson, et al. 1994). It converts androstenedione and testosterone to the estrone and estradiol, respectively. P450 aromatase is located in the smooth endoplasmatic reticulum and its activity is stimulated by LH. In mice the aromatase is expressed in Leydig cells and in seminiferous tubules, especially in spermatids (Carreau, et al. 1999). P450arom is also present in Sertoli cells and it was reported that during the early stages of testicular development the estrogen production is dominant in these cells in rats. However, mature Leydig cells secrete more estrogen, whereas Sertoli cells continue to express aromatase, but at a lower rate (Hess 2003; O'Donnell, et al. 2001). It was shown, that human spermatozoa produce estrogens and that aromatase is expressed, possibly playing role in sperm mortality (Lambard, et al. 2003).

Estrogens act through estrogen receptors (ER α and ER β), which are expressed in most of the testicular cells (Carreau, et al. 2002a; Carreau, et al. 2002b). Different studies showed that estrogens have an important role in the regulation of sperm production and fertility (O'Donnell et al. 2001). Physiological level of estrogens is also necessary for the survival of germ cells (Pentikainen, et al. 2000).

1.1.5. Function of testosterone

The primary role of Leydig cells is to produce testosterone, which in turn is crucial for spermatogenesis and fertility. This action of testosterone is mediated by the Sertoli cells which nourish and support the developing spermatozoa and their function is critically dependent on normal Leydig cell function. Testosterone effects on spermatogenesis via androgen receptors (ARs) that are localized in the Sertoli cells (Silva, et al. 2002). Testosterone is also essential for the testicular formation and differentiation. Testosterone diffuses from Leydig cells to seminiferous tubules and together with FSH induces the Sertoli cells to produce local factors that are required for the normal spermatogenesis. Testosterone acts on the Sertoli cells to increase its response to FSH resulting in increased production of androgen-binding protein (ABP), which binds specifically to testosterone, dihydrotestosterone and 17-beta-estradiol. It serves them to be less lipophilic and concentrated within the luminal fluid of the seminiferous tubules, making the androgens available to bind the intracellular androgen receptor thus exerting the trophic effects on spermatogenesis. Testosterone action is crucial and in an absolute requirement for adult spermatogenesis and the main targets of its action are completion of meiosis and spermatogenesis (Cameron, et al. 1993; Marathe, et al. 1995; McLachlan, et al. 2002a). Moreover, different studies indicate that testosterone is involved in Sertoli cell differentiation in early postnatal life (Buzzard, et al. 2003; Sharpe, et al. 2003). The role of testosterone in germ cell development and for spermatogonial development during the first wave of spermatogenesis is still not clear. It has been also reported that testosterone inhibits germ cell apoptosis (Singh, et al. 1995). Furthermore, Sertoli cell-specific AR knockout mice exhibit an arrest at late spermatocytes and beyond, suggesting that androgen action is crucial for the completion of meiosis and spermatogenesis in the first wave (Chang, et al. 2004; De Gendt, et al. 2004). Thus, spermatogonial development, meiosis and spermiation are the three main processes, where the action of gonadotrophins and testosterone is critical (Matthiesson, et al. 2006; McLachlan, et al. 2002).

1.2. Peroxisomes

Peroxisomes (originally called microbodies) are organelles found in all eukaryotic cells. Peroxisomes were first identified by J. Rhodin in 1954 (Rhodin, et al. 1954), using electron microscopy in a mouse kidney and were identified as spherical organelles of 0.3-1.0µm with a single limiting membrane. Thereafter, peroxisomes as distinct organelles have been described by Christian de Duve in the 1960th (De Duve and Baudhuin 1966). They found that catalase, urate- and D-amino acid oxidases are localized in special particles which differ from microsomes or mitochondria. The term of peroxisome was given by de Duve and Baudhin, as they own both hydrogen peroxide (H₂O₂) producing oxidases and catalase degrading H₂O₂. They contain a fine granular matrix and occasionally a paracrystalline core. Peroxisomes exhibit remarkable morphological as well as metabolic plasticity and they are able to move throughout the cell along microtubule. Their number, size, biochemical function and protein composition differs significantly among various species and tissues (Baumgart 1997; Subramani 1993; Wanders and Tager 1998). Peroxisomes have been identified in every tissue so far with the exception of mature red blood cells and spermatozoa in the testis (Luers, et al. 2006).

Peroxisomes and mitochondria share similarity in size, and both organelles are very dynamic. They are able to adapt their shape and number depending on the cells requirements (Bonekamp, et al. 2013; Polyakov, et al. 2003; Schrader, et al. 2012). Peroxisomes differ from mitochondria by their homogenous matrix, single membrane, an electron dense core as well as by absence of cristae. Lysosomes can be differentiated from peroxisomes by their heterogeneous matrix and staining for acid phosphatase (Baumgart, et al. 1989; Fujiki, et al. 1982).

1.2.1. Peroxisome biogenesis

More than 30 *PEX* genes encoding proteins (peroxins) were discovered, which are divided into the following groups required for peroxisomal biogenesis (Distel, et al. 1996): for formation of the peroxisomal membrane (PEX3, PEX16, PEX19), for transport in the cytoplasm (PEX5, PEX7, PEX19), for docking (PEX13, PEX14, PEX17), import of proteins into the peroxisomal matrix (PEX10, PEX12), proliferation of the organelles (PEX11) and for organelle degradation (PEX4) (Baumgart et al.

1989). In contrast to mitochondria, peroxisomes do not contain DNA. Thus, peroxisomal matrix and membrane proteins are synthesized on free polyribosomes in cytoplasm and imported later into peroxisomes (Lazarow and Fujiki 1985). Peroxisomal matrix proteins contain peroxisomal targeting signals (PTS) either at the C terminus (PTS1) or at their N terminus (PTS2). They are recognized by the peroxisomal targeting sequence soluble receptors (PTS1 by Pex5p, PTS2 by Pex7p) and the receptor-cargo complexes then dock at the peroxisomal membrane with the docking proteins (Pex13p, Pex14p and Pex17p) (Subramani 1993). Thus, PEX13 plays a significant role in importing proteins into the peroxisome via PTS1 and PTS2. Deletion of *Pex13* leads to a loss of both PTS1 and PTS2 protein import, and it was shown that Pex13 functions as a docking protein for the predominantly PTS1 receptor (Gould 1996). *Pex13* gene defect leads to the peroxisomal protein import disruption and peroxisomal metabolic dysfunction (Liu, et al. 1999; Maxwell, et al. 2003; Shimozawa, et al. 1999).

1.2.2. Metabolic functions of peroxisomes

Peroxisomes play a strong role in cellular metabolism, which is especially evident by the devastating consequences in cells in conditions of peroxisome deficiency or absence. Peroxisomal enzyme composition varies depending on a cell type and a distinct organ, as well as they respond differently to developmental and environmental conditions (Baumgart 1997). They proliferate easily after treatment with hypolipidemic drugs and are involved in lipid metabolic pathways (Baumgart 1997). They participate in fatty acid β -oxidation, peroxide metabolism, fatty acid α -oxidation, biosynthesis of ether phospholipids/plasmalogens, retinoid metabolism, cholesterol metabolism, protein /amino acid metabolism as well as conversion and biosynthesis of bile acid and polyunsaturated fatty acids (PUFAs).

1.2.2.1. Peroxisomal fatty acid β -oxidation

One of the main functions of peroxisomes is the breakdown of fatty acids. Generally, oxidation of fatty acids occurs in three subcellular organelles: mitochondria, peroxisomes and the CYP4A catalyzed oxidation occurring in the endoplasmic

reticulum (Mannaerts, et al. 2000; Ortiz de Montellano 1995). Mitochondrial β -oxidation is responsible for the oxidation of the bulk of the short, medium and long chain fatty acids and in the process, contributes to energy generation via ATP. Peroxisomes are involved in the β -oxidation of lipids which cannot be oxidized by mitochondria (Wanders and Tager 1998). These include: very-long-chain fatty acids (VLCFA), notably hexacosanoic acid (C26:0), the 2-methyl branched-chain fatty acids (pristanic acid) long-chain dicarboxylic acids, the bile acid synthesis intermediates (di and trihydroxycholestanoic acid, prostaglandins, leukotriens and certain xenobiotics. Fatty acids are taken into the peroxisome and esterified to CoA by the solute carrier family member proteins ABCD1/ALDP, ABCD2/ALDRP, or ABCD3/PMP70. ABCD1 and ABCD3 are strongly expressed in Sertoli cells, whereas peroxisomes in Leydig cells show the highest expression levels of ABCD2 (Neniciu et al. 2007). The substrates transported by ABCD2 are ill-defined. Several studies indicate the role of ABCD2 in the synthesis of the poly-unsaturated fatty acid, which requires chain shortening by peroxisomal β -oxidation. The peroxisome β -oxidation pathway consists of the similar reaction steps as the mitochondrial, but the enzymes involved are different and also oxidation does not go to completion. In contrast to the mitochondria, peroxisomal β -oxidation of fatty acids does not yield ATP. Products formed are transported out of peroxisomes to the mitochondria for full oxidation to CO₂ and H₂O. β -oxidation of fatty acids as the main function of peroxisomes also leads to the formation of H₂O₂. Peroxisomal β -oxidation systems consist of a classical peroxisome proliferator-activated receptor (PPAR)-inducible pathway for catabolism of eicosanoids and straight-chain acyl-CoAs by fatty acyl-CoA-oxidase (ACOX1), multifunctional protein 1 (MFP1) and thiolase A (pTH1), and a second non-inducible pathway catalyzing the oxidation of the cholesterol side chain and 2-methyl-branched fatty acyl-CoA by a branched-chain acyl-CoA oxidase in humans ACOX2, (ACOX3 in mice)(Baumgart, et al. 1996a; Baumgart, et al. 1996b), multifunctional protein 2 (MFP2) (Novikov et al. 1997), also known as (HSD17B4), and sterol carrier protein X (SCPX). MFP-2 is involved in the peroxisomal β -oxidation of very-long- chain fatty acids, pristanic acid, C27-bile acid intermediates as well in the synthesis of PUFA (Wanders, et al. 2001b).

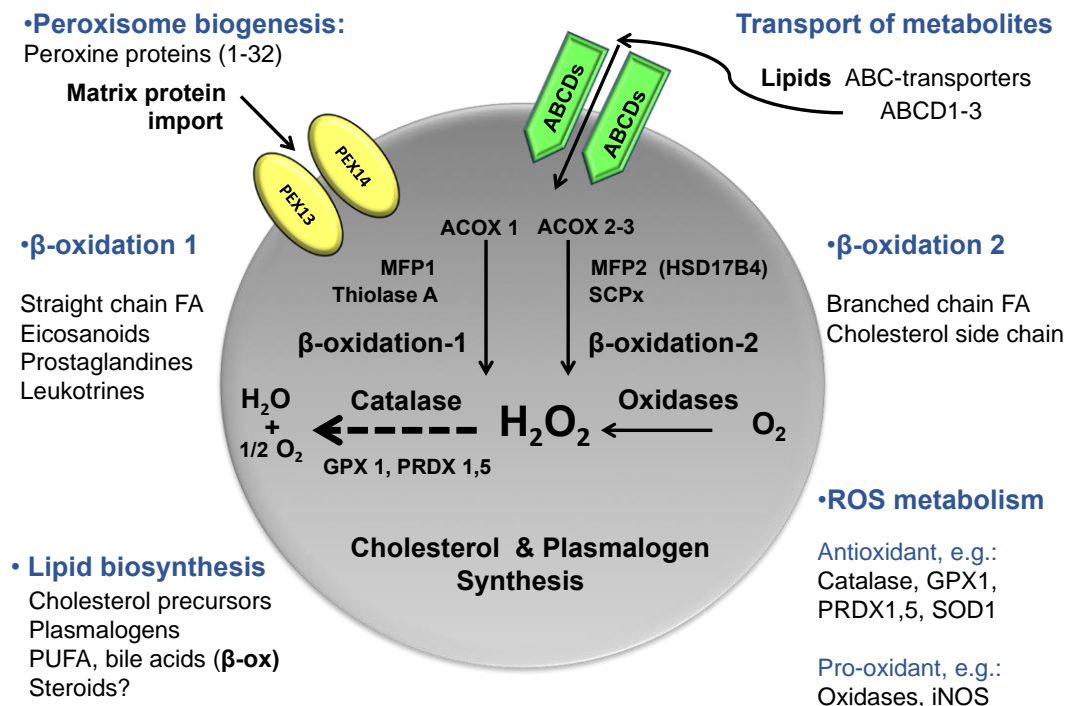


Figure 3. Model for a peroxisome

1.2.2.2. The role of peroxisomes in cholesterol synthesis

Peroxisomes are also involved in the de novo cholesterol synthesis and in cholesterol oxidation (Biardi, et al. 1994; Krisans 1992; Krisans, et al. 1994). Cholesterol synthesis begins from acetyl-CoA, which is derived mostly from an oxidation reaction in mitochondria. Enzymes involved in cholesterol synthesis are in the cytoplasm, endoplasmic reticulum (ER) and peroxisomes. Peroxisomes contain acetoacetyl-CoA thiolase, 3-hydroxy-3-methylglutaryl coenzyme A (HMG-CoA) reductase, HMG-CoA synthase, mevalonate kinase, and farnesyl diphosphate (FPP) synthase. Under the enzymatic reaction of an acetoacetyl-CoA thiolase, two acetyl-CoA are condensed to create acetoacetyl-CoA. It has been shown, that this enzyme has a peroxisomal target signal 1 (Song, et al. 1994). HMGCoA reductase, which catalyzes the conversion of HMG-CoA into mevalonate, is the rate limiting enzyme of the cholesterol biosynthetic pathway. Different studies showed that this enzyme is located in the sER and in the peroxisomes (Engfelt, et al. 1997; Keller, et al. 1985; Kovacs, et al. 2001). The next steps of cholesterol biosynthesis occur exclusively in

peroxisomes, since the following enzymes contain peroxisomal targeting signal: phosphomevalonate kinase (PMVK), mevalonate diphosphate decarboxylase (MPD) and isopentenyl phosphase (IPP) isomerase and farnesyldiphosphate synthase (FPP) (Biardi and Krisans 1996). FPP is utilized further by the ER for squalene synthesis resulting final product cholesterol (Goldstein and Brown 1990), which occurs only in the sER.

1.2.3. Oxidative stress in the cells

Oxidative stress arises due to a significant increase in the concentration of reactive oxygen species (ROS) and reactive nitrogen species (RNS) and/or a decrease of antioxidant mechanisms. Production of free radicals is a natural and continuous process in the body. ROS are generated as common by-products of normal cellular metabolism, and in normal physiological levels they act as intracellular signaling molecules in different biological mechanisms: cell proliferation, cell differentiation, cell apoptosis, immune reactions, inflammatory processes, aging (Fialkow, et al. 2007). ROS are highly reactive molecules, which include oxygen radicals such as superoxide anion (O_2^-), hydroxyl radical ($\cdot OH$), nitric oxide ($\cdot NO$), also non-radical species such as hydrogen peroxide (H_2O_2), peroxyxynitrite and other compounds. Increased, harmful levels of ROS in the cells are usually decomposed by protective detoxifying mechanisms, which include antioxidant enzymes, such as catalase, glutathione peroxidase, superoxide dismutase 2 or mitochondrial SOD2, superoxide dismutase 1 or SOD1, peroxiredoxins 1-6, epoxide hydrolase and antioxidant molecules, such as glutathione, alpha tocopherol (Vit E), ascorbic acid (Vit C).

The major sources of ROS in cells are mainly generated as a by-product of mitochondrial respiration (Boveris 1984; Mammucari and Rizzuto, 2010). Other than mitochondrial respiration, peroxisomes are also playing an important role as in production as well as in scavenging of oxygen free radicals in cells, particularly H_2O_2 (Dansen and Wirtz 2001; Nordgren and Fransen 2014; Schrader and Fahimi 2006).

ROS lead to cell damage through different mechanisms: DNA damage, peroxidation of lipids, oxidation of proteins. Moreover, they mediate an increased release of pro-inflammatory cytokines. The major interest to oxidative stress arises considering

their significant role in the pathogenesis of different pathologies including atherosclerosis, inflammation, hypertension, diabetes, cancer, ischemia, injury, fibrosis, aging and other conditions (Chapple 1997; Madamanchi, et al. 2005; Raha and Robinson 2000).

1.2.3.1. Mitochondria and oxidative stress

The mitochondrion consists of two major membranes: inner and outer mitochondrial membranes separated by an intermembrane space. The inner membrane surrounds the mitochondrial matrix, which contains its own DNA and the enzymes responsible for the central reactions of oxidative metabolism.

Mitochondria are known as the powerhouses of the cell, as they are responsible for the energy generated from the oxidative breakdown of fatty acids and carbohydrates, which are converted to ATP through oxidative phosphorylation (ox-phos). Cellular ATP is mainly generated through mitochondrial oxidative phosphorylation, a process where electron transport occurs along four enzyme complexes located at the inner mitochondrial membrane: mitochondrial complex I (NADH dehydrogenase), complex II (succinate dehydrogenase), complex III (cytochrome bc1), complex IV (cytochrome oxidase) and complex V (ATP synthase). Electrons are generated by citric acid cycle in the mitochondrial matrix. During electron transport, protein complexes push protons from the matrix into intermembrane space, creating a proton gradient, which generates the mitochondrial membrane potential ($\Delta\Psi_m$) and pH differential (ΔpH). Mitochondrial membrane potential is essential for the physiological function of the respiratory chain to generate ATP, including the powering the ATP synthase.

Mitochondrial respiration with energetic processes is not without dangers. It consumes 85-90% of the oxygen necessary inside the cells, making them a major producer and the greatest potential source of ROS in the cells. Mitochondrial electron transport chain with molecular oxygen directly generates primarily the superoxide radical and via SOD2 hydrogen peroxide (Chance, et al. 1979; Hansford, et al. 1997). The two major respiratory chain regions responsible for ROS production are complex I and complex III (Baumgart, et al. 2001; Cross and Jones 1991; Shimomura, et al. 1985).

1.2.3.2. Peroxisomes and oxidative stress

Oxygen is necessary for many metabolic reactions in different cellular locations with mitochondria, endoplasmic reticulum (ER) and peroxisomes being the major sites. Respiratory pathway in peroxisomes and the role of this organelle in the metabolism of ROS have been already described by early investigators (De Duve and Baudhuin 1966; Oshino, et al. 1973; Sies 1974). β -oxidation of fatty acids is the most important metabolic process in peroxisomes contributing to the formation of hydrogen peroxide by fatty acyl-CoA oxidases. There are also other oxidases in peroxisomes such as urate oxidase, D-amino acid oxidase, D-aspartate oxidase, xanthine oxidase, pipelicolic acid oxidase, polyamine oxydase and nitric oxide synthase. To maintain the balance between production and scavenging of ROS, peroxisomes house a variety of other antioxidant enzymes for the cell rescue from the damaging effects of ROS. Catalase is one of the most important antioxidant enzymes, which has a protective function against the peroxides generated in peroxisomes, and is considered as a marker enzyme for peroxisomes. It has been revealed, that catalase is highly expressed in peroxisomes in Leydig cells (Neniciu et al. 2007). The high amount of catalase in peroxisomes of Leydig cells can play a protective and beneficial role for steroidogenesis.

As mentioned above, there are also other antioxidant enzymes which are mainly localized in mitochondria and/or cytosol, but they are present in peroxisomes as well. Different isoenzymes of glutathione peroxidases present in all cell compartments including peroxisomes (Singh, et al. 1994), and their role is to reduce lipid hydroperoxides as well as hydrogen peroxide. SOD1, which is mainly present in the cytoplasm and SOD2, primarily localized in mitochondria, was reported to be localized in peroxisomes as well (Dhaunsi, et al. 1992; Keller, et al. 1991; Singh 1996). Recently in our laboratory was shown that mammalian SOD2 is exclusively located in mitochondria, but not in peroxisomes (Karnati, et al. 2013). Both enzymes protect cells against superoxide anions by converting them into H_2O_2 . The production of hydrogen peroxide, superoxide anion, hydroxyl radicals, as well as the discovery of different antioxidant enzymes in these organelles has supported the notion, that peroxisomes play a key role in both the generation of ROS with grave consequences for the cell fate, and scavenging of ROS in a cell, in particular hydrogen peroxide (Schrader and Fahimi 2006). Peroxiredoxin I (PRDX1) is also playing an important

role in oxidative cell protection. It was reported to be present in rat liver peroxisomes as well as in cytoplasm, mitochondria and nucleus (Immenschuh, et al. 2003). It has been reported, that increased levels of hydrogen peroxide can inhibit steroidogenesis via blockage of the mitochondrial P450_{scc}, StAR protein expression (Tsai, et al. 2003) and also 3 β -HSD (Stocco, et al. 1993).

1.2.4. Peroxisomal disorders

There are more than 20 human peroxisomal disorders with severe clinical manifestation, which reveal the relevance of the peroxisome for proper functioning of the cell and for human health. Severe inherited peroxisomal diseases can lead to death at early age and are usually characterized by an accumulation of VLCFAs, BCFAs or bile acid intermediates and also other components in the plasma. The peroxisomal disorders are divided into two classes: peroxisome biogenesis disorders and the single peroxisomal enzyme deficiencies (Fujiki 2016).

1.2.4.1. Peroxisome biogenesis disorders

Peroxisome biogenesis disorders (PBDs) include Zellweger syndrome (ZS), neonatal adrenoleukodystrophy (NALD), infantile Refsum disease (IRD)(Wanders, et al. 2001a), which are collectively called the Zellweger spectrum disorders (ZSDs) as well as rhizomelic chondrodysplasia punctata (RCDP) type 1 (Goldfischer, et al. 1973; Govaerts, et al. 1982; Steinberg, et al. 2006; Wanders and Waterham 2005). The molecular defects of these diseases are deletions or mutations of PEX genes, which are responsible for peroxisome biogenesis. PBDs are autosomal recessive disorders, in which functional peroxisomes are absent. The Zellweger syndrome (cerebrohepatorenal syndrome) is considered to be the most severe form of peroxisomal biogenesis disorders leading to early death of the children. Patients demonstrate developmental brain disorders, malformation in the central nervous system, skeletal dysmorphisms, liver dysfunction, adrenal insufficiency and retinopathy. In these patients very long chain fatty acids and branched chain fatty acids, such as phytanic acid are accumulated in plasma as well as in other cell

types. In addition, plasmalogens and ether-phospholipids levels are deficient, which is necessary for normal brain and lung function.

1.2.4.2. Single Peroxisomal enzyme deficiencies

Several diseases resulting from single peroxisomal enzyme deficiencies exist, where one of the peroxisomal metabolic pathways is affected. It can be enzyme defect in (1) peroxisomal β -oxidation, (2) ether phospholipid synthesis, (3) peroxisomal α -oxidation, (4) glyoxylate detoxification or (5) H_2O_2 -metabolism (Wanders 2004; Wanders and Waterham 2006).

One of the single peroxisomal enzyme disorders is X-linked adrenoleukodystrophy (X-ALD) primarily occurring in males, which is classified in two most frequent phenotypes: childhood cerebral ALD (CCALD) and adrenomyeloneuropathy (AMN) (Powers 1985). Also, adolescence cerebral ALD exists, where symptoms manifest in adolescence. In these diseases an ABCD1 gene defect was described, an ABC-transporter on the peroxisomal membrane, leading to the dysfunction of the transport of very long-chain fatty acids into the peroxisomal matrix (Kemp and Wanders 2007) thus leading to the disruption of transport and subsequent breakdown of VLCFAs. The biochemical hallmark of X-ALD is the accumulation of VLCFAs in plasma as well as in different cell types. The accumulation of VLCFAs is mainly toxic to the adrenal cortex and myelin. CCALD usually manifests between 3 and 10 years of age with progressive behavioral and neurologic deterioration, whereas AMN starts at a later age of onset between 28-35 years.

Patients with a MFP-2 deficiency mostly die in their first years of life, exhibiting severe hypotonia, developmental abnormalities, neuronal migration defects and convulsions in the neonatal period. Clinically they are strongly similar to patients with Zellweger syndrome or cerebrohepatorenal syndrome (Gould, et al. 1996; Wanders et al. 2001b).

1.2.5. Peroxisomes and testis

In the testis, peroxisomes were discovered first in interstitial Leydig cells via routine electron microscopy and through positive peroxidase staining for the localization of the peroxidatic activity of peroxisomal catalase (Reddy and Svoboda 1972; Reddy and Svoboda 1972a). Catalase is generally used as peroxisomal marker, because it is the most abundant peroxisomal protein found in other organs and tissues. They were the first to speculate that Leydig cell peroxisomes play a role in cholesterol and steroid biosynthesis and/or catabolism. Through the analysis of the expression of catalase mRNA in male reproductive tract, peroxisomal marker protein was detected in peritubular and interstitial Leydig cells (Zini and Schlegel 1996). Later it has confirmed by in situ hybridization that catalase expression is restricted to Leydig cells (Baumgart, et al. 1997). The localization of peroxisomes only in Leydig cells as well as in epididymis was also shown by Western and Northern blotting (Reisse, et al. 2001). However, later through visualization of different peroxisomal proteins, it was shown that peroxisomes are present in most cell types in the testis, except for mature spermatozoa (Luers, et al. 2003; Luers et al. 2006; Nenicu et al. 2007). These studies show the difference of peroxisomal protein composition dependent of specific cell type. Leydig cells express high level of catalase and peroxisomal lipid transporter ABCD2, whereas ABCD1, ABCD3 as well as the acyl-CoA oxidase 2 (ACOX2) were found mostly in Sertoli cells (Nenicu et al. 2007).

1.2.6. Peroxisomal dysfunction and testicular impairment

Peroxisomes play a significant role in human testis development and function. This is stressed by gonadal impairment such as impaired spermatogenesis, primary hypogonadism and infertility in patients with peroxisomal dysfunction. Male patients with X-ALD demonstrate an adreno-testiculo-leukomyeloneuropathic-complex of symptoms with central and peripheral nerve disturbance, as well as impairment of endocrine system such as adrenal cortex and the gonads (Brennemann, et al. 1997; Powers 1985; Powers and Schaumburg 1981). Histological findings of testicular tissue of adult patients show hypocellularity and vacuolation of seminiferous tubules, germinal cell arrest and disturbed maturation of spermatogenesis. In some patients, the decrease in the number of Leydig cells was detected. Light microscopy of the

testis tissue revealed striations in Leydig cells, suggesting an accumulation of VLCFA in the cytoplasm in these cells (Powers and Schaumburg 1981). Sixty three percent of the AMN patients exhibit elevated serum LH and low levels of testosterone, confirming an impairment of the Leydig cells. Additionally, they possess increased serum FSH, which is the result of impaired Sertoli cell function consequently of deficient spermatogenesis (Brennemann et al. 1997). ALD-patients suffer from infertility, which can develop within one year (Aversa, et al. 1998). Poor response of hCG treatment was also demonstrated in many patients. Assies et al 1998 demonstrated that some X-ALD patients exhibit reduced levels of DHEA (Assies, et al. 1998).

Due to early postnatal death of patients with peroxisomal biogenesis disorders, very sparse information is known about the role of peroxisomes for male fertility and testicular function. However, Zellweger spectrum patients, surviving to adolescence also show testicular abnormalities with vacuolated Sertoli cells, a complete degeneration of Leydig cells and an arrest of spermatogenesis. Patients with a severe form of peroxisomal biogenesis disorders show cryptorchidism (Dimmick 1997). It was suggested that cryptorchidism could be a result of androgen insufficiency or disturbed androgen signaling pathways in patients with peroxisomal disorders (Foresta, et al. 2008). Moreover, several studies with mouse models associated with peroxisome dysfunction show impaired testicular function. Testicular impairment was demonstrated in different mouse models with single peroxisomal enzymes deficiencies i.e. acyl CoA oxidase (Fan, et al. 1996a, b), MFP-2 (Huyghe, et al. 2006a), and dihydroxyacetonephosphate acyltransferase (DAPAT) (Rodemer, et al. 2003) knockout mice and mouse model with peroxisome biogenesis disturbance i.e Sertoli cell specific Pex 5 knockout mice (Huyghe et al. 2006a).

In ACOX1 deficient mice with defects in peroxisomal β -oxidation, testes were smaller compared to wild-type controls. A strong decrease in Leydig cell population, and reduction of spermatogenesis, but no changes in Sertoli cells were seen in the testis of ACOX $-/-$ mice (Fan et al. 1996b).

DAPAT is a key enzyme in plasmalogen biosynthesis. Studies revealed that male adult DAPAT knockout mice were infertile and showed an arrest in spermatogenesis with a complete absence of elongated spermatids and spermatozoa. Moreover, partial arrest and apoptosis of spermatocytes was detected. Proliferation of

interstitial Leydig cells in clusters was noted in knockout mice compared to controls (Rodemer et al. 2003).

MFP-2- knockout mice partly mimicked the human diseases. In contrast to human disease they did not show severe neurodevelopmental problems and the survival into adulthood permitted to observe a significance of this enzyme in several organs, including testis. Knocking out of MFP-2 leads to an inactivation of peroxisomal β -oxidation. It causes severe male infertility, exhibiting a strong accumulation of neutral lipids in Sertoli cells in the prepubertal stages. Studies show that germ cells gradually disappeared from the tubulus seminiferous, spermatogenesis was already severely impaired by the age of 5 weeks. At the age of 5 months, the testes demonstrated a complete fatty degeneration and obliteration of the seminiferous tubules till complete testicular atrophy. Biochemical analyses showed that peroxisomal β -oxidation substrates, such as VLCFA and pristanic acids were elevated in the testis. According these studies interstitial Leydig cells were normal until the age of 12 weeks, thereafter the number of Leydig cells was difficult to estimate due to disintegrating seminiferous epithelium. The basal and hCG-stimulated testosterone levels were not changed in knockout mice whereas quantitative PCR results of the Leydig cell-specific gene expression, 3β -HSD, P450 cholesterol side chain cleavage enzyme and P450c17 were lower with no statistical significance. Interestingly female MFP-2 knockouts exhibited only a reduced fertility (Huyghe et al. 2006a). In this study, also shortly Sertoli cell-specific *Pex5* knockout mice were described, where they show severe affected spermatogenesis, testicular atrophy and infertility similar to MFP-2 knockout mice.

Different mouse models with generalized inactivation of *Pex* genes involved in PTS1- and PTS2-dependant matrix protein import (*Pex2*-, *Pex5*- and *Pex13*-knockouts) have been developed to investigate the underlying pathogenesis of the most severe peroxisomal biogenesis disorder, Zellweger syndrome (Baes, et al. 1997; Faust and Hatten 1997; Liu et al. 1999). All knockout models demonstrated different organ impairments typical for ZS, including disturbed neocortex neuronal migration and development as well as hypotonia. Due to their early postnatal mortality, it was not possible to investigate the role of peroxisomes in adult tissues in *Pex*-knockout mice, losing their usefulness as models for postnatal disease pathogenesis. Particularly, these *Pex*-KO mice were not suitable to study testicular pathologies observed in

patients with Zellweger syndrome. Later, through advanced Cre-loxP technology was possible conditionally inactivate genes in specific cell type. Conditional knockout of *Pex13* and *Pex5* specifically in Sertoli cells were generated to study the functional importance of peroxisomes in these cells. Both knockouts showed severe impaired spermatogenesis, with lipid accumulation in Sertoli cells leading to arrest of spermatogenesis (Huyghe, et al. 2006b; Nenicu et al. 2007). In *Pex13*-KO mice the proliferation of Leydig cells with hormonal alterations was observed, which is considered to be a compensatory alteration in response to the loss of Sertoli cells. The morphological and biochemical phenotyping on the protein level of the Sertoli-cell-specific *Pex13*-knockout mouse has been largely done in our lab (Nenicu 2010).

To clarify the role of peroxisomal function in Leydig cells, we were able to establish a conditional knockdown of *Pex13* in Leydig cells. *Pex13* gene encodes a protein that is essential for PTS1 and PTS2 protein import into the peroxisome. Pex13p is the putative docking protein which interacts not only with the PTS1-receptor Pex5p, but also with PTS2-receptor Pex7p (Stein, et al. 2002). Deletion of *Pex13* leads to a loss of both PTS1 and PTS2 protein import. If the import of matrix proteins is defective, this results to a complete disruption of peroxisomal metabolism (Gould et al. 1996).

In the *Pex13*^{-/-} mouse, morphologically detectable peroxisomes were absent in the liver and peroxisomal ghosts in cultured fibroblast were detected with peroxisomal metabolic deficiency (Maxwell et al. 2003).

2. Materials and Methods

2.1. Materials

2.1.1. Laboratory Instruments

Table 1. All laboratory instruments used for experiments in this thesis are summarized with appropriate supplier.

Instruments	Manufacturer
AGFA Horizon Ultra Color Scanner	AGFA, Mortsels, Belgium
Biocell A10 water system	Milli Q-Millipore, Schwalbach, Germany
Biofuge Fresco	Heraeus, Hanau, Germany
Biofuge Pico	Heraeus, Hanau, Germany
Dish washing machine (G 78 83 CD)	Miele, Gütersloh, Germany
Gel-Doc 2000 gel documentation system	Bio-Rad, Heidelberg, Germany
Hera cell 240 incubators	Heraeus, Hanau, Germany
Hera safe, clean bench KS-12	Heraeus, Hanau, Germany
Ice machine, Scotsman AF-100	Scotsman Ice Systems, Vernon Hills, IL, USA
I Cycler PCR machine MiQ2 optical module	Bio-Rad, Heidelberg, Germany
Leica DMRD fluorescence microscope	Leica, Bensheim, Germany
Leica DC 480 camera	Leica, Bensheim, Germany
Leica TCS SP2 confocal laser scanning microscope	Leica, Nussloch, Germany
Microwave oven MB-392445	LG, Willich, Germany
Mini-Protean 3 cell gel chamber	Bio-Rad, Heidelberg, Germany
Multifuge 3 SR centrifuge	Heraeus, Hanau, Germany
pH meter E163649	IKA, Weilheim, Germany

Pipettes	Eppendorf, Hamburg, Germany
Pipette-type electroporator Microporator MP-100	PeQLab, Digital Bio Technology,
Power supply - 200, 300 and 3000 Xi	Bio-Rad, Heidelberg, Germany
Pressure/Vacuum Autoclave FVA/3	Fedegari, Albuzzano, Italy
Sorvall Evolution RC centrifuge	Kendro, NC, USA
Smartspec™ 3000 spectrophotometer	Bio-Rad, Heidelberg, Germany
Thermo plate HBT 130	Medax, Kiel, Germany
Thermo mixer HBT 130	HLC, BioTech, Bovenden, Germany
Trans-Blot SD semi dry transfer cell	Bio-Rad, Heidelberg, Germany
TRIO-thermoblock	Biometra, Göttingen, Germany
Ultra-balance LA120 S	Sartorius, Göttingen, Germany
Vortex M10	VWR International, Darmstadt, Germany
Water bath shaker GFL 1083	GFL, Burgwedel, Germany

2.1.2. General materials, culture media, buffers and solutions

Table 2. Details for culture media, buffers and solutions used in this thesis.

Cell Culture Media

MLTC-1 medium	RPML-1640 containing 25mM HEPES and supplemented with 10% fetal calf serum (FCS), 2Mm L-glutamine
MA-10 medium	Waymouth's complete medium MB752/1 supplemented with heat inactivated horse serum, penicillin G (100 units/ml), and streptomycin (100ug/ml)
Mouse primary Leydig cell culture	DMEM/F12 supplemented with 15% horse serum, 2.2µg/l sodium bicarbonate, 10mm HEPES, 1mg/ml BSA, 500ng/ml insulin, 100IU/ml penicillin,

medium (first day)	100µg/ml streptomycin
Mouse primary Leydig cell culture medium	DMEM/F12 supplemented with 2.2µg/l sodium bicarbonate, 10mm HEPES, 1mg/ml BSA, 500ng/ml insulin, 100IU/ml penicillin, 100µg/ml streptomycin
Testis enzymatic digestion medium for isolation of primary cells	DMEM/F12 supplemented with 10 mM HEPES (pH 7.4), collagenase A (1 mg/ml), hyaluronidase (1 mg/ml), 0,07% BSA
Stock Solution Percoll (90%)	Percoll +10 X Earle's balanced salt containing 0,7% BSA and 250 mM HEPES
Percoll gradient	Percoll solution (21, 26, 34, 40 and 60%) in isotonic Earle's salt buffer containing 0.07% BSA

Solutions for Molecular Biology and Western Blotting

Cell lysis buffer	50mM Tris, 400mM NaCl, 100mM EDTA, 0.5% SDS
Loading dye (10 ml)	16µl saturated aqueous bromophenol Blue, 80µl 500mM EDTA, pH 8.0, 720µl 37% formalin stock solution, 4ml 10X gel buffer fill up to 10 ml ddH ₂ O
1X Formaldehyde gel	100 ml 10x RNA transfer buffer 10x, formaldehyde, 880ml ddH ₂ O ₂
Agarose gel 2%, 120 ml	2,4g of agarose, 120 ml of 1x TAE, Stain G 4,5µl
10X RNA transfer buffer	200nM MOPS, 50 mM sodium acetate, 10 mM EDTA, pH 7.0
LB medium	0.17M sodium chloride + 1% Trypton + 0.5% Yeast extract, pH 7.0
LB-Agar	LB medium + 1g/50ml Agar + 100 µg/ml Ampicillin

Homogenization buffer	50mM Tris + 150mM NaCl+1% Triton-X-100 (pH 7.4), before using add 10% protease inhibitor
Resolving gel (12%) for SDS-PAGE gels	6.7 ml ddH ₂ O, 8ml of 30% acrylamide, 5 ml 1.5 M Tris buffer (pH 8.8), 200µl SDS (10%), 120 µl 10% APS, 10 µl TEMED
Stacking gel for SDS-PAGE gels	6.0 ml ddH ₂ O, 1300µl of 30% acrylamide, 2,5 ml 0.5 M Trisbuffer (pH 6.8), 100µl SDS (10%), 60 µl 10% APS, 10 µl TEMED
10 X Electrophoresis buffer	2 M glycine +250 mM Tris + 1% SDS
10X Sample Buffer	3.55 ml ddH ₂ O +1.25 ml 0.5 M Tris-HCl (pH 6.8), + 2.5 ml 50% glycerol +2 ml 10% SDS, a tip of 0.05% bromophenol blue. Prior to use add 50 µl β-Mercaptoethanol
20 X Transfer Buffer	NuPAGE transfer buffer (Invitrogen), Heidelberg Germany
10 X TBS	0.15 M NaCl, 0.1 M Tris, 0.05% Tween 20, pH 8.0
1 X TBST (washing buffer)	1ml (for 100ml) of 10X TBS + 0.05% Tween 20, pH 8.0
10% Blocking Buffer	10 g fat free milk powder in 100 ml 1X TBST C

Solutions for Immunofluorescence

Fixative solution	4% depolymerized paraformaldehyde, containing 2% sucrose in 1X PBS (150mM NaCl, 13.1 mM K ₂ HPO ₄ , 5mM K ₂ HPO ₄ , pH 7.4
Citrate buffer	Buffer A: 1 mM C ₆ H ₈ O ₇ H ₂ O; Buffer B: 50 mM C ₆ H ₅ Na ₃ O ₇ 2H ₂ O; Citrate buffer: 0.15 mM buffer A, 8.5 mM buffer B, pH 6.0

Glycine (1%)	1g Glycine in 100 ml of 1X PBS buffer
Glycine (1%) + Triton X-100 (0.3%)	1g Glycine in 100 ml of 1X PBS buffer + 0.3 ml Triton X-100
IF Blocking buffer	4% bovine serum albumin (BSA) in Tris-buffered saline containing 0.05% Tween 20 (TBST)
Buffer for diluting antibody	1% TBST (150 mM NaCl, 50 mM Tris, 0.05% Tween 20, pH 7.4)
Mowiol 488 solution	Overnight stirring of 16.7% Mowiol 488, 80 ml 1x PBS; add 40 ml glycerol stir again overnight; centrifuge at 15,000 g for 1h and store supernatant at -20°C
Anti-fading agent (2.5%)	2.5g N-propyl-gallate in 50 ml of 1 x PBS +50 ml of glycerol
Mounting medium	1 part anti-fading agent, 3 parts Mowiol 488 solution
PBS 10X	1.5 M NaCl, 131 mM K ₂ HPO ₄ , 50 mM KH ₂ PO ₄ , pH 7.4
TBS 10X	0.5 M Tris, 1.5 M NaCl, fill up to 1l ddH ₂ O, pH 7.4
Trypsin (0.01%)	0,01g trypsin in 100 ml PBS buffer

2.1.3. Chemicals

Table 3. List of reagents and media ingredients used in this study.

Reagent	Company name
Abiraterone Acetate	Cayman Chemical, Michigan, USA
Acrylamide	Roth, Karlsruhe, Germany
Agarose LE	Roche, Grenzach Wyhlen, Germany
Ampicillin	Difco, MI, USA
Bradford reagent	Sigma, Steinheim, Germany
Btomophenol blue	Riedel-de-Haen, Germany
BSA	Sigma, Steinheim, Germany
Catalase assay kit	Cayman Chemical, Germany
Collagenase Type I	Sigma, Steinheim, Germany
Deoxyribonuclease I, Amplification Grade	Invitrogen, Heidelberg, Germany
Diethyl ether	Sigma-Aldrich, Germany
Dihydroethidium	Molecular Probe, Oregon, USA
Dimethyl Sulfoxide (DMSO)	Sigma, Steinheim, Germany
Dithiotreitol (DTT)	Sigma, Steinheim, Germany
DMEM/F12	GIBCO, New York, USA
dNTPs	Promega GmbH, Madison, USA
Dulbecco's Modified Eagle's Medium/Ham's F-12	GIBCO, New York, USA
Dnase	Sigma, Steinheim, Germany
Earle's balanced salt solution 10x	Sigma, Steinheim, Germany

Earle's balanced salt solution	Sigma, Steinheim, Germany
Ethanol	Riedel-de-Haen, Germany
Ethylenediaminetetraacetic acid (EDTA)	Fluka, Biochemik, Steinhaeim, Germany
Fetal calf serum	PAA, Pasching, Austria
Formaline	Sigma, Steinheim, Germany
FuGENE HD Transfection Reagent	Promega, Madison, USA
Gentamycin	Sigma, Steinheim, Germany
GSH-Glo™ Glutathione Assay	Promega, Madison, USA
Glycine	Roth, Karlsruhe, Germany
Glycerol	Sigma, Steinheim, Germany
HEPES	Biochrom, Berlin, Germany
Horse serum	PAA, Pasching, Austria
Hyaluronidase	Sigma, Steinheim, Germany
22(R)-Hydroxycholesterol	Santa Cruz Biotech, Heidelberg, Germany
Immun-Star™ AP	Bio-Rad, Heidelberg, Germany
Insulin	Sigma, Steinheim, Germany
INTERFERin Transfection Reagent	Polyplus-transfection Inc, New York, USA
Interleukin-1 beta (IL-1 beta)	Biomol, Hamburg, Germany
Interleukin-6 (IL-6)	Biomol, Hamburg, Germany
Isopropanol	Sigma, Steinheim, Germany
Isotonic Earle's salt buffer	Sigma, Steinheim, Germany
Lipofectamin RNAiMAX	Invitrogen, Heidelberg, Germany
Mowiol 4-88	Polysciences, Eppelheim, Germany

N-Propyl-gallate	Sigma, Steinheim, Germany
Oil O Red	Fluka, Steinheim, Germany
OPTI-MEM	GIBCO, New York, USA
Paraffin (Paraplast)	Sigma, Steinheim, Germany
Paraformaldehyde (PFA)	Sigma-Aldrich, Germany
Penicillin/Streptomycin	Sigma, Steinheim, Germany
Percoll	Sigma, Steinheim, Germany
Potassium carbonate	Sigma-Aldrich, Germany
Protease inhibitor mix M	Serva, Heidelberg, Germany
Protease K	Sigma, Steinheim, Germany
PCR kit	QIAGEN, Hilden, Germany
PVDF membranes	Bio-Rad, Heidelberg, Germany
QIAGEN Plasmid midi kit	Qiagen, Hilden, Germany
RNeasy kit	QIAGEN, Hilden, Germany
RNAzol	Sigma-Aldrich, Germany
RPMI-1640	GIBCO, NY, USA
RT-PCR kit	Invitrogen, Karlsruhe, Germany
ScreenFect A Transfection Reagent	InCella GmbH, Mannheim, Germany
Sodium bicarbonate	Sigma, Steinheim, Germany
Sodium chloride (NaCl)	Sigma, Steinheim, Germany
Sodium dodecyl sulfate (SDS)	Sigma, Steinheim, Germany
Sucrose	Merck, Darmstadt, Germany
Taq polymerase	Promega GmbH, Madison, USA
Tetramethylenediamine (TEMED)	Roth, Karlsruhe, Germany

TransIT-LT1 Transfection Reagent	Mirus, Madison, USA
Trilostane	Sigma-Aldrich
Trishydroxymethylaminomethane (Tris)	Merck, Darmstadt, Germany
Tris-HCL	Sigma, Steinheim, Germany
Triton X-100	Sigma, Steinheim, Germany
Trypan blue	Sigma, Steinheim, Germany
Trypsin	Sigma, Steinheim, Germany
Tween 20	Merck, Darmstadt, Germany
Viafect TM Transfection reagent	Promega, Madison, USA
Viomer Blue, Green Transfection Reagent	Lipocalyx, Halle, Germany

2.1.4. Antibodies

Table 4. List of primary and secondary antibodies, which were used for immunofluorescence and for Western blots.

Host	Primary antibodies	Methods and dilution	Supplier
rabbit	Mouse Catalase polyclonal antibody	IF 1:2.000 WB 1: 40.000	Gift from Denis I Crane Biomol.Biomed. Sci., Griffith Univ., Nathan, Brisbane, Qld 4111, Australia
rabbit	Mouse Cytochrome P450 side chain cleavage enzyme (P450scc)	IF 1:1.000	Chemicon International CA,

	polyclonal antibody	1: 5.000	Temecula, 92590 CA, USA Cat. No. AB12 44
rabbit	Mouse Glutathione Reductase polyclonal antibody	WB 1:2.000	Biozol, Diagnostica Vertrieb GmbH; D-85380 Eching Cat. No: ab 16801
mouse	Mouse Glyceraldehyde-3-phosphate dehydrogenase (GAPDH) monoclonal antibody	WB 1:10.000	HyTest Ltd, 20520 Turku, Finland Cat. No: 5G4
mouse	Mouse Oxidative Phosphorylation Complex III (OxPhos III) polyclonal antibody	IF 1:2.000 WB 1:500	Molecular Probes/Invitrogen, Carlsbad, CA 92008, USA Cat. No: A 11143
rabbit	Mouse Peroxin13 (PEX13) polyclonal antibody	IF 1:1.000 WB 1: 6.000	Gift from Denis I. Crane (address see above)
rabbit	Mouse Peroxin14 (PEX14) polyclonal antibody	IF 1: 2.000 WB 1: 30.000	Gift from Denis I. Crane
rabbit	Mouse Steroidogenic acute regulatory protein (StAR), monoclonal antibody	IF 1:100 WB 1:1.000	Cell Signaling Technology Cat. No: 8449P
rabbit	Mouse Steroidogenic Acute Regulatory protein (StAR) polyclonal antibody	IF 1:100 WB 1:1.000	Abcam, Cakmbridge, CB4 0FW, UK, Cat. No. (ab3343)

rabbit	Mouse Superoxide dismutase 1 (SOD1) (Cu/Zn SOD) polyclonal antibody	WB 1: 1.500	Fitzgerald Industries International, Inc. Concord, USA Cat. No: RDI-RTSODabR
rabbit	Mouse Superoxide dismutase 2 (SOD2) (Mn-SOD) polyclonal antibody	WB 1:4.000	RDI, Research Diagnostics, Inc, Flanders, NJ 07836
rabbit	Mouse Tubulin (alpha) polyclonal antibody	WB 1:4.000	SIGMA, Saint Louis, Missouri 63103 USA, Cat. No: T 3526

Host	Secondary antibodies	Methods and dilution	Supplier
donkey	Anti-Mouse IgG TexasRed, Kit	IF 1:300	VECTOR, Burlingame, CA, USA, Cat. No: Ti-2000
donkey	Anti-Rabbit IgG AlexaFluor488	IF 1:300	Molecular Probes/Invitrogen, Carlsbad, CA, USA, Cat. No: A21206
goat	Anti-Rabbit IgG alkaline	WB 1:20.000	Molecular Probes/Invitrogen, Carlsbad, CA, USA,

	phosphatase conjugate		Cat. No: A0545
goat	Anti-Mouse IgG alkaline phosphatase conjugate	WB 1:20.000	Molecular Probes/Invitrogen, Carlsbad, CA, USA, Cat. No: A3562
donkey	Anti-Rabbit IgG horseradish peroxidase conjugate	WB 1:10.000	Jackson Immuno Research Cat. No: 715035152
donkey	Anti-Mouse IgG horseradish peroxidase conjugate	WB 1:10.000	Jackson Immuno Research Cat. No: 715035150

Counterstaining of nuclei		Supplier
Hoechst 1:500		
TOTO-3 nucleic acid staining 1:1,000	IF 1:1.000	Molecular Probes/Invitrogen, Carlsbad, CA, USA

2.1.5. Primers

Table 5. List of primers

Gene	Accession no.	Forward/reverse primers	length	Ann temp in °C
28 S ribosomal RNA (28S rna)	NR_003279	For CCTTCGATGTCGGCTCTTCCTAT Rev GGCGTTCAGTCATAATCCCACAG	254	65
Acyl-Coenzyme A oxidase 1, palmitoyl (Acox1)	NM_015729	For CTGAACAAGACAGAGGTCCACGAA Rev TGTAAGGGCCACACACTCACATCT	565	60
Acyl-Coenzyme A oxidase 2, branched chain (Acox2)	NM_053115	For CTCTTGACGTATGAGGGTGAGAA Rev CTGAGTATTGGCTGGGGACTTCTG	688	58
Acyl-Coenzyme A oxidase 3, pristanoyl (Acox3)	NM_030721	For GCCAAAGCTGATGGTGAGCTCTAT Rev AGGGGTGGCATCTATGTCTTTCAG	813	55
ATP-binding cassette, subfamily D, member1 (ABCD1) or (ALDP)	NM_007435	For GAGGGAGGTTGGGAGGCAGT Rev GGTGGGAGCTGGGGATAAGG	440	63
ATP-binding cassette, subfamily D, member 2 (ABCD2) or (ALDPR)	AK134763	For TGCAAATTCTGGGGAAGA Rev TGACATCAGTCCTCCTGGTG	405	58
ATP-binding cassette, subfamily D, member 3 (ABCD3) or (PMP70)	NM_008991	For CTGGGCGTGAAATGACTAGATTGG Rev GGGATAAGGTCCCCAGTCAAGTG	523	65
ATP-binding cassette, subfamily D, member 4 (ABCD4) or (PMP70R)	BC050102	For TGAAAGGCTCAGTGCAGATG Rev GGCTGCAGGTAGAAGAGACG	304	62
Catalase (Cat)	NM_009804	For ATGGTCTGGGACTTCTGGAGTCTTC Rev GTTTCCTCTCCTCCTCGTTCAACAC	312	65
Cytochrome P450, family 11, subfamily a polypeptide 1, (P450 scc) or (Cyp11a1)	NM_019779	For GCTGGAAGGTGTAGCTCAGG Rev TTCTTGAAGGGCAGCTTGTT	432	58

Cytochrome P450, family 17, subfamily a, polypeptide 1, (P450c17) or (Cyp17a1)	NM_007809	For ACCAGCCAGATCGGTTTATG Rev AGGGCAGCTGTTTGTCATCT	204	58
Cytochrome P450, family 19, subfamily a, polypeptide 1 (P450 arom) or (Cyp19a1)	NM_007810	For GACACATCATGCTGGACACC Rev CAAAGCCAAAAGGCTGAAAG	722	58
Enoyl-coenzyme A hydratase/3- hydroxyacyl coenzyme dehydrogenase (multifunctional protein 1) (Ehhadh) or (MFP1)	NM_023737	For ATGGCCAGATTTTCAGGAATG Rev TGCCACTTTTGTTGATTTGC	211	56
Follicle stimulating hormone receptor (Fshr)	NM_013523	For CCAGCCTTACCTACCCCAGT Rev CTGTGGTGTTCACAGTGATG	345	58
Glutathione peroxidase1 (Gpx1)	BC086649	For GGGACTACACCGAGATGAACGA Rev ACCATTCACTTCGCACTTCTCA	430	55
Glutathione S- transferase 1 (Gsta1)	BC132572	For GCAGACCAGAGCCATTCTCAACTAC Rev CTGCCAGGCTGTAGGAACTTCTTC	480	55
β (3b-HSD III) or (Hsd3b3)	NM_001012 306	For TCAATGTGAAAGGTACCC Rev ATCATAGCTTTGGTGAGG	499	55
17b-Hydroxysteroid dehydrogenase 4 (multifunctional protein 2) (MFP2) or (Hsd17b4)	NM_008292	For GAGCAGGATGGATTGGAAAA Rev TGA CTGGTACGGTTTGGTGA	223	66
3-Hydroxy-3- methylglutaryl-				

Coenzyme A reductase (Hmgcr) or (HMG-CoAR)	NM_008255	For CCCACGAGCAAACATTGTC Rev TGAGCCCCACACTGATCAACC	741	55
3-Hydroxy-3-methylglutaryl-Coenzyme A synthase 1 (Hmgcs1) or (MGC36662)	NM_145944	For CTTTGCCTGACTGTGGTTCA Rev GACCACAGGGTACTCGGAGA	447	62,7
Isopentenyl-diphosphate isomerase (Idi1) or (MGC8139)	NM_145360	For GGGCTGACACCAAGAAAAAC Rev ACTGGCTGCCTTCTTCAAAA	470	62,7
Luteinizing hormone/choriogonadotropin receptor (LH-R)	NM_013582	For ATGGATCCCTCTCACCTATCTCCCTGT RevAGTCTAGATCTTTCTTCGGCAAATT CCTG	702	58
Peroxiredoxin 1 (Prdx1) or (PAG)	NM_011034	For TCTCTTTCAGGGGCCTTTTT Rev CCAAACACAGCTCAGACCA	396	35
Peroxiredoxin 5 (Prdx5) or (Pmp20)	NM_012021	For GAAAGAAGCAGGTTGGGAGTGT Rev CCCAGGGACTCCAAACAAAA	182	35
Peroxisome biogenesis factor 13 (Pex13)	NM_023651	ForGACCACGTAGTTGCAAGAGCAGAGT RevCTGAGGCAGCTTGTGTGTTCTACTG	717	65
Peroxisome biogenesis factor 14 (Pex14)	NM_019781	For CACCTCACTCCGCAGCCATA RevCTGACAGGGGAGTGCTCACTGCT	298	56
Steroidogenic acute regulatory protein (StAR) or (Star)	NM_011485	For GTTCCTCGCTACGTTCAAGC Rev TTCCTTCTTCCAGCCTTCCT	292	58
Sterol-carrier protein X (ScpX) or (SCPX)	M91458	For GGCCTTCTTTCAAGGGAAAC Rev ACCACAGCCCAATTAGCAAC	230	56
3-Ketoacyl-CoA thiolase (Thiolase A) or (pTH1)	AY273811	For TCAGGTGAGTGATGGAGCAG Rev CACACAGTAGACGGCCTGAC	241	60

2.2. Cell Culture

2.2.1 Mouse Leydig Tumor cells (MLTC-1 and MA-10 cells)

MA-10 and MLTC-1 cells which are by far the most widely used and the best characterized tumor cell lines of mouse Leydig cells (Ascoli 1981a; Rebois 1982) were used in this study. They were established from the M548O transplantable Leydig cell tumor carried in C57BL/6 mouse. Two variants of the M5480 tumor were later identified: M5480A (MA-10) and M5480P (MLTC-1).

2.2.1.1. Culture of MLTC-1 cells

The MLTC-1 cell line was bought from the American Type Culture Collection (ATCC), ATCC number CRL-2065 TM. The base medium for this cell line is ATCC-formulated RPMI-1640 Medium, Catalog No. 30-2001 (see Table 2).

MLTC-1 cells were cultured in RPMI-1640 containing 25mM HEPES and supplemented with 10% fetal calf serum (FCS), without antibiotic, pH 7.3 at 37°C under a humidified atmosphere of 95% air and 5% CO₂. Cells were cultured at a density 1×10^6 in 10cm Petri dishes. At 60% confluence, the cells were disaggregated with trypsin-EDTA (0.05%) for 3 min. and dissolved in growth medium. During splitting the viability of the cells was determined with 0.4% trypan blue (w/v) exclusion. Cells were sub-cultured at 1.5×10^5 in per well 6 well plates, 7.5×10^4 in per well 12 well plates, 3.8×10^4 in per well 24 well plates for different experiments and grown for 3 days prior to their use in experiments.

2.2.1.2. Culture of MA-10 cells

MA-10 cells were a gift from Prof. Dr. Ralf Middendorff (JLU-Giessen), a colleague in our institute. MA-10 cells were cultured in RPMI 1640 containing 10% of heat inactivated horse serum, penicillin G (100 units/ml), and streptomycin (100ug/ml). Cells were incubated at 37°C in 5% CO₂ in a humidified incubator. Cells were sub-cultured at a density of 1×10^6 in 10cm Petri dishes, 1.5×10^5 in per well 6 well plates, 7.5×10^4 in 12 well plate for different experiments and grown for 3 days prior to their use in experiments.

2.2.2. Isolation and primary culture of mouse Leydig cells

Primary mouse Leydig cells were isolated according to the method of Schumacher and colleges (Schumacher, et al. 1978) with some modifications using a procedure involving enzymatic dissociation and Percoll-gradient centrifugation. For each experiment 6 -12 adult mice (3-4 months of age) were sacrificed by cervical dislocation. Testes were removed aseptically under sterile hood and collected into chilled Dulbecco's Modified Eagle Medium/ Ham's F-12 (DMEM/F12; 1:1, v/v) with gentamycin. All following steps were performed under sterile conditions. Testes were transferred in a new sterile medium and the tunica albuginea was carefully removed from the testes. De-capsulated testes were put into a 50ml tube containing 10ml (for 2 testes 2 ml medium) medium DMEM/F12 with collagenase 1.0 mg/ml, 10 mM HEPES, 0.07% BSA, hyaluronidase 1.0 mg/ml, pH 7.4. The incubation was carried out for 15 min at 34°C in a water bath shaker. After collagenase digestion, tubules and the suspension of cells were left for sedimentation on ice for 2-3 min. The suspension obtained was filtered through 70µm Nylon gauze (BD Falcon) and the crude interstitial cells were collected by centrifugation at 300 x g for 10 min. Cells were washed twice with DMEM/F12 by centrifuging at 200 x g for 8 min to remove the collagenase. Finally, collagenase-dispersed cells were re-suspended in 6ml (for 6 mice) of Leydig cell medium (DMEM/F12 supplemented with 10mM HEPES (pH 7.4), 1mg/ml BSA, 500ng/ml insulin, 100 units/ml penicillin, 100µg/ml streptomycin). Three ml was loaded (3ml for each Percoll tube) on top of a discontinuous Percoll gradient and centrifuged for 30 min at 800 x g. In order to prepare a gradient, the osmolality of Percoll (undiluted) had to be first adjusted with saline or cell culture medium to make the Percoll isotonic with physiological salt solutions. Adding 9 parts (v/v) of Percoll to 1 part (v/v) 10 x concentrated cell culture medium was the way of preparing a Stock Isotonic Percoll (SIP) solution. Nine parts Percoll were mixed with 1 part 10 x Earle's balanced salt solution containing 0.7% serum albumin and 250mM HEPES, pH 7.4 to prepare a 90% stock solution Percoll. Discontinuous Percoll gradient (25, 35, 50 and 60%) were prepared by diluting the 90% Percoll stock solution with isotonic Earle's salt buffer containing 0.07% BSA. Following centrifugation, 4 visible bands were detected and the highly purified Leydig cells were found in the third band. Leydig cells formed a distinct band close to the interphase between 50 % and 60% of Percoll. This band was isolated and added to

3 volumes of serum free medium DMEM/F12 with 10mm HEPES and the isolated Leydig cells were washed twice by centrifuging at 100 x g for 10 min. The purified Leydig cells were plated on day 1 in DMEM/F12 medium containing 15% horse serum and supplemented with 10mm HEPES, 1mg/ml BSA, 500ng/ml insulin, 100IU/ml penicillin, 100µg/ml streptomycin at a density of 1×10^5 cells/cm² in 24 well plate and incubated in a humidified atmosphere of 95% air-5%CO₂ at 34°C. On the following day cells were changed to serum free but supplemented with 10mm HEPES, 1mg/ml BSA, 500ng/ml insulin, 100IU/ml penicillin, 100µg/ml streptomycin, DMEM/F12 medium and they were maintained under this culture condition for additional 3 days with daily medium change. Cells were treated on day 4 with 100ng/ml hCG for 6h. After treatment, the medium from each well was removed and stored at -20°C for assay of progesterone, testosterone by radioimmunoassay and by ELISA. The percentage and purity of Leydig cells in the identified fraction was determined by staining with an antibody against the mitochondrial P450scc, as a further Leydig cell marker. Primary mouse Leydig cells were stained immediately after isolation according to cyto-spin protocol (Cytospin Centrifuge, Hettich Lab Technology). 200ul of each cell suspension (with a concentration of approximately 5×10^5 cells/ml) was added to a slide chamber and spined at 800 rpm for 5 minutes. Slides were carefully removed from cytocentrifuge and allowed to air dry prior to staining. Additionally, cells were plated in 24 well plates with collagen coated coverslips. Following 4 days of culture cells were stained with P450scc. The percentage of Leydig cells in this fraction varied between 80 and 90% of all nucleated cells.

2.3. Transformation of E.coli and preparation of plasmid DNA

The tube containing the competent E.coli cells was removed from -80°C storage and bacteria were thawed on ice. One hundred ng plasmid DNA was pipetted into a 50µl competent cells and mixed gently tapping the side of the tubes. Immediately the tube was incubated on ice for 20 min, which allows bacteria to take up plasmid DNA through the cell membrane. The cells in the tube were subjected to a heat shock for exactly 90 seconds at 42°C and the tube was returned quickly to the ice for 2 minutes in order to stop the heat shock. 200µl of LB medium without antibiotics was added to the tube and the cells were incubated for 30 min at 37°C in a water bath.

Using a sterile glass spreader 50-200µl of transformation mixture was spread all over the plates (Ampicillin-LB-Agar plates, pre-warmed at RT). After the soaking of the fluid into the agar, plates were inverted and incubated overnight, at 37°C.

2.3.1. Endotoxin-free, midi preparation of plasmid DNA

The next morning, a single colony was picked from the agar plate and inoculated into 3-5ml of LB medium. Culture was grown overnight at 37°C and 300 rpm for 8-12h. Thereafter 700 µl of culture bacteria were mixed with 300 µl of 50% glycerol and stored at -80°C as frozen stock. The plasmid DNA purification was done with NucleoBond columns according to the protocol of Macherey-Nagel. 1 ml of the bacterial suspension was centrifuged at 6,000 x g for 10min at 4°C and the supernatant was discarded completely. The pellet was re-suspended in 8ml of Resuspension Buffer RES-EF and RNase A by pipetting the cells up and down. Eight ml of Lysis Buffer LYS-EF was added to the suspension and was mixed gently by inverting the tube 5 times after which the mixture was incubated at RT for 5 min. NucleoBond^R Xtra Column together with the inserted column filter was equilibrated with 15ml of Equilibration Buffer (EQU-EF). Eight ml of Neutralization Buffer NEU-EF was added to the suspension and was mixed immediately gently by inverting the tube 15 times after which was incubated on ice for 5 min. The lysate was loaded onto the column and was allowed the column to empty by gravity flow. Thereafter, the column filter was washed with the 5ml Equilibration Buffer EQU. NucleoBond^R Xtra Column Filter was discarded by turning the column upside down and the NucleoBond^R Xtra Column was washed with 8ml of Wash Buffer. Plasmid DNA was eluted with 5ml of Elution Buffer ELU and the eluate was collected in a 50ml centrifuge tube. 3.5 ml of room-temperature isopropanol was added to precipitate the eluted plasmid DNA and was centrifuged at 15,000 x g for 30 min at 4°C. The supernatant was removed carefully and discarded whereas the pellet was washed with 2ml of room-temperature 70% ethanol and centrifuged at 15,000 x g for 5min at RT. The ethanol was removed carefully with a pipette tip and the pellet was left to air dry at RT for 5-10 min. The plasmid DNA pellet was dissolved in an appropriate volume of buffer TE or sterile H₂O.

2.4. Transfection

2.4.1. Transfection via microporation with *Pex13* shRNA in MLTC-1 cells

For the analysis of the effects of peroxisomal deficiency in Leydig cells, we used specific shRNA plasmid to knock down *Pex13* in MLTC-1 cells via microporation. Microporation is a unique electroporation technology developed by NanoEnTek. It uses a pipette Tip as an electroporation space. Through microporation the transfection efficiency and cell survival rate are high. In our laboratory, we used the Pipette-type electroporator Microporator MP-100 (peQLab, Biotechnologie GmbH, Digital Bio).

We established a transfected *Pex13* shRNA knockdown model using microporation to study the consequences of peroxisomal deficiency in MLTC1 cells. shRNA plasmid enable efficient gene knockdown using short-hairpin RNA

. shRNA plasmids were purchased from Qiagen (Catalog no.: 336311 KM37506G), where 5 plasmids were provided for each gene: four *Pex13* gene-specific shRNA plasmids and one negative control plasmid. Each plasmid carries an shRNA under the control U1 promoter and a green fluorescent protein (GFP) reporter gene to detect transfected cells by fluorescence microscopy.

Table 6. *Pex13* specific shRNA plasmids (1-4) and NC (scr-shRNA).

Clone ID	Insert Sequence
1 (<i>Pex13</i> shRNA)	agacctgcttacagttcattt
2 (<i>Pex13</i> shRNA)	acaggacttatacctgcaaatt
3 (<i>Pex13</i> shRNA)	tgccgtgtctgatgaagaaatt
4 (<i>Pex13</i> shRNA)	tgatttgggccctactttatt
NC	ggaatctcattcgatgcatac

The above mentioned *Pex13* specific shRNA plasmids were used to transfect MLTC-1 cells and in our hands clone 3 with insert sequence (tgccgtgtctgatgaagaaatt) gave the most efficient knockdown (Table 6). One scrambled shRNA (scr-shRNA) plasmid

vector was used as a negative control. The scr-shRNA has no significant sequence homology to mouse, rat or human gene sequences.

Materials: Cell, DNA, culture medium (+FBS without antibiotics), 24 well plate, 1.5 ml tube Kit components: Gold-Tip, Microporation Tube (MPT-100) BufferR (resuspension buffer), Buffer E (electrolytic buffer).

Transfection was done according to the manufacturer's manual instruction. Briefly, MLTC-1 cells were cultured at density 1×10^6 in 10cm Petri dish in RPMI-1640 containing 25mM HEPES and supplemented with 10% fetal calf serum (FCS), pH 7.3 at 37°C under a humidified atmosphere of 95% air and 5% CO₂. At 60% confluence, the cells were rinsed using 1 X PBS and disaggregated with trypsin-EDTA (0.05%) for 3 min. Trypsin was neutralized by adding medium containing serum and cells were dissolved in growth medium. They were centrifuge at 1000 rpm for 3 min at room temperature. Media was aspirated and pellets were rinsed using culture media (+FBS, antibiotic). One aliquot of cell culture was taken and the cells were counted to determine the cell number and calculate the volume to be used for seeding. Cells were centrifuged at 1000 rpm for 2 min at room temperature. 500µl of culture medium containing serum (with supplements, but without antibiotics) was added in each well of 24 well plates and pre-incubate plates at 37°C in 5% CO₂ in a humidified incubator. To avoid cell from damage, it was necessary to transfer the cells directly into pre-warmed medium (37°C). Cell pellets were re-suspended the in R-buffer. 1×10^5 MLTC-cells per 10µl of R-buffer was used for transfection. Re-suspended cells were transferred to a 1.5 ml tube. Plasmid DNA was added into re-suspended cells. The concentration of DNA is dependent on the cell type. A DNA amount of 0,5µg/10µl was used for the beginning. For MLTC-1 cells the optimal DNA amount for transfection was 1µg/10µl concentration. The quality of plasmid DNA strongly influences the results of transfection experiments. Therefore, care has been taken to isolate high quality plasmid and to adjust to the optimal concentrations to obtain the highest transfection efficiency. Three ml Buffer E was added in Microporation Tube (MPT-100). The cells and DNA was mixed by pipetting. The microporator pipette was inserted into the pipette station. The cells were immediately plated after microporation into the media in the culture well plate. Desired pulse conditions for microporation were set on the microporator MP-100 (peQLab).

To obtain the highest transfection efficiency via microporation for MLTC-1 cells several different conditions were tested (Table 7). Optimal conditions were found for MLTC-1 cells with 90% transfection efficiency as controlled via GFP fluorescence by using condition 3, which was applied thereafter for all shRNA plasmid experiments (1350 Pulse Voltage, 20 Pulse Width, 2 Pulse Number). Following 72 h of transfection, cells were used for different experiments. Treatment with hCG to stimulate the steroid production was done after 72h of transfection.

Table 7. Microporation parameters for transfection with shRNA plasmids in MLTC-1 cells.

Conditions	1	2	3	4	5	6
Pulse Voltage	1050	1275	1350	1400	1400	1700
Pulse Width	30	40	20	10	20	20
Pulse Number	2	1	2	1	2	1
Transfection efficiency %	5%	25%	85%	10%	70%	20%

2.4.2. Transfection of MLTC-1 cells via lipofection using shRNA

Since the widely used lipofection method of transfection is more cost-effective, we tried to compare the transfection efficiency of a few transfection reagents available in the market with microporation. Transfections of MLTC-1 cells via lipofection using shRNA have been done according to the protocols given by the manufacturers with the following compounds tested: 1. ViaFect (ViaFectTM Transfection Protocol), 2. Attractene (Attractene-QIAGEN Supplementary Protocol), 3. InCella (Davidson), 4. Fugene (Corporation), 5. TransIT®-LT1 (TransIT_LT1_Transfection Protocol).

After several experiments a relatively high transfection rate of 70% could be obtained with ViaFectTM (results not shown). However, microporation was chosen to be the

desired transfection procedure for this study owing to the higher transfection efficiency and reproducibility

Table 8. Conditions for lipofection of MLTC-1 cells with shRNA using different transfection reagents.

Compounds	Viafect TM	Attractene	InCella	FuGENEHd	TransIT®-LT1
Transfection Reagent	3µl	1.5µl	2µl	1.5µl	1,5µl
shRNA (µg)	1µg	1µg	1µg	1µg	2.5µg
Cell number per well	30.000 cells	30.000 cells	30.000 cells	30.000 cells	30.000 cells
Final volume per well	500 µl	500µl	500µl	500µl	500µl
Transfection efficiency	70%	50%	30%	10%	5%

2.4.3. *Pex13* or *Mfp2* (*Hsd17b4*) silencing by RNA interference technology (RNAi) in MLTC-1 and in primary Leydig cells

As an alternative approach to microporation and shRNA mediated knockdown, MLTC-1 cells and primary Leydig cells were also transfected by a small interfering RNA approach for the mouse *Pex13* gene or *Mfp2* (*Hsd17b4*) gene. The mouse *Pex13* siRNA (siRNA ID# 176738) or *Mfp2* siRNA (siRNA ID#: s67849) was purchased from Ambion (Austin,TX). Sequence: Length: 21

Pex13: Sense: 5' GCUAUAGCCCUUAUAGUUAAdTdT
Antisense: 5' UAACUAUAAGGGCUAUAGCdTdT 3'

Mfp2: Sense: CAUUAGUCAUUGUUAACGAtt
 Antisense: UCGUUAACAAUGACUAAUGct

One scrambled siRNA (scr-siRNA) was used as a negative control. This control siRNA did not possess any significant sequence homology to mouse, rat or human gene sequences.

Different transfection reagents were tried according to the protocols given by manufacturers 1. InCella (Davidson), 2. Viromer Green (Weber), 3. INTERFERin (INTERFERin Transfection Protocol), 4. Lipofectamin RNAiMAX (Technologies). Different concentrations of siRNA (15, 30 or 40 nM) and different volumes of transfection reagents were used in order to obtain high transfection efficiency. Conditions used for transfection of MLTC-1 cells are presented in table 9.

Table 9. Conditions for transfection of MLTC-1 cells with siRNA using different transfection reagents in 24 well plate.

Compound	InCella Screenfect	INTERFERin	Viromer green	Viromer blue	RNAimax
Transfection Reagent used amount of	1.7µl	1.7µl	1.7µl	2µl	1,5µl
siRNA (nM)	40nM	40nM	40nM	40nM	40nM
Cell number per well	30.000 cells	30.000 cells	30.000 cells	30.000 cells	30.000 cells
Final volume per well	500 µl	500µl	500µl	500µl	500µl
Transfection efficiency	65%	50%	20%	10%	10%

The best transfection efficiency with low toxicity and reproducibility was achieved using InCella (Davidson) (Table 9).

Similarly, primary Leydig cells were also transfected using InCella ScreenFect. Briefly, purified primary Leydig cells were plated at a density of 2×10^5 in 24 well plates and cultured for 24h in the aforementioned medium. The following day, Leydig cells were transfected with *Pex13* or *Mfp2* siRNA (40nM) and control scr-siRNA (40 nM) using the ScreenFect transfection reagent (InCella). Transfection complex (ScreenFect A and siRNA) were first mixed with an appropriate volume of serum free DMEM/F12 medium with the aforementioned supplements and added to adherent cells. The medium was replaced with fresh medium after 24 h. After 48 h of transfection, cells transfected were treated with hCG (100ng/ml) for 6h. At the end of the experiment, the medium from each well was collected and stored at -80°C for assay of hormones and the cells were processed for total protein isolation. The optimal conditions for the amount of transfection reagent (ScreenFect A), the dilution of the siRNA and the number of cells are presented in table 10.

Table 10. Optimal conditions for the transfection of primary Leydig cells using *Pex13*- and *Mfp2*- siRNA.

ScreenFect A	2µl in 40µl of supplied Dilution Buffer
<i>Pex13</i> -, <i>Mfp2</i> or scr-siRNA	40nM in 40µl of supplied Dilution Buffer
Combined complex volume	80µl
Cell number per well	$1.5-2 \times 10^5$
Cells/media	420µl
Final volume	500µl

2.5. RNA expression analysis by semi-quantitative RT-PCR

RNA isolation

Total RNA isolation from cells was performed using the RNeasy kit (cat. No 74101 Qiagen, Hilden, Germany) as well as RNAzol RT (RNAzol RT, Sigma-Aldrich Co).

Homogenization of cells in RLT buffer was carried out through a QIAshredder spin column placed in a 2-ml collection tube, and centrifuged for 2 min at 15.000g speed. RNA extraction was performed with the RNeasy Mini Kit from Qiagen according to the manufacturer's protocol.

Homogenization of cells in RNAzol RT (1ml per cm²) was done directly on the culture dish. To form a homogenous lysate, the cell lysate was passed several times through a pipette. RNA extraction was performed according to the manufacturer's protocol (RNAzol RT (Sigma-Aldrich Co) (Catalog no.: FRT4533).

Dnase I digestion

Prior to reverse transcription, a DNase I digestion step was carried out for RNA samples to remove residual genomic DNA. The DNase digestion mixture was prepared and incubated for 15 min at RT 25°C after which the DNase was inactivated by the addition of 1µl of 25Mm EDTA to the mixture and heated for 10 min at 65°C (Table 11).

Table 11. Conditions for Dnase I digestion.

RNA sample	1µg
10X DNase I reaction buffer	1µl
DNase I, Amp Grade, 1U/ul	1µl
DEPC-treated water	to 10µl

First-strand cDNA was synthesized from total RNA (0.5-1µg) with oligo (dT) 12-18 primers using the Superscript II reverse transcriptase (#18064-022, Invitrogen, Germany).

The polymerase chain reaction (PCR) was set up in a final volume of 25 μ l using 1 μ l cDNA. PCR conditions and all primers were optimized with gradient PCRs on a BioRad iCycler. 28S rRNA was used as a control to normalize the levels of cDNA (Table 12).

Table 12. Protocol for the polymerase chain reaction (PCR).

Template	1.0 μ l
10x PCR buffer	2.5 μ l
10mM dNTPs	0.2 μ l
Forward primer	1.0 μ l
Reverse primer	1.0 μ l
Taq DNA polymerase	0.2 μ l
Sterile H ₂ O	19.1 μ l
Total volume	25.0 μ l

2.6. Western Blot analysis

Isolation of the whole cell lysates

Cells were washed twice with 1 X PBS and 50-150 μ l of cell lysis buffer was added to each well of 24 well plates. Using a rubber policeman, cells were scraped thoroughly and placed to Eppendorff tubes. Tubes were transferred on ice for 30 min and were vortexed at intervals every 10 min. Afterwards tubes were centrifuged for 10 min at 1,000 x g at 4°C, thereafter the supernatants were collected and stored at -20°C.

Preparation of Western Blots

The protein samples (15 μ g-30 μ g) were separated on 12% SDS polyacrylamide gels and transferred onto polyvinylidene fluoride (PVDF) membranes (Catalog no.: 162-0218, BioRad, Munich, Germany) by electrotransfer with a BioRad blotter. To block nonspecific protein-binding sites, membranes were incubated with Tris-buffered saline (TBS) containing 10% nonfat milk powder and 0.05% Tween-20 for 1h at RT.

The membranes were incubated with the primary antibody for 1 h, at RT or overnight at 4°C. Thereafter, the blots were washed 3 times for 10 min with TBST buffer and then incubated with alkaline phosphatase-conjugated secondary antibodies for 1h at RT. The concentrations of the antibodies used for WB are given in Table 4. Alkaline phosphatase activity was detected using Immun-StarTMAP (No.: 170-5018) substrate from BioRad (Munich, Germany). Blots were exposed to Kodak Biomax MR films and the bands on films were quantified with ImageJ. All Western Blot analyses were done and analyzed with different membranes at least three times.

2.7. Immunofluorescence for MLTC-1 and mouse primary Leydig cells

Cells were plated on coverslips and allowed to grow for 3-4 days. The cells were washed with warm (37°C) 1x PBS (pH 7.4) and fixed with 4% paraformaldehyde (PFA) +2% saccharose in PBS for 20 min at RT. Then the coverslips containing the cells were washed three times with 1x PBS for 10 min. Thereafter, the cells were incubated in PBS containing 1% glycine for 10 min at RT and additionally with PBS containing 1% glycine and 0.1% Triton for 25 min at RT. Cells were incubated for 45 min in PBS containing 1% BSA and 0.05% Tween to block nonspecific protein binding sites. After blocking, cells were incubated with primary antibodies in a moist chamber overnight at 4°C. The next day cells were washed three times with 1X PBS for 5 min and incubated with secondary antibodies for 1h at RT. Thereafter, cells were washed once with 1X PBS and nuclei were counter-stained with Hoechst 22358 and TOTO-3 iodide (Molecular Probes/ Invitrogen, Carlsbad, USA) for 10 min at RT. Samples were inspected with a LEICA fluorescence microscope or with a LEICA TCS SP2 confocal laser scanning microscopy (CLSM).

2.8. ROS detection by staining with dihydroethidium (DHE)

Dihydroethidium, (DHE), also called hydroethidine, which is a cell permeable reagent was used to evaluate reactive oxygen species (ROS) production. DHE upon reaction with superoxide anions forms the red fluorescent product which intercalates with DNA. MLTC-1 cells were treated with dihydroethidium (D-23107, Invitrogen) after 72 h of transfection. 5µmol of DHE was added to 1 ml (24 well plate) of normal MLTC-1

medium and incubated at 37°C for 30 min. Thereafter, cells were washed three times for 5 min with 1 X PBS and incubated with 4% PFA for 20 min at RT for fixation. The cells were washed three times for 10 min with 1X PBS and nuclei were counter-stained with Hoechst 22358 for 10 min at RT. The samples were inspected with a LEICA fluorescence microscope or with a LEICA TCS SP2 confocal laser scanning microscopy (CLSM).

2.9. Detection of glutathione using GSH-Glo™ Glutathione Assay

The GSH-Glo™ Glutathione Assay was used to detect and quantify the reduced glutathione (GSH) level in cells. Reduced glutathione is an important antioxidant, the level of which in the cells is an indicator of oxidative stress. Reduced form of glutathione is able to donate an electron donor to other reactive oxygen species. Thereby, GSH is changed to the oxidized form becoming itself reactive, oxidized form, which readily reacts with another reactive glutathione to form the glutathione disulfide (GSSG).

The GSH-Glo™ Glutathione Assay is a luminescence-based assay, which was done according to the manufacturer's protocol (GSH-Glo Glutathione Assay, Promega). The signal is a result of two chemical reactions and based on the conversion of a luciferin derivative into luciferin in the presence of GSH, which is catalyzed by a glutathione S-transferase (GST) enzyme supplied in the kit. Generated luciferase is proportional to the amount of reduced glutathione present in the sample.

After 72 h of transfection, the medium from the transfected MLTC-1 cells were removed and GSH-Glo™ Reagent was added. The Luciferin Detection Reagent was added to the plate after 30 min of incubation. Following a 15min incubation, the plate was read in a luminometer.

2.10. Determination of catalase activity

Catalase (CAT) activity measurements were performed using Cayman's Catalase Assay Kit assay, which uses the peroxidase function of catalase to determine the enzyme activity, based on the reaction of CAT with methanol in the presence of hydrogen peroxide (H₂O₂).

Briefly, MLTC-1 cells were transfected with *Pex13*shRNA and control shRNA via microporation in 12 well plates. After 72 h of transfection, cells were collected using a rubber policeman and centrifuged at 2.000 x g for 10 min at 4°C. The cell pellet was homogenized on ice in 1 ml of cold buffer (50 mM potassium phosphate containing 1mM EDTA, pH 7.0) and centrifuged at 10,000 x g for 15 min at 4°C. Thereafter, the supernatant was removed and stored on ice for the Catalase (CAT) activity assay, done according to the manufacturer's protocol (Catalase Assay Kit). Formaldehyde standard wells, positive control wells and sample wells were prepared by adding 100µl of diluted assay buffer, 30µl of methanol and 20µl of standard or diluted catalase or sample respectively. Reaction was initiated by adding 20µl of H₂O₂, after which plate was covered and incubated on a shaker for 20 min at RT. Thereafter, 30µl of diluted potassium hydroxide and 30 µl of Catalase Purpald (Chromogen) were added to each well and incubated for 10 min on the shaker at RT. After adding 10µl of Catalase Potassium Periodate and incubating on a shaker for 5 min at RT, the absorbance was read at 540 nm using a plate reader.

2.11. Detection of the Mitochondrial Membrane Potential ($\Delta\Psi_m$)

The DePsipher™ Kit (TREVIGEN, Catalog# 6300-100-K) was used for the detection of the mitochondrial membrane potential ($\Delta\Psi_m$) in MLTC-1 cells transfected with *Pex13* siRNA and control siRNA. The experiment was done according to the protocol provided with the DePsipher™ Kit. 1X Reaction buffer was prepared from 10X Reaction Buffer by diluting with distilled water. 1 µl of DePsipher™ solution was added to 1 ml of 1X Reaction Buffer and were vortexed to homogenize the solution. After 72 h of transfection, the medium was collected and MLTC-1 cells were covered with diluted DePsipher™ solution. Cells were incubated at 37°C in a 5% CO₂ incubator for 15-20 minutes. Thereafter, the cells were washed with 1 X Reaction Buffer with stabilizer solution and observed immediately under the microscope using a fluorescein long-pass filter. A lipophilic cation, a unique cationic dye (5, 5', 6, 6', tetrachloro-1, 1', 3, 3'- tetraethylbenzimidazolyl carbocyanin iodide) was used to detect the loss of the mitochondrial potential. It enters cells forming a red fluorescent compound within healthy mitochondria. If the mitochondrial potential is disturbed, the

dye cannot accumulate within the mitochondria, remains in cytoplasm showing primarily green fluorescence.

2.12. Enzyme-linked immunosorbent assays (ELISA) and radioimmunoassay's (RIAs)

Measurement of different steroid hormone production in MLTC-1 and in primary mouse Leydig cells was done by enzyme-linked immunoassays (ELISA) (DRG Instruments GmbH, Germany). The principle of the test is based on typical competitive binding scenarios. The wells in the microplate are coated with an antibody directed towards an antigenic site of the hormone molecule.

The hormone (antigen) in the sample competes with a hormone-horseradish peroxidase conjugate for binding to the antibodies coated on the microtiter wells. The amount of bound peroxidase conjugate is inversely proportional to the concentration of hormone in the sample. Following the incubation, the unbound conjugate was washed off and the enzyme substrate was added. After addition of the substrate solution, the intensity of color (blue) formed is inversely proportional to the concentration of hormone in the sample. The enzymatic reaction was stopped by adding stop solution (H_2SO_4) in each well, where a blue color changes into yellow. The absorbance of each well was determined at $450 \pm 10 \text{ nm}$ with a microtiter plate reader.

Pregnenolone, progesterone, testosterone, dehydroepiandrosterone (DHEA), estrone and estradiol production in MLTC-1 as well as in primary Leydig cells was measured according to the protocols given by the manufacturers (ELISA kit) (DRG Instruments GmbH, Marburg, Germany). For progesterone measurement, the samples from MLTC-1 cells were diluted 1/80 and samples from primary Leydig cells were diluted 1/15. For pregnenolone measurement samples from MLTC-1 and primary Leydig cells were diluted 1/45. Dilution factor was taken into account for the calculation of the hormone concentrations.

A set of standards was used to plot a standard curve from which the hormone concentration in the samples and controls was calculated.

Radioimmunological measurements of testosterone and progesterone

Measurements of testosterone and progesterone from MLTC-1 cells and primary Leydig cells by RIA were performed in the laboratory of the Clinic for Obstetrics,

Gynecology and Andrology of Animals, Justus Liebig University, Giessen (Prof. Dr. Gerhard Schuler). Radioimmunological measurements in the lab were set up as competitive assays as previously described by (Hoffmann, et al. 1973).

2.13. Experiments with different treatments of MLTC-1 cells and primary Leydig cells

2.13.1. Treatment with human chorionic gonadotropin (hCG)

Human chorionic gonadotropin (hCG) is a glycoprotein hormone normally synthesized by trophoblastic cells of the placenta after embryo implantation during pregnancy. hCG is a vital hormone during early pregnancy to support the production of progesterone by the corpus luteum (Fritz and Speroff 2011; Mesiano 2009). hCG consists of α and β subunits, where the alpha-subunit is identical to other three hormones such as luteinizing hormone (LH), follicle-stimulating hormone (FSH), and thyroid-stimulating hormone (TSH) and is coded by a single gene. However, the β subunits are unique and define their biological specificity. In conclusion, LH and hCG have similar structure and function to bind and activate a common receptor, the LH/choriogonadotropin receptor (LHCGR), also known as the LH or lutropin receptor (Lhr) (Ascoli et al. 2002; Puett, et al. 2007). To determine if MLTC-1 cells produce steroids in response to hCG, MLTC-1 cells were seeded at a density $1,5 \times 10^5$ per well in 6 well plates and cells were allowed to grow for 3 days. On the day preceding an experiment, cells were washed and replaced with serum-free RPMI 1640 medium. hCG (Predalon 5000 IU) at 100ng/ml or 1,49 IU/ml was constituted fresh, diluted in serum-free RPMI1640 medium and applied to MLTC-1 cells. Cells were incubated in 800 μ l (per well) of serum free medium with 100ng/ml hCG for 6 and 24 h. After the incubation, the medium from each well was removed, the supernatants were collected, centrifuged at 670 x g for 10 min, at 4°C) and the final supernatant was stored at -20°C for assay of progesterone, testosterone by radioimmunoassay and by ELISA. Cells were processed for total RNA or protein isolation. Steroid production was normalized as mass per μ g of total protein.

2.13.2. Treatment with 22 (R)-Hydroxycholesterol

22(R)-Hydroxycholesterol (22R-HC) is a cholesterol substrate derivative and hydrosoluble form of cholesterol that readily passes through cell and organelle membranes. 22R-HC is a membrane-permeable substrate for CYP11A1 in the mitochondria and enters the inner mitochondrial membrane without the help of StAR, which is a limiting factor in the steroidogenesis and is responsible for the transfer of cholesterol from the outer mitochondrial membrane to the inner mitochondrial membrane.

MLTC-1 cells were transfected with *Pex13* shRNA and control shRNA as mentioned in chapter (transfection via microporation) and seeded at 1×10^5 per well in 24 well plates. After 72 h of transfection cells were treated with 40 μ M 22R-HC in serum free medium for 6h.

Mouse primary Leydig cells after isolation were plated at density 1.5×10^5 /per well in 24 well plates. On the following day cells were transfected with *Pex13*siRNA and control siRNA. Following 48h of transfection cells were treated with 40 μ M 22R-HC for 6h. All treatments were performed in serum-free media. Final concentrations of ethanol used as chemical solvents were less than 0.4% and included in controls. At the end of all experiments, medium samples were taken and stored at -20°C for the hormone measurements by ELISA.

2.13.3. Treatment of MLTC-1 cells with trilostan and abiraterone acetate

MLTC-1 cells were transfected with *Pex13* shRNA and control shRNA as mentioned above. After 72 h of transfection, cells were pre-incubated for 30 min with trilostane (5 μ M) and abiraterone acetate (17nM). At the end of preincubation cells were washed and incubated with hCG (100 ng/ml) and 22R-HC (40 μ M) in serum free media for another 6h. Trilostan was used as an inhibitor of 3 β -hydroxysteroid dehydrogenase to block the formation of progesterone. Abiraterone acetate blocks CYP17A1 by potently inhibiting both the 17 α -hydroxylase and the 17, 20-lyase activities thus inhibiting further conversion of pregnenolone to DHEA. After incubation, cells were processed for total protein isolation. Medium from each well was removed and stored at -20°C for assay of pregnenolone by ELISA. Steroid production was normalized as mass per μ g of total protein.

2.13.4. Treatment of MLTC-1 cells with antimycin A

Antimycin A is known to bind the Qi site of cytochrome c reductase in the mitochondrial complex III to inhibit the mitochondrial electron transfer between cytochrome b and c. The disruption of electron transport causes a collapse of the proton gradient across the mitochondrial inner membrane, leading to the loss of the mitochondrial membrane potential ($\Delta\psi_m$) and a reduction in the cellular levels of ATP (Balaban, et al. 2005; Campo, et al. 1992; Pham, et al. 2000). MLTC-1 cells were cultured at a density 5×10^4 /per well in 24 well plates for 3 days in RPMI-1640 medium supplemented with 10% fetal serum. On the 3rd day cells were pre-incubated with antimycin A (5 μ M) for 30 min. Thereafter, cells were stimulated during 4h with hCG (100ng/ml) or 22R-HC (40 μ M) in the serum free RPMI 1640 medium in the presence or absence of antimycin A (1 μ M). Progesterone production in the incubation media was measured by ELISA.

3. Aims of the study

Prior to this dissertation, no study in the international literature was providing direct evidence for the involvement of peroxisomes in steroid synthesis in Leydig cells. At the very beginning, Reddy and Svoboda in 1972 hypothesized on the involvement of peroxisomes in cholesterol and steroid metabolism. Thereafter, Mendis-Handagama and colleagues showed that the number of peroxisomes and peroxisomal volume in Leydig cells as well as testosterone production were increased upon LH treatment, whereas LH deprivation resulted in a strong reduction in the number of these organelles and testosterone secretion, suggesting that the peroxisomal compartment is involved in steroid synthesis (Mendis-Handagama 1997; Mendis-Handagama, et al. 1992; Mendis-Handagama, et al. 1990a). Moreover, patients with peroxisomal disorders demonstrated testicular pathologies, which indicated that peroxisomal metabolism is crucial for normal testicular function. Nevertheless, till now the role of peroxisomes in steroid metabolism in Leydig cells and its influence on male fertility is not completely understood. Therefore, the aim of this study was to investigate the role of peroxisomes in steroid synthesis in Leydig cells.

The major aims of this study were:

1. To establish a good cell culture model for functional studies with mouse Leydig tumor cell lines (MLTC-1 and MA-10 cells).
2. To analyze and compare the expression of steroidogenic enzymes in MLTC-1 and MA-10 cells.
3. To analyze the steroid synthesis of MLTC-1 cells stimulated by hCG.
4. To establish optimal mouse Leydig cells isolation and primary culture to study the functional aspects in primary Leydig cells.
5. To investigate the expression, abundance and relevance of peroxisomes in Leydig cells.
6. To analyze the effects of peroxisome deficiency in Leydig cells on steroid metabolism by generating a knock down of *Pex13* gene.
7. To analyze the consequences of *Pex13* knockdown on redox state and mitochondrial function in Leydig cells.

8. To investigate the biological potency of androgens and estrogens in Leydig cells with MFP2 (17 β -HSD4) knockdown.

4. Results

4.1. Comparison of genes involved in steroidogenesis in MA-10 and MLTC-1 cells

Exploring different aspects of Leydig cell physiology using primary Leydig cell cultures in vitro is particularly difficult due to their low abundance in the testis and methods to isolate them are quite laborious. Moreover, primary Leydig cells in culture lose their ability to respond to LH treatment after a few days, resulting in decrease steroid production. Internationally, the mouse Leydig tumor cell lines MLTC-1 and MA-10 are therefore widely used as in vitro models to study Leydig cell physiology and to investigate the regulation of steroidogenesis.

The first aim of this thesis work was to characterize MA-10 and MLTC-1 cells for the expression of enzymes involved in steroidogenesis and to analyze if they are suitable models to study the involvement of peroxisomes in steroidogenesis.

Using semi-quantitative RT-PCR, the steady state levels for the mRNAs encoding different steroidogenic enzymes, carrier proteins and receptors were determined in total RNA of the two murine tumor Leydig cell lines, MA-10 and MLTC-1 cells in comparison to each other.

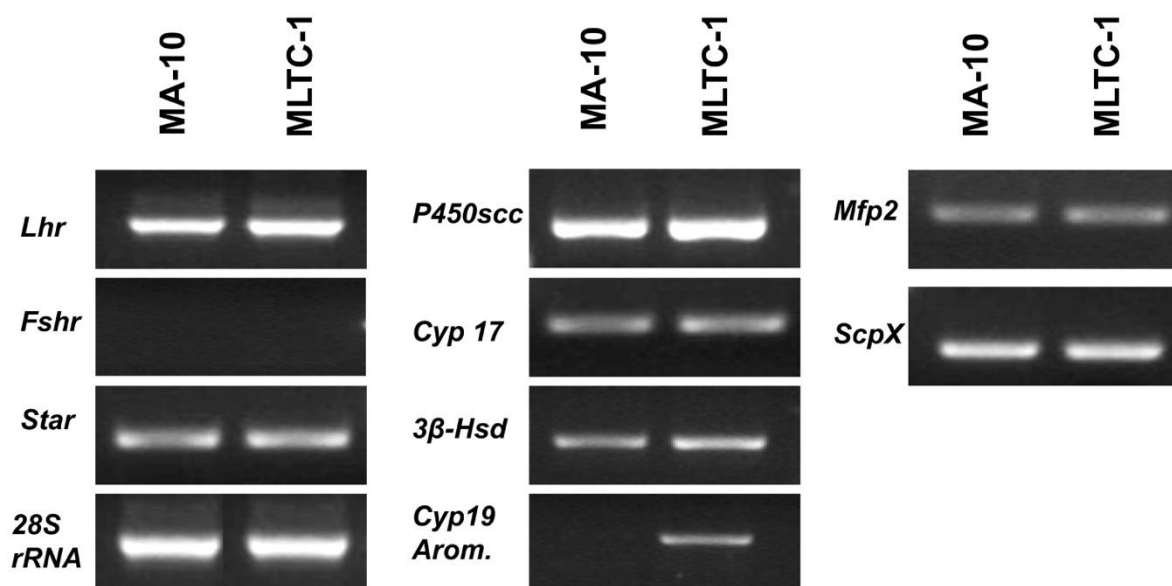


Figure 4. Semiquantitative RT-PCR analyses on cDNAs prepared from total RNA of MLTC-1 and MA-10 cells. The RT-PCR products of Lh-r: Luteinizing hormone/chorion gonadotropin receptor; Fsh-r: follicle stimulating hormone receptor; Star: steroidogenic acute regulatory protein; P450scc: mitochondrial cytochrome P450 side chain cleavage enzyme; Cyp17: cytochrome P450c17; 3 β -Hsd: 3 β -hydroxysteroid dehydrogenase; Cyp19: cytochrome P450aromatase; MFP2: peroxisomal 17 β -hydroxysteroid dehydrogenase 4; Scpx: sterol carrier protein x, 28S rRNA: 28 S ribosomal RNA as internal control in MA-10 and in MLTC-1 cells without treatment with hCG. To calculate the differences in mRNA expression levels, the RT-PCR band intensities of steroidogenesis-related genes were normalized for the band intensity of the house keeping gene 28S rRNA of the same cDNA samples.

Semi-quantitative RT-PCR analysis revealed that MA-10 and MLTC-1 cells differentially express the genes involved in steroidogenesis. In strong contrast to MLTC-1 cells, the expression of the aromatase gene was absent in MA-10 cells. MLTC-1 cells exhibited a higher steady state expression levels of LHr, P450scc and 3 β -HSD genes, whereas, other proteins or enzymes involved in steroidogenesis such as Star, Cyp17 and MFP2 were expressed in a similar fashion between MLTC-1 and MA-10 cells. Both MA-10 and MLTC-1 cells did not express the FSH receptor, a typical Sertoli cell gonadotropin receptor (Fig. 4).

Interestingly, it was observed during cell culture that MA-10 cells in culture were loosely attached to culture flask bottom and formed clusters. Moreover, in comparison to MLTC-1 cells, MA-10 cells showed a decreased rate of proliferation (results not shown).

Considering these factors, mouse Leydig tumor cell line (MLTC-1) was chosen as a better model in comparison to MA-10 cells to study steroidogenesis.

4.2. MLTC-1 cells respond to human chorionic gonadotropin (hCG) treatment

Next, MLTC-1 cells were stimulated with hCG to test their ability to produce steroids. 1.5×10^5 MLTC-1 cells were grown for 3 days in 6-well-plates after which cells were treated with hCG (100ng/ml) in serum-free medium for 6h and 24h. Semi-quantitative RT-PCR was done for determination of StAR, P450scc and Lhr mRNA expressions.

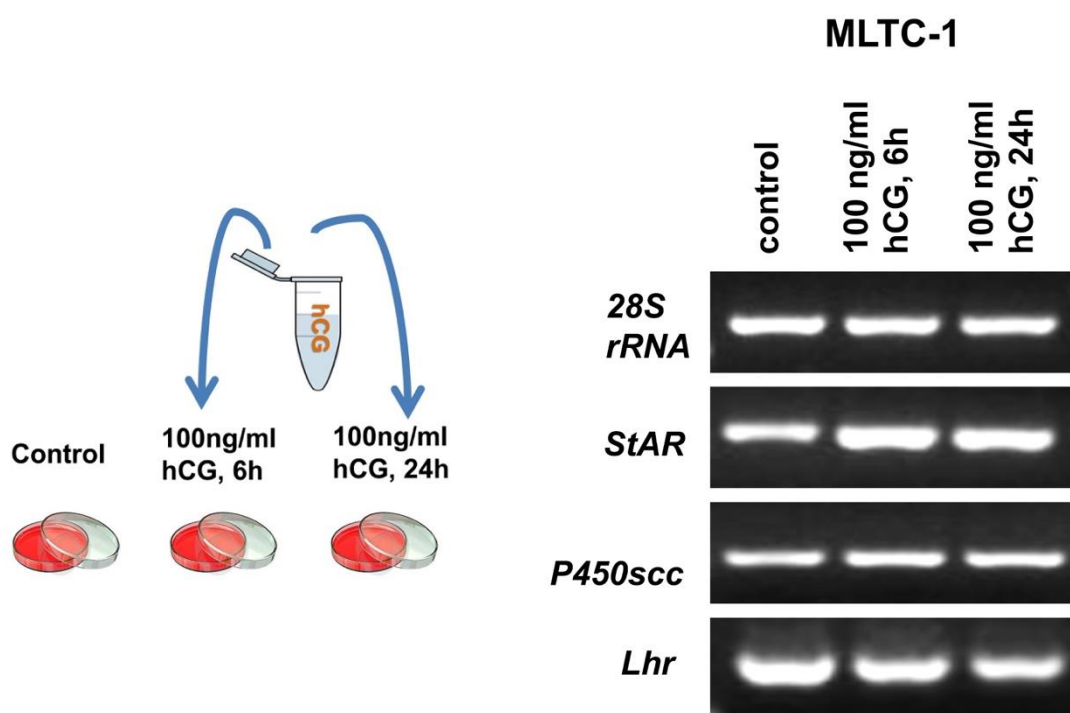


Figure 5. Semiquantitative RT-PCR analyses on cDNAs prepared from total RNA of MLTC-1. 28S rRNA (28S ribosomal RNA) as internal control, StAR (Steroidogenic acute regulatory protein), P450scc (mitochondrial cytochrome P450 side chain cleavage enzyme), Lhr (Luteinizing hormone/chorion gonadotropin receptor), in MLTC-1 cells after exposure to hCG (100ng/ml) for 6 h and 24 h.

Stimulation of MLTC-1 cells with hCG resulted in an induction of StAR mRNA expression. hCG-induced StAR mRNA expression was found to be significant at 6h in comparison to 24h (Fig. 5), wherefore mainly 6h treatment with hCG was used for all following analyses.

It was previously shown, that the stimulation with hCG down-regulate the mRNA levels of Lhr (Menon, K M J et al. 2004). This feature was also noted in MLTC-1 cells, which also served as an indirect confirmation, that these cells respond to hCG treatment (Fig. 5).

At the protein level, stimulation with hCG caused a strong increase in the induction of StAR especially that of the 30kDa cleaved form of StAR, which is responsible for cholesterol transport from outer mitochondrial membrane into the inner mitochondrial membrane for further pregnenolone synthesis. Moreover, also a slight increase of the 37kDa precursor form of StAR was noted. Similarly, the mitochondrial cholesterol side-chain cleavage enzyme, P450scc was also up-regulated after hCG stimulation (Fig. 6).

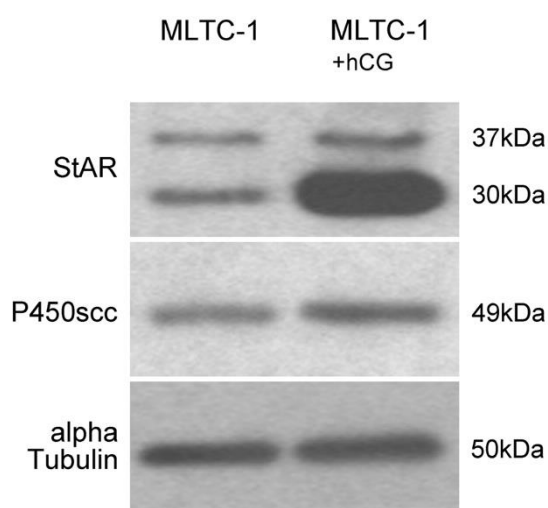


Figure 6. Western blot analysis for steroidogenic acute regulatory protein (StAR) and mitochondrial cytochrome P450 side-chain cleavage enzyme (P450scc) of the whole the cell lysate from MLTC-1 cells without and with 6h hCG stimulation. Cells were lysed and 20µg of proteins were loaded in each lane on 12.5% SDS gels. The same blots were stripped and re-probed several times with specific antibodies. StAR - steroidogenic acute regulatory protein, P450scc-

cytochrome P450 side chain cleavage enzyme, alpha Tubulin- as an internal control.

Collectively, these results indicate that MLTC-1 cells respond to hCG treatment and are a good cell culture model to study steroidogenesis.

4.2.1. Hormone production in MLTC-1 cells.

Next, we were interested to check the ability of MLTC-1 cells to produce hormones. Therefore, progesterone and testosterone secretion by MLTC-1 cells with hCG stimulation were determined by RIA, the most sensitive method for analysis also of smaller steroid amounts.

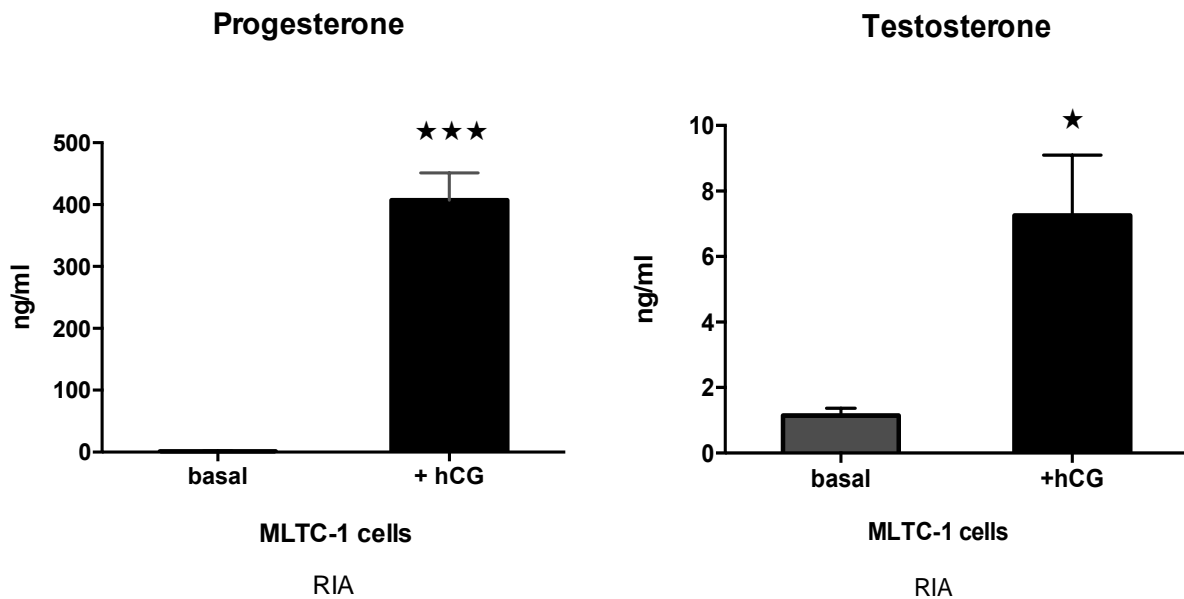


Figure 7. Progesterone and testosterone production by MLTC-1 cells per well in response to 6h hCG (100ng/ml) treatment measured by RIA. MLTC-1 cells were grown in culture to 60% confluency and after 3 days of culture cells were treated with hCG (100ng/ml) for 6h. Media were collected and subjected to measurement of progesterone and testosterone by RIA. Hormones concentrations were normalized according to each sample cell pellet protein concentration. Basal progesterone (1,6ng/ml), hCG-mediated progesterone (428 ng/ml), basal testosterone (1,15 ng/ml), hCG-mediated testosterone (7,25ng/ml).

RIA results revealed that MLTC-1 cells produce high levels of progesterone as reported in many different studies. Interestingly, we found that there is significant production of testosterone by MLTC-1 cells after culturing those for 3 days and treating for 6 h with hCG (100ng/ml).

Similar results were also obtained by measuring progesterone and free testosterone concentration produced by MLTC-1 via ELISA (Fig. 8).

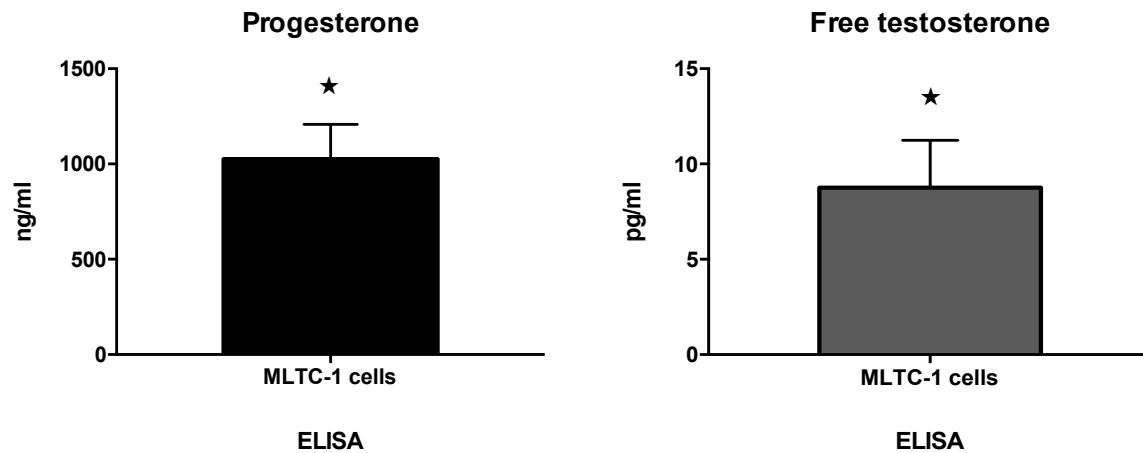


Figure 8. Progesterone and testosterone production by MLTC-1 cells per well in response to hCG (100ng/ml) treatment measured by ELISA. MLTC-1 cells were grown in culture to 60% confluency. After 3 days of culture they were treated with hCG (100ng/ml) for 6h. Media were collected and subjected to measurement by ELISA. Hormones concentrations were normalized according to each sample cell pellet protein concentration.

Furthermore, ELISA revealed that MLTC-1 cells can also produce DHEA, estradiol and estrone (Fig. 9).

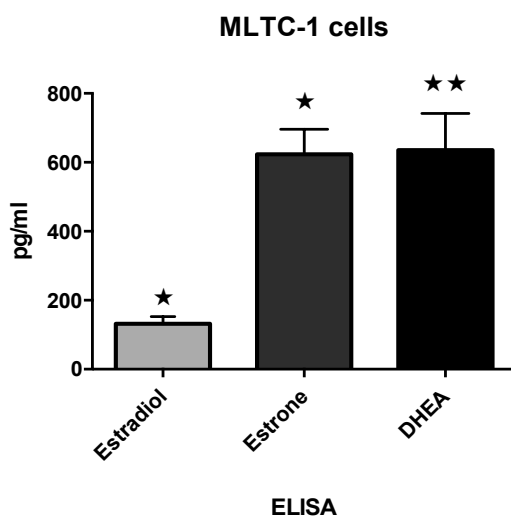


Figure 9. Estradiol, estrone and DHEA production by MLTC-1 cells per well in response to hCG (100ng/ml) treatment measured by ELISA. MLTC-1 cells were grown in culture to 60% confluency and after 72 h of culture cells were treated with hCG (100ng/ml) for 6h. Media were collected and subjected to measurement by ELISA. Hormones concentrations were normalized according to each sample cell pellet protein concentration.

4.3. Peroxisomal genes and proteins are differently expressed in MLTC-1 cells

Having confirmed the ability of MLTC-1 cells to produce steroids, we next profiled these cells for the expression of peroxisomal genes. Semi-quantitative RT-PCR analyses revealed that majority of peroxisomal genes are well expressed in MLTC-1 cells (Fig. 10). The antioxidant enzyme catalase was found to be highly expressed in MLTC-1 cells at the RNA level.

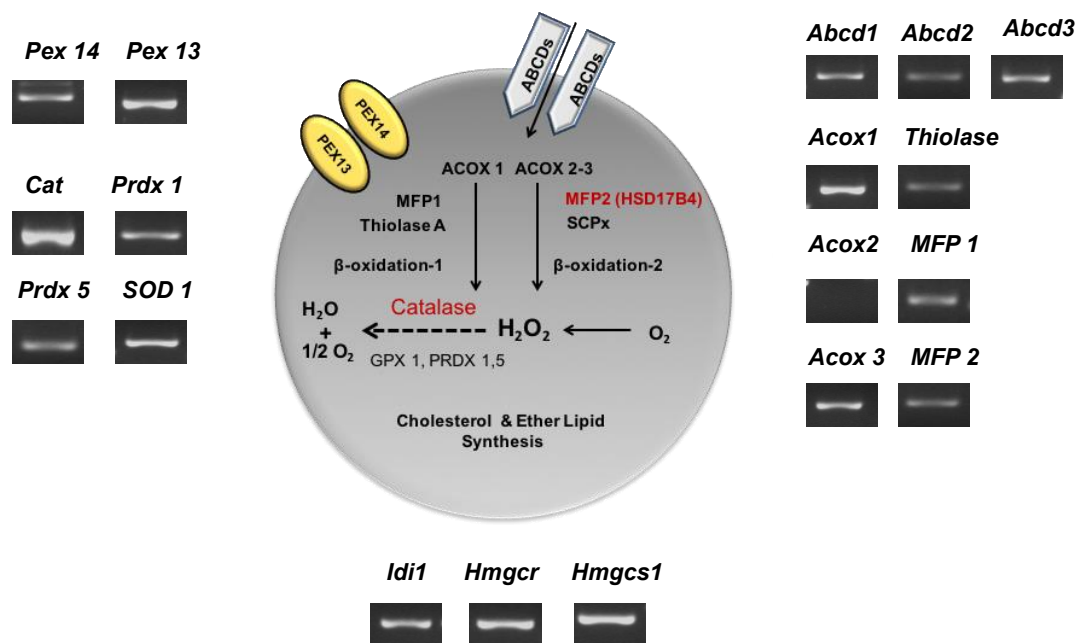


Figure 10. Semiquantitative RT-PCR analysis on cDNAs prepared from total RNA of MLTC-1 cells. Peroxisomal biogenesis genes *Pex13*, *Pex14*. Peroxisomal ABCD-transporters *Abcd1-3*. Enzymes of the β -oxidation pathway 1, *Acox1*: acyl-CoA oxidase 1, Ehhadh multifunctional protein 1 (*MFP1*), Thiolase A: peroxisome 3-ketoacyl-CoA thiolase; Enzymes of the β -oxidation pathway 2, *Acox2* and *Acox 3*: acyl-CoA oxidase 2 and 3, Hsd17 β 4: Multifunctional protein 2 (*Mfp2*); ScpX: sterol carrier protein X. Antioxidants in peroxisomes, *Cat*: catalase, *Prdx1*: peroxiredoxin-1, *Prdx5*: peroxiredoxin-5, *Sod1*: superoxide dismutase 1. Enzymes for cholesterol synthesis, *Idi 1*: isopentenyl-diphosphate delta isomerase 1, *Hmgcr*: 3-hydroxy-3-methylglutaryl-CoA reductase, *Hmgcs1*: 3-hydroxy-3-methylglutaryl-CoA synthase 1.

Moreover, a high abundance of peroxisomes in MLTC-1 cells as shown by immunofluorescence analysis with the peroxisomal marker protein catalase and peroxisomal biogenesis proteins PEX13 and PEX14 corroborated the high expression of mRNAs for peroxisomal biogenesis genes and catalase in MLTC-1 cells.

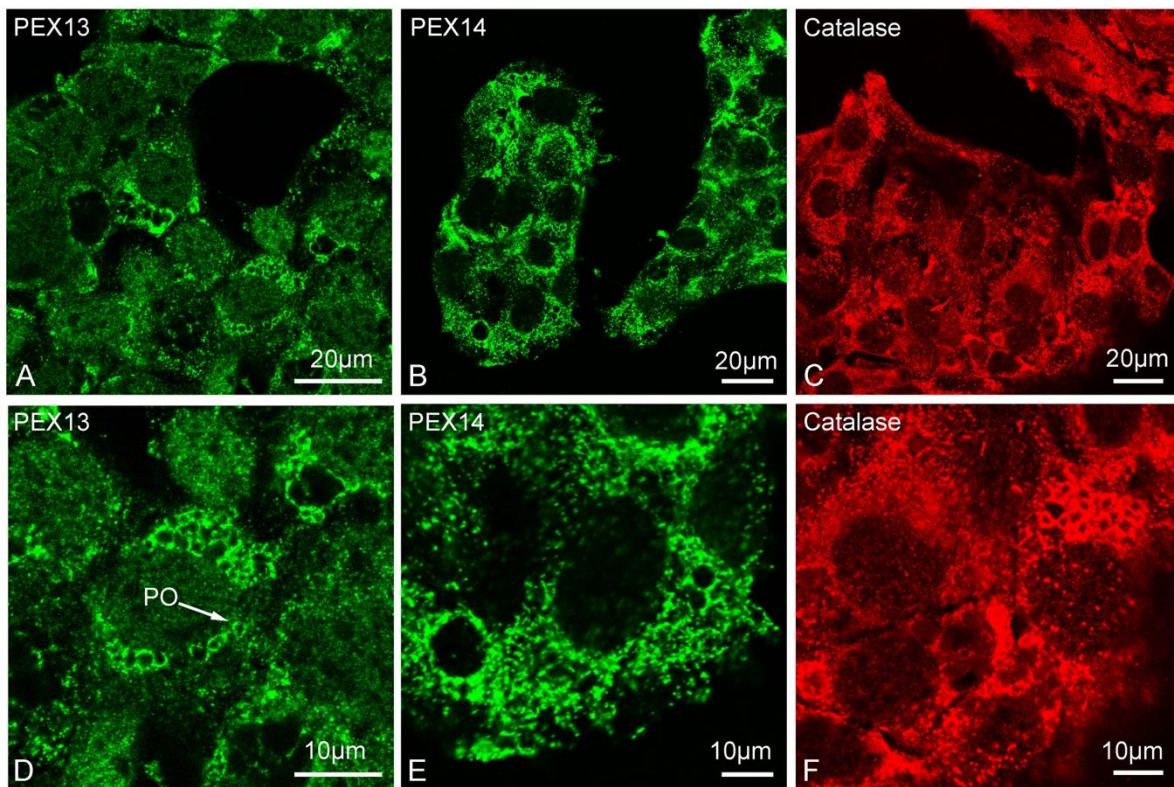


Figure 11. Immunofluorescence detection of peroxisomal proteins in MLTC-1 cells
MLTC-1 cells were stained for the peroxisomal biogenesis proteins: A. Peroxin 13 (PEX13); B. Peroxin 14 (PEX14) and for the localization of peroxisomal antioxidant enzyme C. Catalase. Bars represent in A-C 20µm, in D-F 10µm (D magnification from A, E magnification from B, F magnification from C). Pictures were taken by confocal laser scanning microscopy (CLSM). Representative pictures were obtained from 3 different experiments.

As described previously (Nenicu et al 2007), peroxisomes are abundant in Leydig cells, which is also the case in MLTC-1 cells. Similar to Leydig cells in testis sections, peroxisomes are surrounding lipid droplets. In addition,

immunofluorescence staining confirmed the high abundance of the catalase protein, exhibiting a similar distribution pattern as PEX13 and PEX14.

To summarize, these findings indicate that MLTC-1 cells are abundant in peroxisomes and serve as a good model to study the influence of peroxisomes on steroidogenesis.

4.4. shRNA mediated knock-down of *Pex13* in MLTC-1 cells

To investigate the specific role of peroxisomes in Leydig cells, we were interested to establish a cell culture model with peroxisome deficiency. As mentioned above, the *Pex13* gene encodes a protein that is essential for the biogenesis of peroxisomes. *Pex13* is responsible for the import of matrix proteins into the peroxisomes. Therefore, if the import of matrix proteins is defective, it will lead to a complete disruption of peroxisomal metabolism. To achieve this, we were first interested to obtain an efficient transfection protocol with minimal toxicity and high transfection rate in MLTC-1 cells.

As mentioned in Materials and Methods (chapter 2.4.1., table 7) different conditions for microporation were used to check the transfection efficiency using a control shRNA plasmid also expressing the green fluorescent protein (GFP). Detection of GFP after microporation via fluorescence microscopy was done to check the transfection efficiency in MLTC-1 cells. After trying different conditions for microporation, we found that MLTC-1 cells were highly transfectable with an efficiency of 85% using the following microporation parameters: voltage-1350, pulse width- 2, pulse number-2. Viability and the proliferation rate of the transfected cells were normal indicating no toxicity after control shRNA transfection.

4.4.1. Establishing the *Pex13* knockdown in MLTC1 cells

Next, MLTC-1 cells were transfected with a shRNA plasmid for *Pex13* and a control non-targeting shRNA as described under Materials and Methods (chapter 2.4.1). After 72 h of transfection, cells were processed for total RNA and protein isolation.

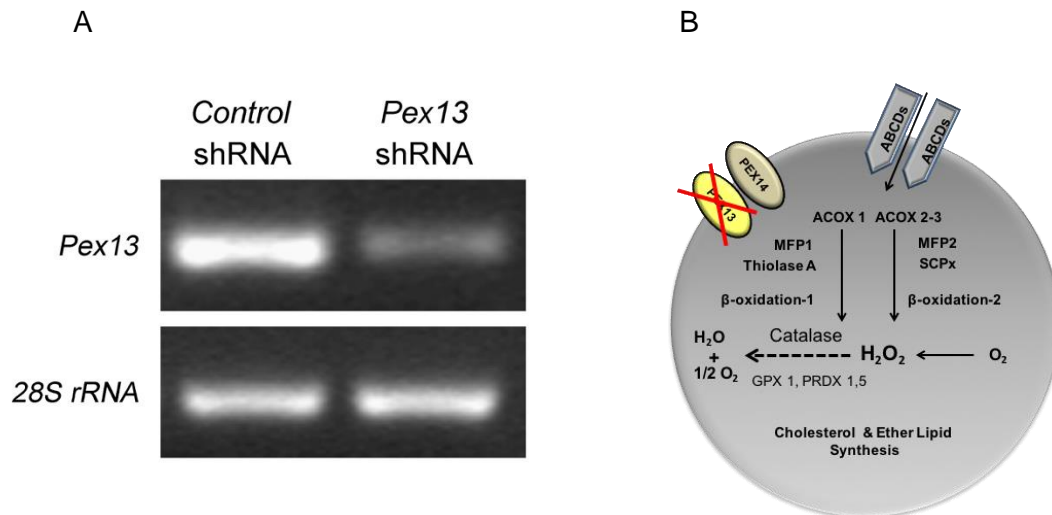


Figure 12. Semi-quantitative RT-PCR analysis of *Pex13* from total RNA of MLTC-1 cells transfected with *Pex13* shRNA- and control shRNA-palmsids (A). *Pex13*: Peroxisomal biogenesis gene 13; 28S rRNA: 28S ribosomal RNA as internal control. B. Model of a peroxisome.

Semi-quantitative RT-PCR analyses revealed that the *Pex13* mRNA was significantly reduced in MLTC-1 cells transfected with the *Pex13* shRNA plasmid in comparison to cells transfected with control shRNA (Fig. 12).

Similarly, Western blot analysis showed that PEX13 protein level in MLTC-1 cells transfected with the *Pex13* shRNA plasmid was reduced approximately by 80% in comparison to control shRNA plasmid transfected MLTC-1 cells (Fig. 13).

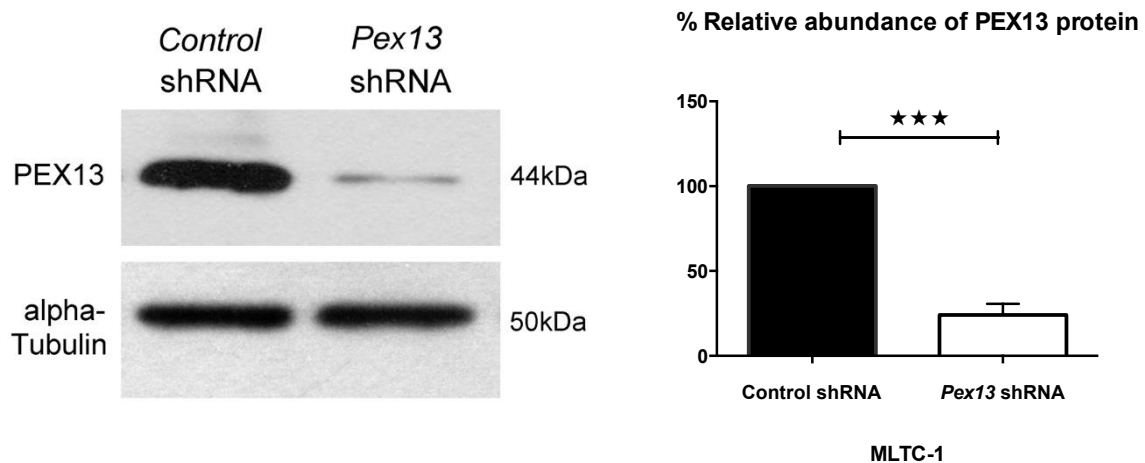


Figure 13. Western blot analysis for the peroxisomal biogenesis protein PEX13 in MLTC-1 cells transfected with the *Pex13* shRNA plasmid. After 72h of transfection cells were lysed and subjected to Western blot analysis. Twenty micrograms of total proteins were loaded in each lane on 12.5% SDS gels. First the membrane was incubated with antibody against PEX13: peroxin13. The same blot was stripped and reprobed for the α tubulin as an internal control. Chemiluminescent signals were visualized and quantified through ImageJ. Data are representatives of similar results obtained from three independent experiments (* $p \leq 0.05$, ** $p \leq 0.01$, *** $p \leq 0.001$) (N=3).

4.4.2. shRNA mediated knock-down of *Pex13* leads to mistargeting of catalase into the cytoplasm in MLTC-1 cells

Loss of functional peroxisomes results in the mistargeting of peroxisomal proteins to the cytoplasm. Previous studies have reported that the highly abundant catalase protein is mistargeted into the cytoplasm in peroxisomal knockout cells (Baes et al. 1997). Moreover, this is also observed in the cells of patients with peroxisomal biogenesis disorders (Sheikh, et al. 1998).

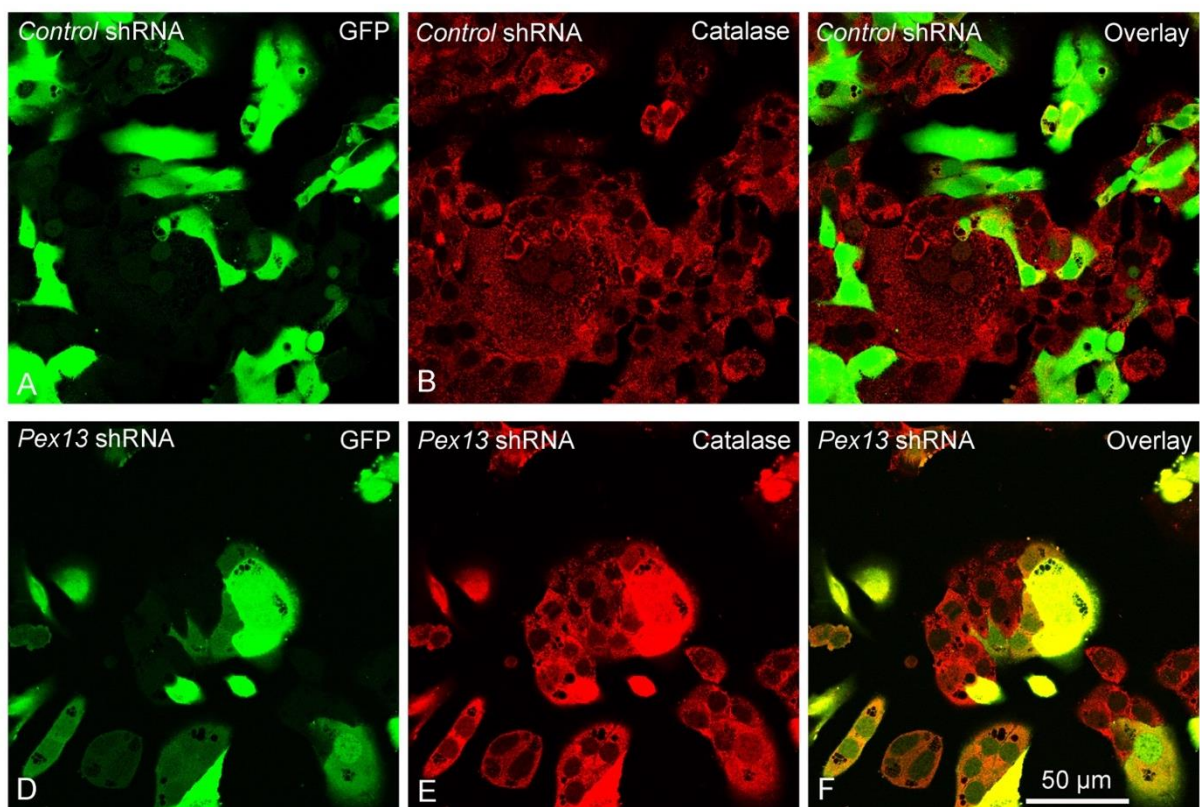


Figure 14. Double-fluorescence of green fluorescent protein (GFP) and catalase immunolocalisation in MLTC-1 cells transfected with the *Pex13* shRNA plasmid also expressing GFP. MLTC-1 cells were transfected with the control shRNA and with *Pex13* shRNA plasmids. Immunostaining for the peroxisomal matrix protein catalase was done following 72 h of transfection. Pictures were taken by confocal laser scanning microscopy (CLSM). The immunofluorescence staining revealed that the catalase is localized in peroxisomes in the cells transfected with the control shRNA (A,B,C,). In contrast, in the MLTC-1 cells transfected with the *Pex13* shRNA, the catalase protein was mistargeted to the cytoplasm (D,E,F). Bars A-F represent: 50µm. Similar pictures were obtained in 3 different experiments.

To understand if the knockdown of *Pex13* in MLTC-1 cells would lead to the loss of functional peroxisomes we performed immunofluorescence studies for staining the peroxisomal matrix protein catalase in *Pex13* shRNA transfected MLTC-1 cells.

Immunofluorescence staining revealed that the catalase staining was clearly present in peroxisomes in the cells transfected with the control shRNA. In contrast, the catalase protein was mistargeted to the cytoplasm in the cells transfected with the *Pex13* shRNA plasmid, demonstrating the loss of matrix protein import due to *Pex13* deficiency. In summary, the *Pex13* knockdown in MLTC-1 cells leads to an impaired import of matrix proteins, such as catalase, into peroxisomes (Fig. 14).

4.5. hCG-induced up-regulation of StAR is strongly inhibited in MLTC-1 cells with *Pex13* knockdown

Next, to understand the influence of peroxisomes on steroidogenesis we decided to analyze and compare hCG-stimulated control and *Pex13* shRNA-transfected MLTC-1 cells. At first, we examined the effects of hCG stimulation on StAR protein which regulates the rate-limiting step in steroid biosynthesis. The cholesterol transport from the outer to the inner mitochondrial membrane is mediated by StAR. StAR is rapidly synthesized in cytoplasm in response to cAMP, which is translated as a 37kDa precursor. After phosphorylation by PKA-A, it is cleaved within the mitochondria to generate the intramitochondrial 30kDa form.

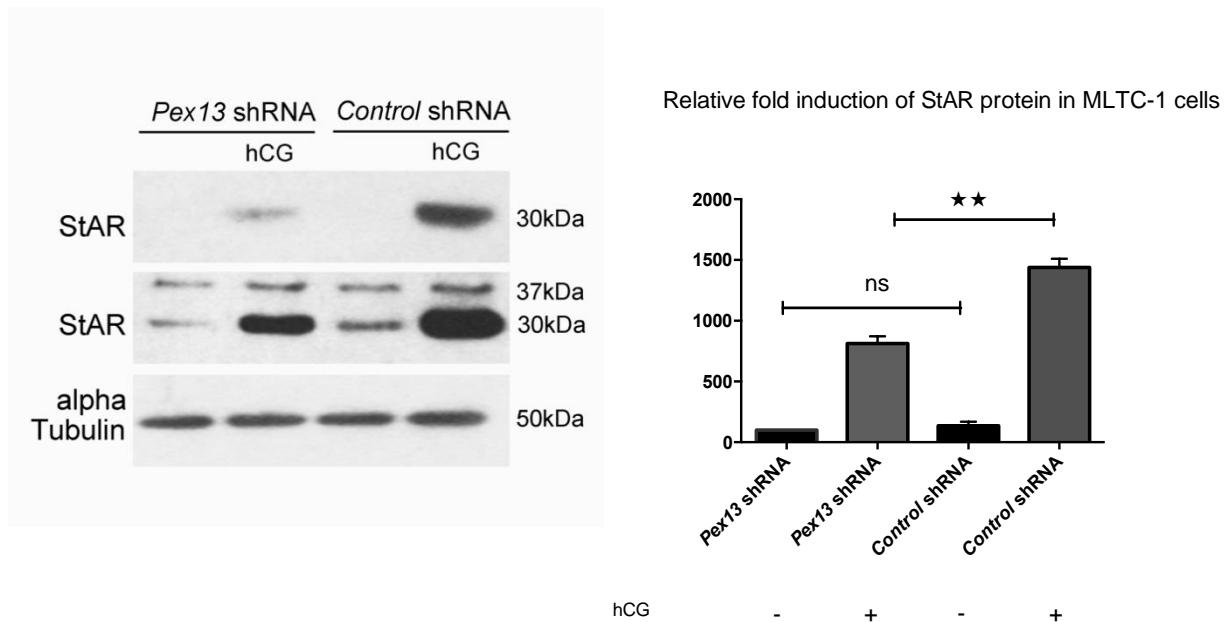


Figure 15. Western blot analysis for StAR abundance in response to hCG treatment after *Pex13* knockdown in MLTC-1 cells. MLTC-1 cells were transfected with *Pex13* shRNA and control shRNA plasmids. Following 72h of transfection cells without and with treatment (100ng/ml hCG for 6h) were lysed and subjected to Western blot analysis. Twenty micrograms of proteins were loaded in each lane on 12.5% SDS gels. First the membrane was incubated with anti-StAR antibody (StAR- Steroidogenic acute regulatory protein). The same blot was stripped and reprobed for the localization of α tubulin as an internal control. Chemiluminescent signals were visualized and quantified through ImageJ. Data are representative of similar results obtained from three independent experiments (* $p \leq 0.05$, ** $p \leq 0.01$, *** $p \leq 0.001$) (N=3).

As expected hCG stimulation in control shRNA plasmid transfected cells induced the protein levels of StAR with specific induction of the intramitochondrial cleaved form of 30kDa StAR (Fig. 15). Interestingly, hCG stimulation in *Pex13* shRNA transfected MLTC-1 cells resulted in a reduced up-regulation of StAR (approximately to 56%) protein in comparison to control shRNA transfected cells. More specifically, this impaired induction of StAR protein was clearly seen for the mature 30kDa form of StAR after hCG stimulation. Basal 37kDa StAR protein level is reduced in *Pex13* knockdown MLTC-1 cells in the represented picture, but in different other experiments we did not notice the significant difference between 37kDa StAR protein levels in *Pex13* shRNA and control shRNA transfected MLTC-1 cells without hCG stimulation. In short, peroxisomal knockdown leads to a decrease in the hCG-

induced up-regulation of the intramitochondrial form of 30 kDa StAR protein (Fig. 15).

4.6. Mouse primary Leydig cell isolation, culture and treatment with hCG

To confirm the importance of peroxisomes for steroid synthesis in Leydig cells, and to rule out the possibility that the observed findings in MLTC-1 cells are a cell-line specific phenomenon, it was important to induce a *Pex13* gene knockdown in murine primary Leydig cells. Moreover, isolated primary Leydig cells are ideal for direct biochemical and acute functional studies on steroidogenesis and they are often better suited than intact animals.

To study the relevance of peroxisomal metabolism and effects of peroxisomal deficiency on different steps of steroid synthesis, the establishment of the primary mouse Leydig cell isolation and Leydig cell culture model was crucial.

4.6.1. Isolation of primary Leydig cells

Leydig cells were isolated using enzymatic dissociation and Percoll density gradient centrifugation as described in Materials and Methods (Chapter 2.2.2.). When the cell suspension was loaded on top of a discontinuous Percoll gradient and centrifuged for 30 min, separation into 4 visible bands was obtained. The upper band consisted mainly of damaged cells whereas the second band consisted of mainly of germ cells and single Leydig cells. The fraction of most intact Leydig cells formed a third distinct band at the interphase between 50% and 60% of Percoll. A purity of isolated Leydig cells was reached of ca. 90% depending on the experiment as tested by immunofluorescence staining for cytochrome P450 side-chain cleavage enzyme (P450_{scc}), a marker specific for this cell type (Fig. 16). The fourth band in the gradient predominantly contained erythrocytes.

Immediately after isolation most of Leydig cells were round in shape and some of them were single in the suspension and some of them appeared in clusters. Leydig cells required an initial 24h culture period to attach to the culture plates. After 4 day of culture, Leydig cells were elongated in spindle, triangular or polygonal shapes. They grew in aggregation and some cells grew individually (Fig. 16).

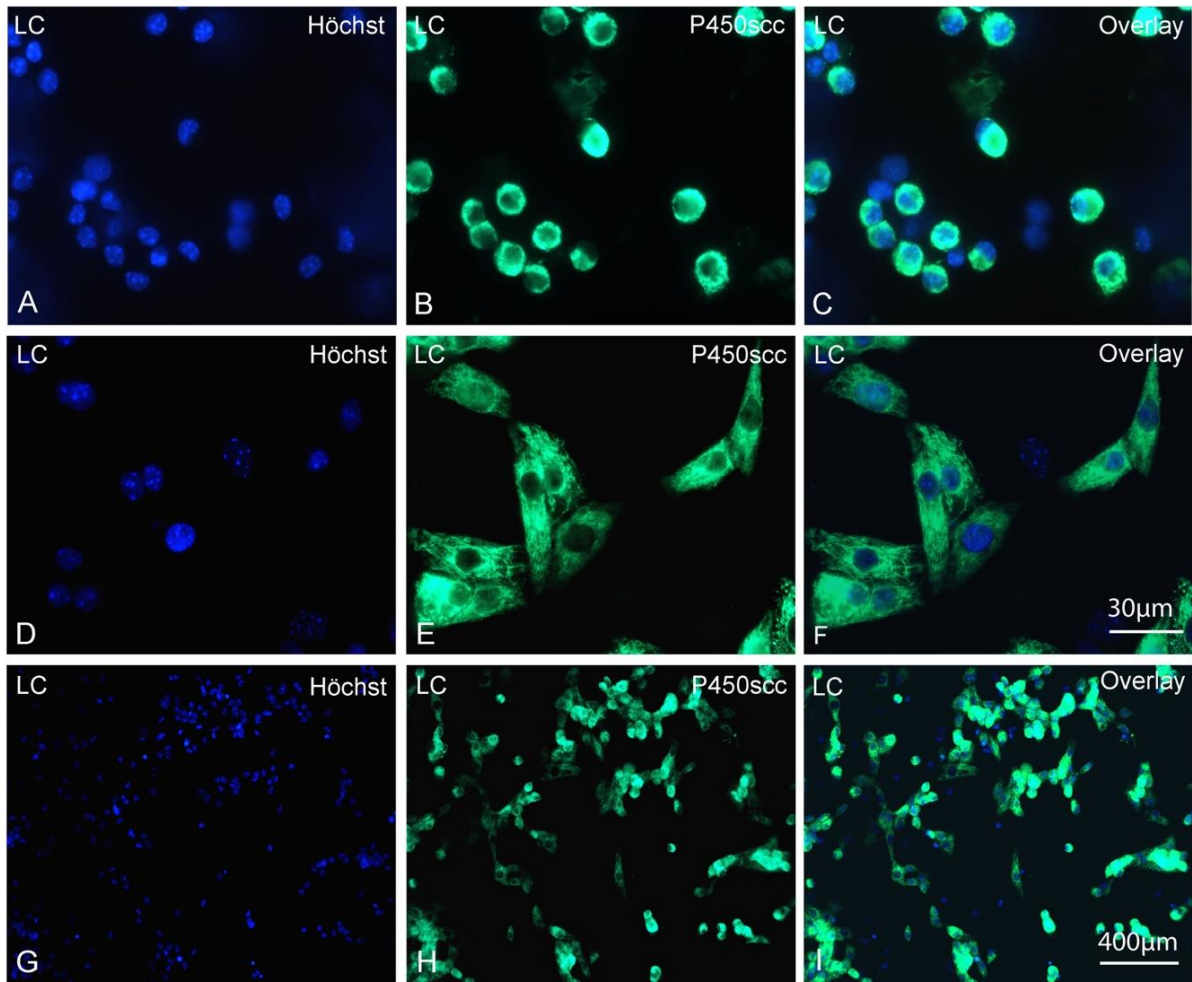


Figure 16. Immunofluorescence staining of primary mouse Leydig cell cultures (LC) stained for the mitochondrial cytochrome P450 side-chain cleavage enzyme (P450scc), a marker specific for this cell type.

Cells were stained in suspension immediately after isolation. (A,B,C).

Staining of four-day-old cultures of Leydig cells (D,E,F,G,H,I). Cells were plated in 24 well plates with collagen coated coverslips. After 4 days of culture cells were stained for P450scc. Nuclei were counterstained with TOTO-3 iodide (blue). Bars represent in A-F 30 µm, in G-I 400µm. Representative pictures were similar in 3 different experiments.

4.6.2. Treatment of primary Leydig cells with hCG.

Isolated Leydig cells in culture are known to lose their responsiveness with time to gonadotropin treatment, due to the down regulation of their LH/hCG receptors (Chen, et al. 2002; Hsueh 1980; Janszen, et al. 1976; Klinefelter, et al. 1987). Therefore, primary cultures of mouse Leydig cells were maintained as described in Materials and Methods (chapter 2.2.2) and tested for their ability to respond to hCG treatment.

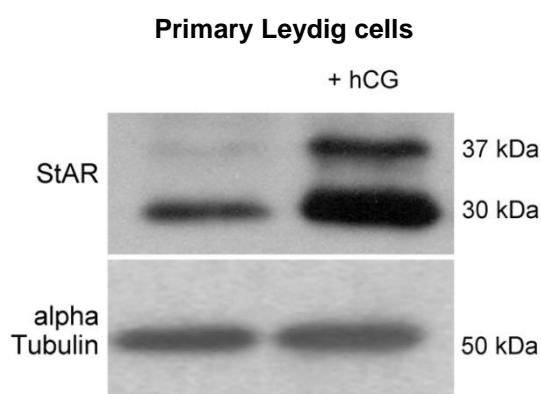


Figure 17. Western blot analysis for the steroidogenic acute regulatory protein (StAR) of the whole the cell lysate from primary mouse Leydig cells without and with hCG stimulation. Primary mouse Leydig cells were grown in culture and treated with hCG for 6 h on the 4th day after isolation. Cells were lysed and subjected to Western blot analysis to assess the level of StAR. Twenty-five microgram of proteins was loaded in each lane on 12.5% SDS gels. First the membrane was incubated with anti-StAR antibody: StAR-Steroidogenic acute regulatory protein. The same blot was stripped and reprobed for the localization of α tubulin as an internal control.

As shown in figure15 stimulation with hCG induced the protein levels of StAR (37kDa and 30kDa) and confirmed the ability of the primary Leydig cell model to respond to hCG stimulation.

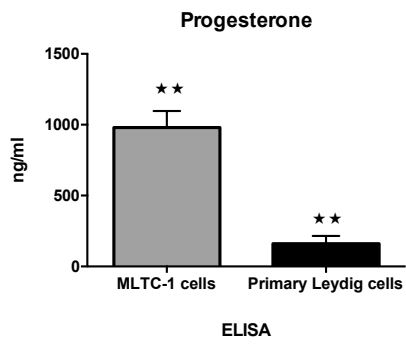
4.6.3. Hormone production in primary mouse Leydig cells and comparison with hormone secretion in MLTC-1 cells.

The functional relevance of hCG induced StAR protein expression in MLTC-1 cells was also confirmed in isolated mouse primary Leydig cells by quantifying their ability to produce hormones upon stimulation. For a comparison, the culture supernatants from hCG-stimulated MLTC-1 cells were also used for analysis to understand the differences (if any) in the steroid synthesis capacity between these two models.

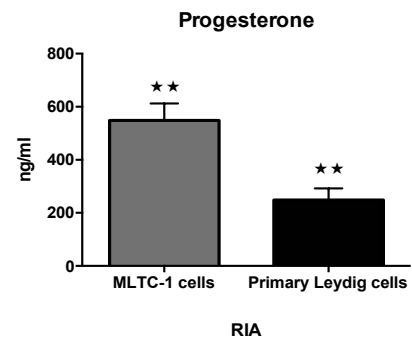
ELISA and RIA revealed that primary Leydig cells produce significantly higher levels of testosterone than MLTC-1 cells which corresponds to data in the existing literature (Mellon 1986) that MLTC-1 cells express low or undetectable levels of 17 β -HSD. Similarly, DHEA measurements showed that MLTC-1 cells produce significantly higher amounts in comparison to primary Leydig cells owing to the lack of 17 β -HSD activity in MLTC-1 cells. Moreover, progesterone, pregnenolone and estrone but not estradiol levels were found to be higher in MLTC-1 cells.

In summary, we were able to obtain primary Leydig cell cultures with high purity and these cells in culture respond to hCG-treatment. Moreover, there exist significant differences in the steroid synthesis capacity between MLTC-1 cell line and murine primary Leydig cells with MLTC-1 cells exhibiting more precursor forms and less end products (testosterone and estradiol).

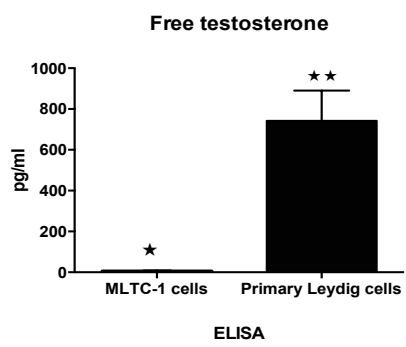
A



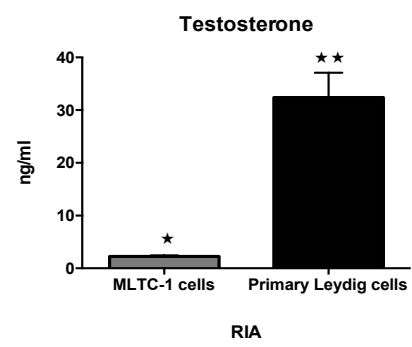
A'



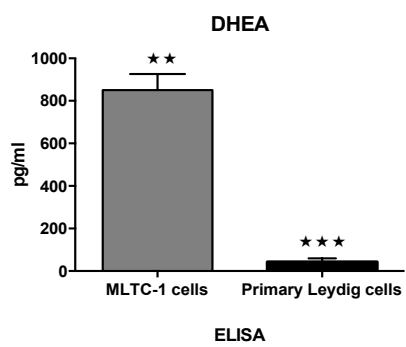
B



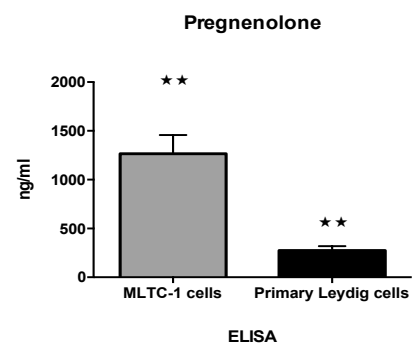
B'



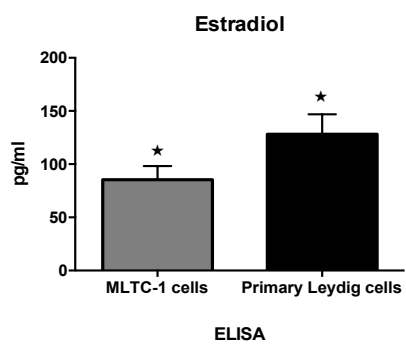
C



D



E



F

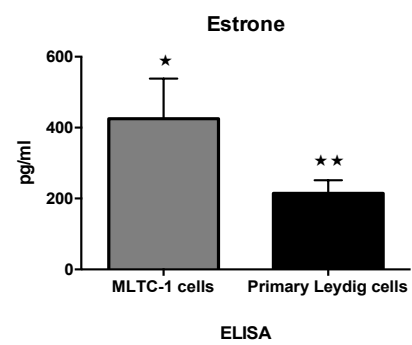


Figure 18. Steroid hormone production by primary mouse Leydig cells and MLTC-1 cells stimulated with hCG (100ng/ml) as measured by RIA and/or ELISA. Primary Leydig cells (pLC) were isolated and grown in culture as described in materials and methods. On the 4th day after isolation cells were treated with 100 ng/ml hCG for 6h. MLTC-1 cells were grown in culture to 60% confluence and after 72 h of culture cells were treated with hCG (100ng/ml) for 6h. Media were collected and subjected to measurement by RIA or/and ELISA. Steroid hormone concentrations were normalized to protein concentrations for each sample and the graphs represent results from three independent experiments (n=3). A. Progesterone concentrations in pLC and MLTC-1 by ELISA (A) and RIA (A'). B. Testosterone concentrations in pLC and MLTC-1 by ELISA (B) and RIA. (B') C. DHEA concentrations in pLC and MLTC-1 by ELISA. D. Pregnenolone concentrations in pLC and MLTC-1 by ELISA E. Estradiol concentrations in pLC and MLTC-1 by ELISA. F. Estrone concentrations in LC and MLTC-1 by ELISA. (* $p \leq 0.05$, ** $p \leq 0.01$, **** $p \leq 0.001$). (N=3)

4.6.4. Establishing a *Pex13* knockdown in mouse primary Leydig cells via a siRNA approach

To verify and confirm the results obtained after *Pex13* knockdown in MLTC-1 cells it was important to establish the knockdown also in isolated primary Leydig cells.

4.6.4.1. Establishment of a siRNA-mediated RNAi-analysis of the functionality of different *Pex13* siRNAs for the knockdown of the *Pex13* gene in MLTC-1 cells and establishing a *Pex13* knockdown in mouse primary Leydig cells via siRNA approach in primary Leydig cells

At first, we transfected primary Leydig cell with *Pex13* shRNA and control shRNA plasmids via microporation. After transfection, the number of primary Leydig cells was extremely low in culture due to the high stress and toxicity caused by microporation (results not shown). Hence we decided to obtain a siRNA mediated knockdown of *Pex13* in primary Leydig cells. To establish the best siRNA conditions and to choose the most efficient *Pex13*si RNA, we first tested the efficiency of the siRNA in MLTC-1 cells and used different lipofection reagents to obtain minimal toxicity and an efficient knockdown as described in Materials and Methods (Chapter 2.4.3., Table 9) (results not shown). Our results showed that the transfection reagent Screenfect (Incella) was the best suited among the ones tested.

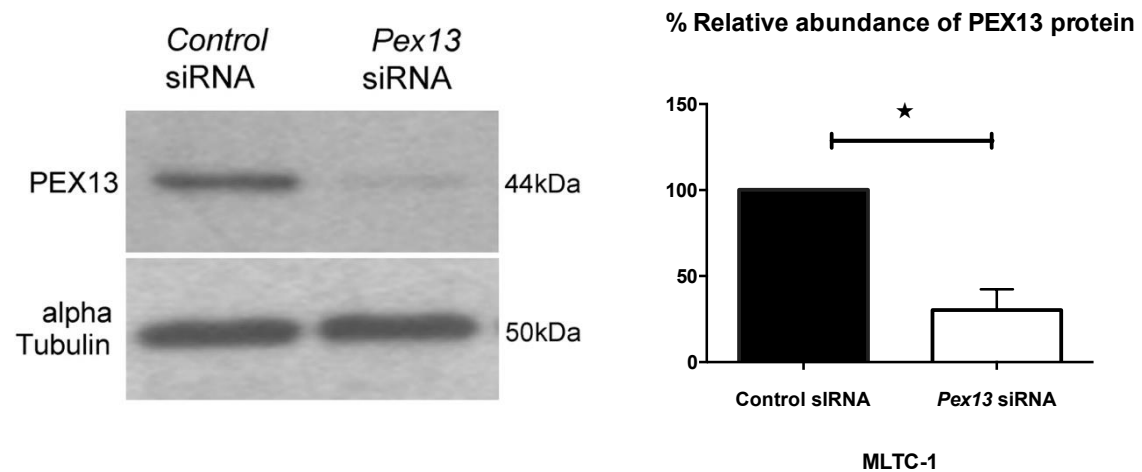


Figure 19. Western blot analysis for the peroxisomal biogenesis protein PEX13 in MLTC-1 cells transfected with *Pex13* siRNA. Twenty micrograms of proteins were loaded in each lane on 12.5% SDS gels. First the membrane was incubated with anti-PEX13 antibody. The same blot was stripped and reprobed for the GAPDH as an internal control. Chemiluminescent signals were visualized and quantified through ImageJ. Data are representatives of similar results obtained from three independent experiments. (* $p \leq 0.05$, ** $p \leq 0.01$, *** $p \leq 0.001$) (N=3).

Western blot analysis revealed that transfection with *Pex13* siRNA significantly reduced the expression of PEX13 protein in MLTC-1 cells in comparison to cells transfected with control siRNA (Fig.19).

Moreover, as observed in case of shRNA-mediated knockdown also *Pex13*-siRNA transfected MLTC-1 cells showed an impaired hCG-mediated StAR up-regulation (approximately to 62%) (Fig.20).

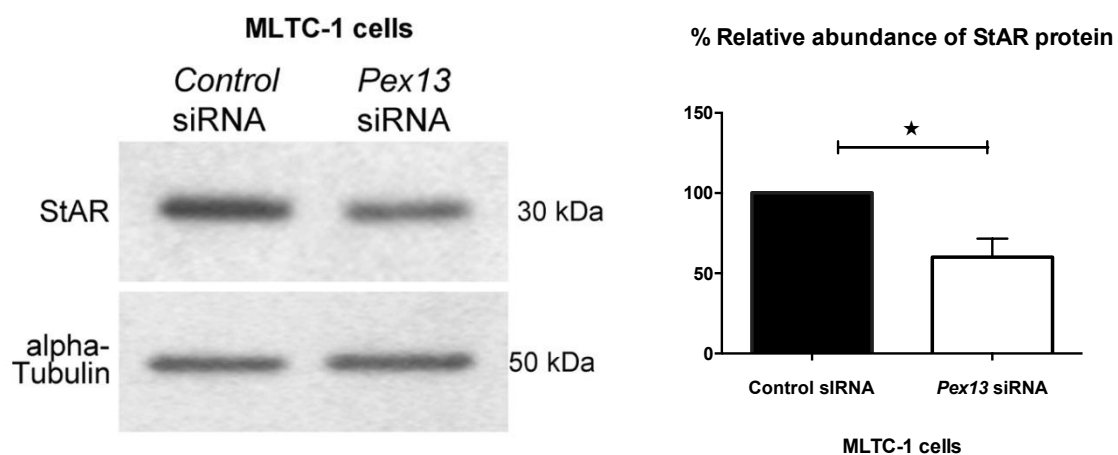


Figure 20. Western blot analysis for StAR abundance in response to hCG treatment in MLTC-1 cells transfected with *Pex13* siRNA. Twenty micrograms of proteins were loaded in each lane on 12.5% SDS gels. First the membrane was incubated with anti-StAR antibody: StAR- Steroidogenic acute regulatory protein. The same blot was stripped and reprobed for the localization of α tubulin as an internal control. Chemiluminescent signals were visualized and quantified through ImageJ. Data are representative of similar results obtained from three independent experiments. (* $p \leq 0.05$, ** $p \leq 0.01$, *** $p \leq 0.001$) (N=3).

A down regulation of *Pex13* in primary Leydig cells was also observed using RNAi approach (Fig. 21). After several experiments the optimal conditions for the amount of transfection reagent Screenfect (Incella), number of cells, the dilution of the siRNA was found and are presented in Materials and Methods (Chapter 2.4.3., Table 10).

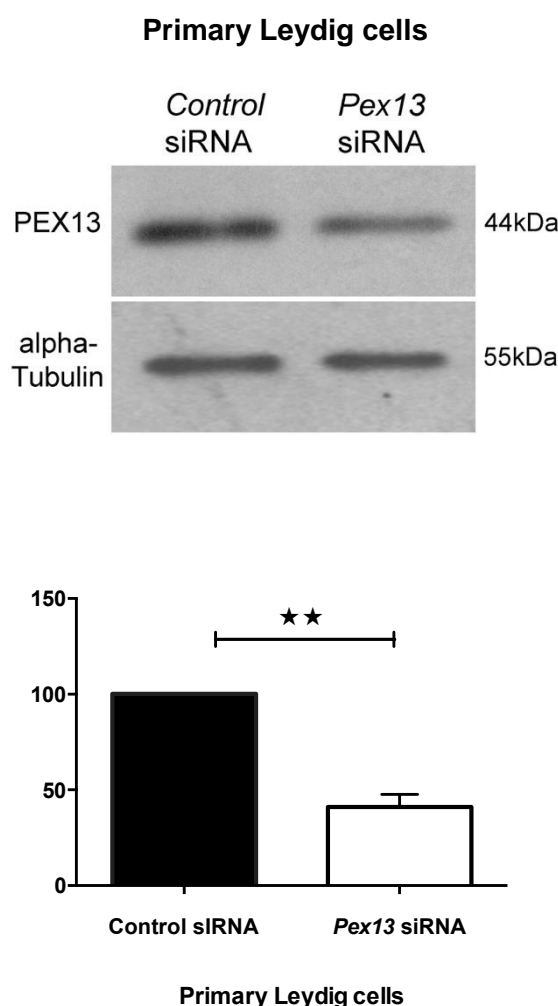


Figure 21: Western blot analysis for the peroxisomal biogenesis protein PEX13 in mouse primary Leydig cells transfected with *Pex13* siRNA. Total protein (20 μ g) from primary Leydig cells were loaded in each lane on 12.5% SDS gels. First the membrane was incubated with antibody against PEX13. The same blot was stripped and reprobed for the localization of α tubulin as an internal control. Chemiluminescent signals were visualized and quantified through ImageJ. Data are representative of results obtained from three independent experiments. (* $p \leq 0.05$, ** $p \leq 0.01$, **** $p \leq 0.001$) (N=3).

Similarly, primary Leydig cells transfected with *Pex13* siRNA showed significantly reduced amount of PEX13 approximately by 60% in comparison to control siRNA transfected cells (Fig. 21).

4.6.5. hCG-induced up-regulation of StAR is inhibited in primary Leydig cells with *Pex13* knockdown

After demonstration of a strong decrease of hCG-stimulated StAR protein expression in MLTC-1 cells transfected with *Pex13*shRNA, we were interested to check hCG-stimulated StAR protein expression in primary Leydig cells after *Pex13* knockdown. Primary Leydig cells were treated with hCG after 48 h of transfection with *Pex13*siRNA. Followed the treatment, cells were processed for total protein isolation and the media were collected for steroid hormones assay by radioimmunoassay and by ELISA.

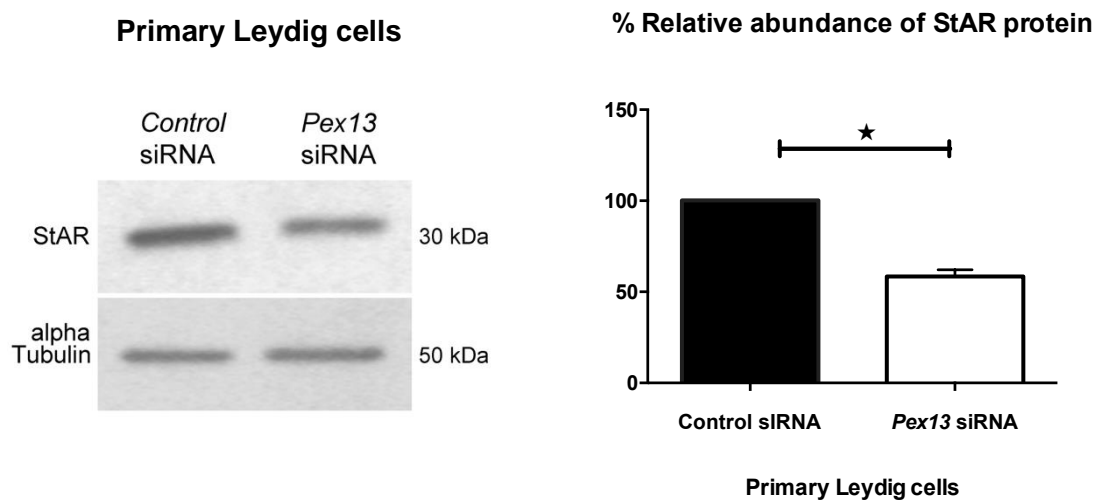


Figure 22. Western blot analysis for StAR abundance in response to hCG treatment after *Pex13* knockdown in mouse primary Leydig cells. Total protein (20µg) from primary Leydig cells were loaded in each lane on 12.5% SDS gels. First the membrane was incubated with antibody against StAR. The same blot was stripped and reprobed for the localization of α Tubulin as an internal control. Chemiluminescent signals were visualized and quantified through ImageJ. Values represent the fold reduction of StAR normalized to α Tubulin from three independent experiments (* $p \leq 0.05$, ** $p \leq 0.01$, **** $p \leq 0.001$) (N=3).

Indeed, also the *Pex13*-RNAi technology in primary Leydig cells induced peroxisomal deficiency in primary Leydig cells leading to a decrease of hCG-mediated induction of 30 kDa intramitochondrial form of StAR (Fig. 22).

4.7. *Pex13* knockdown reduces progesterone secretion in response to hCG treatment in MLTC-1 and in primary Leydig cells

Next the cell culture supernatant from Leydig cells with *Pex13* knockdown were collected for steroid hormones assay by radioimmunoassay and by ELISA. After transport of cholesterol via StAR into the inner mitochondrial membrane, cholesterol is converted to pregnenolone by mitochondrial P450_{scc}. Subsequently, pregnenolone is processed to progesterone by 3 β -HSD. Since knock down of *Pex13* in MLTC-1 cells and in primary Leydig cells leads to a significant decrease of hCG-mediated StAR protein expression, we hypothesized that downstream progesterone production would be also impaired in peroxisome deficient Leydig cells.

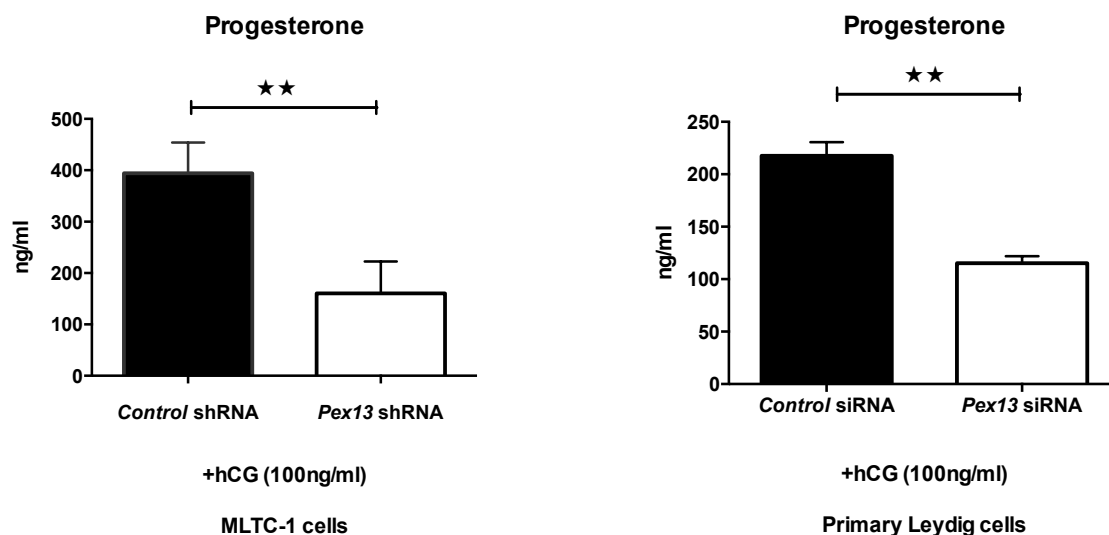


Figure 23. RIA for detection of progesterone in MLTC-1 cells and primary Leydig cells with *Pex13* knockdown. Media were collected from MLTC-1 cells transfected with the indicated shRNA for 72 hours followed by treatment with hCG (100 ng/ml) for 6 h. (B) Media were collected from primary Leydig cells transfected indicated siRNA for 48 hours followed by treatment with hCG (100 ng/ml) for 6 h for steroid hormones assay by RIA. After

treatment, media were collected and subjected to a progesterone production measurement via RIA. Hormone concentration was normalized to protein concentration for each sample. Data are representative of similar results obtained from three independent experiments.

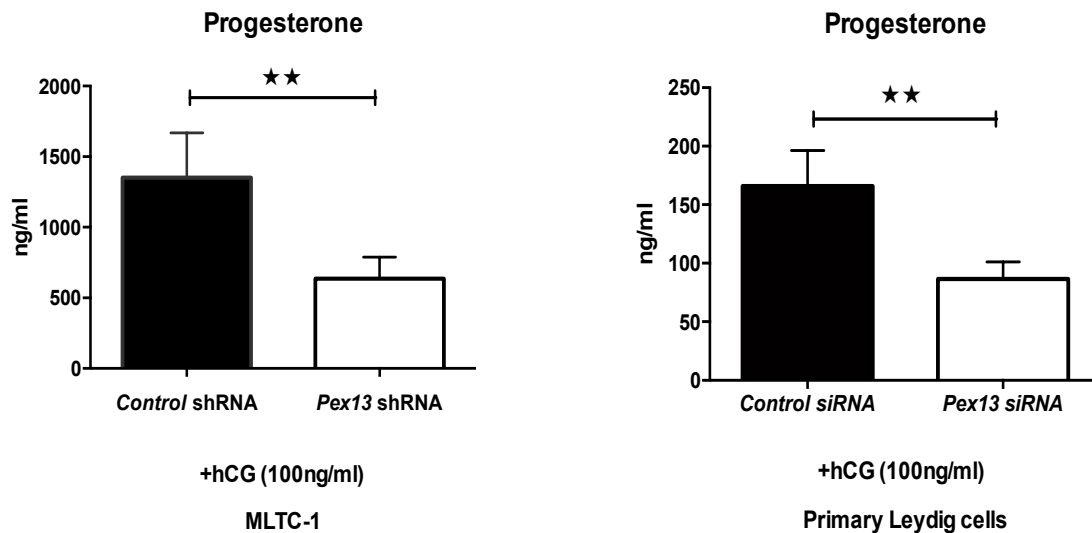


Figure: 24. ELISA for detection of progesterone in MLTC-1 cells and primary Leydig cells with *Pex13* knock-down after treatment with hCG. Media were collected from MLTC-1 and primary Leydig cells with *Pex13* knockdown after treatment with hCG (100 ng/ml) for 6 h for steroid hormones assay by ELISA. Hormones concentrations were normalized to each sample cell pellet protein concentration. Data are representative of similar results obtained from three independent experiments. (* $p \leq 0.05$, ** $p \leq 0.01$, **** $p \leq 0.001$). (N=3)

Accordingly, RIA as well as ELISA revealed that knockdown of *Pex13* in MLTC-1 cells as well as in primary Leydig cells partially inhibited the hCG-stimulated production of progesterone in comparison to the respective controls (Fig. 23 and Fig 24), whereas basal level of progesterone was not changed (results not shown).

4.7.1. Effects of peroxisome deficiency on the activity of P450scc in Leydig cells.

To understand if the decrease in progesterone levels are solely due to the impaired StAR regulation and to test the StAR-independent effects of peroxisome disruption on steroid synthesis we stimulated MLTC-1 cells with 22(R)-hydroxycholesterol

(22R-HC) instead of hCG and the pregnenolone levels were measured. Cholesterol once transported to the mitochondria is converted to pregnenolone by the mitochondrial enzyme P450_{scc}. 22R-HC freely diffuses through the inner mitochondrial membrane without the help of StAR, thereby bypassing the need of StAR function in steroidogenesis. To avoid downstream processing of pregnenolone once it is produced we used the inhibitor of 3 β -HSD (Trilostane), which blocks the conversion of pregnenolone to progesterone. We also pretreated MLTC-1 cells with abiraterone acetate, the inhibitor of P450_{c17} to inhibit the further conversion of pregnenolone to androgens (Fig. 25).

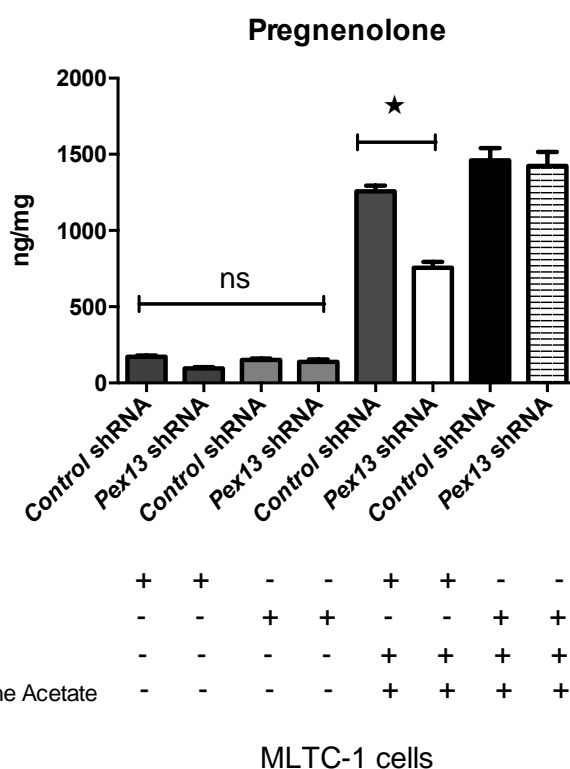


Figure 25. Activity of P450_{scc} in MLTC-1 cells with peroxisome deficiency. MLTC-1 cells were transfected with *Pex13* shRNA and control shRNA. After 72 h of transfection cells were pre-incubated for 30 min with trilostane (5 μ M) and abiraterone acetate (17nM), prior to incubation with hCG (100 ng/ml) and 22R-HC (40 μ M) in serum free media for another 6h. As shown above further conversion of pregnenolone was significantly inhibited in the presence of trilostane and abiraterone. Each sample was collected and subjected

to a progesterone production measurement via ELISA. Hormones concentrations were normalized to each sample cell pellet protein concentration. Results shown are from three independent experiments (* $p \leq 0.05$, ** $p \leq 0.01$, *** $p \leq 0.001$) (N=3).

ELISA measurements revealed that in the presence of trilostane and abiraterone acetate, the pregnenolone production was decreased in *Pex13* shRNA transfected cells stimulated with hCG but not with 22R-HC indicating that the peroxisome knock down in Leydig cells does not influence the activity of P450_{scc} (Fig. 25).

4.7.2. Effects of peroxisomal deficiency on 22R-HC-stimulated progesterone synthesis

To test the effect of peroxisomal disturbance on the activity of 3β -HSD which acts downstream of P450scc we treated MLTC-1 and primary Leydig cells with peroxisome deficiency with 22R-HC. After treatment, the product of 3β -HSD activity, progesterone was measured by ELISA.

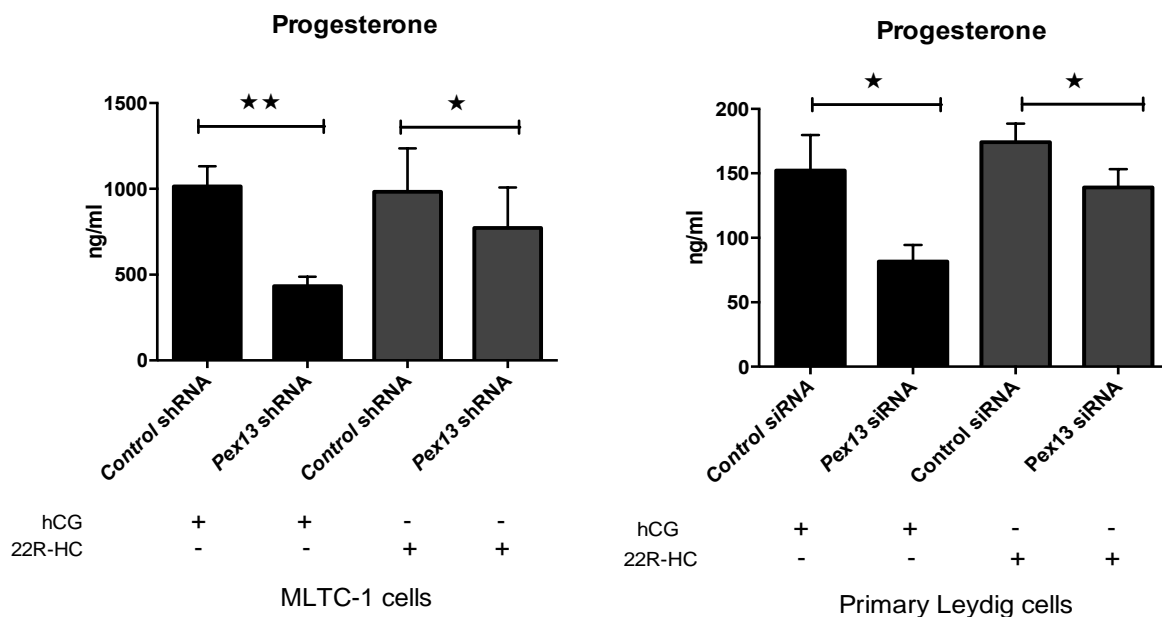


Figure 26. Effects of peroxisomal deficiency on 22R-HC-stimulated progesterone synthesis. MLTC-1 cells after transfection with *Pex13* and control shRNA were cultured in 24 well plates and after 72 hours were treated with 100 ng/ml hCG and 40 μ M 22R-HC for 6 hours. Similarly, primary Leydig cells after transfection with *Pex13* siRNA were treated with above mentioned substances. Following treatment, media were collected and subjected to progesterone production measurements via ELISA. Hormone concentration was normalized to protein concentration for each sample. Data are representative of similar results obtained from three independent experiments (* $p \leq 0.05$, ** $p \leq 0.01$, *** $p \leq 0.001$) (N=3).

As expected, ELISA measurements revealed that in *Pex13*-knockdown cells the amount hCG-induced progesterone was reduced. Surprisingly, the 22R-HC-induced production of progesterone was also significantly reduced although not as strong as

in the case of hCG-mediated progesterone levels in both MLTC-1 cells and primary Leydig cells with *Pex13* knockdown in comparison to the respective control cells (Fig. 26). This finding indicates that peroxisome deficiency in Leydig cells affects 3 β -HSD enzyme activity in both MLTC-1 and in primary Leydig cells independent of StAR.

4.8. *Pex13* knockdown leads to inhibition of testosterone synthesis in MLTC-1 cells and in primary Leydig cells

Since the 22RHC-induced progesterone synthesis was affected in *Pex13* knockdown cells we hypothesized that the downstream steroidogenesis pathways might also be impaired in these Leydig cells. To test this, we measured the final product of steroidogenesis which is testosterone in MLTC-1 cells and primary Leydig cells by RIA as well as by ELISA.

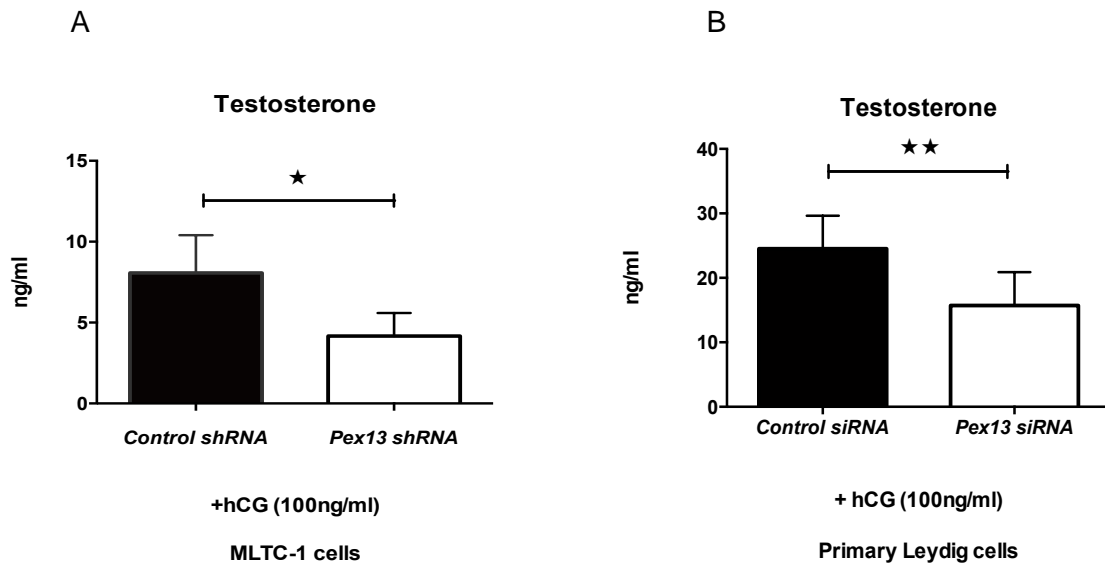


Figure 27. Radioimmunoassay (RIA) for detection of hCG-stimulated testosterone production in MLTC-1 cells and primary Leydig cells with peroxisome deficiency.

(A) Media were collected from MLTC-1 cells transfected with the for 72 hours followed by treatment with hCG (100 ng/ml) for 6 h. (B) Media were collected from primary Leydig cells transfected with *Pex13* siRNA and control siRNA for 48 hours followed by treatment with hCG (100 ng/ml) for 6 h. The collected medium samples were subjected to testosterone production measurements via RIA. Testosterone concentrations were normalized to protein

concentration for each sample. Data are representatives from three independent experiments (* $p \leq 0.05$, ** $p \leq 0.01$, *** $p \leq 0.001$) (N=3).

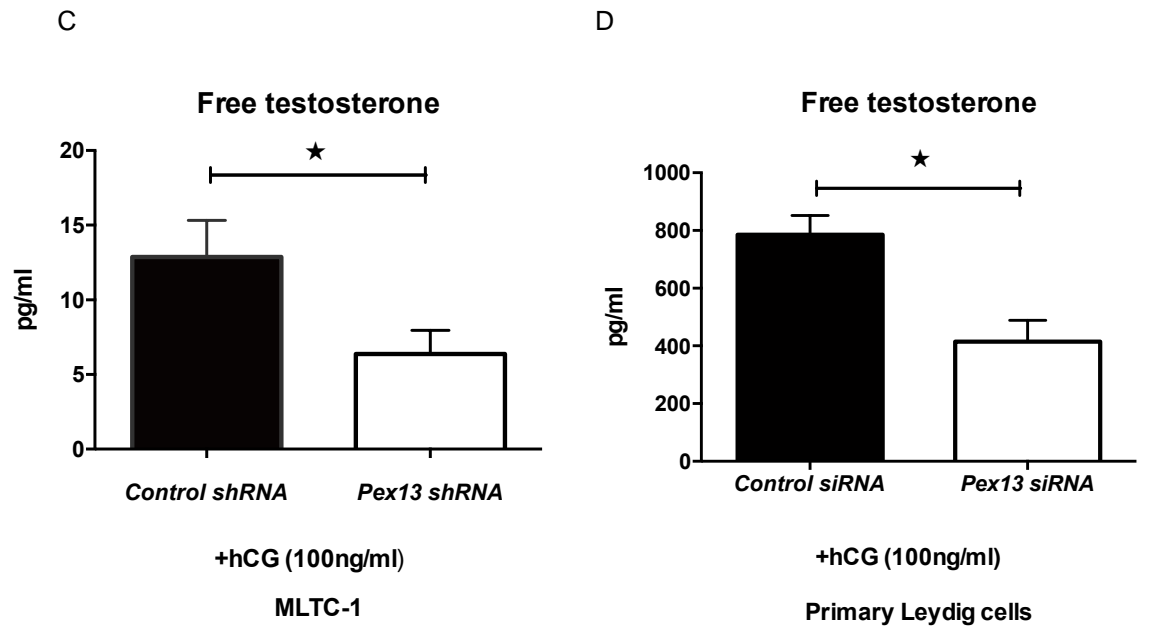


Figure 28. ELISA for detection of testosterone in MLTC-1 cells and primary Leydig cells with *Pex13* knock-down after treatment with hCG as mentioned above. C. Testosterone production in MLTC-1 cells transfected with the *Pex13* shRNA and control shRNA. **D.** Testosterone production in primary Leydig cells transfected with the *Pex13* siRNA and control siRNA.

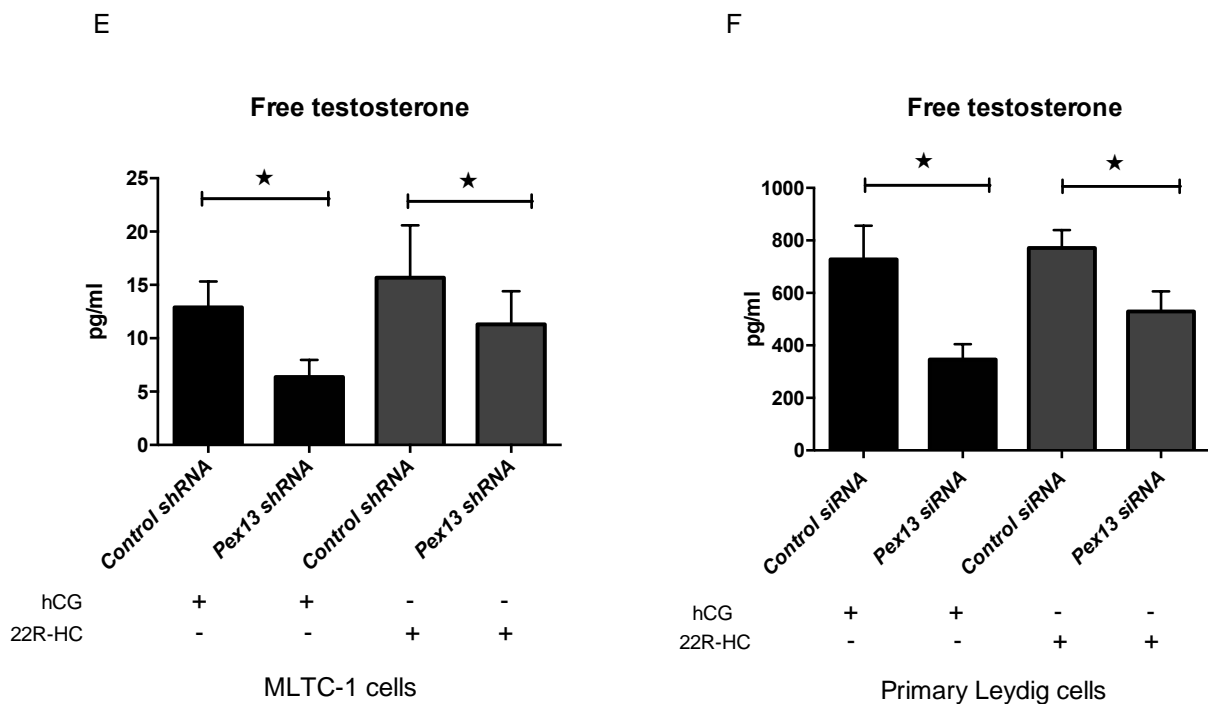


Figure 29. Effects of peroxisome deficiency on 22R-HC-stimulated testosterone secretion. MLTC-1 cells were transfected with *Pex13* shRNA and control shRNA and after 72 h of transfection cells were treated with 100 ng/ml hCG and 40 μ m 22R-HC for 6 hours (E). Similarly, primary Leydig cells after transfection with *Pex13* siRNA were treated with above mentioned substances (F). Following treatment, media were collected and subjected to testosterone level measurements via ELISA. Hormone concentrations were normalized to protein concentration for each sample. Data are representative of similar results obtained from three independent experiments (* $p \leq 0.05$, ** $p \leq 0.01$, *** $p \leq 0.001$) (N=3).

As hypothesized treatment with hCG in *Pex13* knockdown in MLTC-1 cells and in primary mouse Leydig cells led to the inhibition of hCG-stimulated testosterone secretion in comparison to cells transfected with control shRNA (Fig 27 and Fig. 28). Similarly, the 22R-HC-stimulated testosterone secretion was also impaired by the knockdown of *Pex13* in both MLTC-1 and primary Leydig cells (Fig. 29). These results suggest that the *Pex13* knock down in Leydig cells affects steroidogenesis downstream of StAR activity (3 β -HSD, P450c17 and 17 β -HSD) in Leydig cells.

4.9. A down regulation of *Pex13* leads to an inhibition of DHEA production in Leydig cells

Similarly, as described in previous paragraphs, we measured also the level of DHEA in *Pex13* knockdown MLTC-1 and in primary Leydig cell after treatment with hCG and 22R-HC.

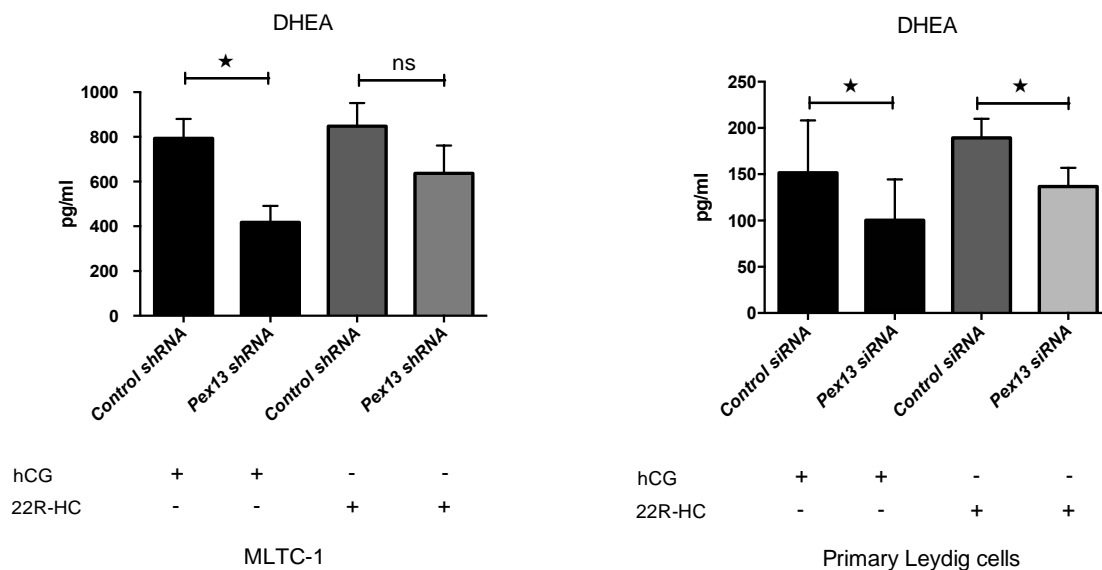


Figure 30: Effects of *Pex13* knockdown on hCG and 22R-HC-stimulated DHEA secretion in Leydig cells. MLTC-1 cells were transfected with *Pex13* shRNA and control shRNA. After 72 h of transfection cells were treated with 100ng/l hCG and 40 μ M 22R-HC for 6 hours. Similarly, primary Leydig cells after transfection with *Pex13* siRNA were treated with the above mentioned substances. Following treatment, media were collected and subjected to estradiol level measurements via ELISA. Hormone concentrations were normalized to protein concentrations for each sample. Data are representative of similar results obtained from three independent experiments (* $p \leq 0.05$, ** $p \leq 0.01$, *** $p \leq 0.001$) (N=3).

Results show, that *Pex13* knock down in Leydig cells leads to lower levels of hCG- as well as 22R-HC stimulated DHEA production (Fig. 30).

4.10. Detection of reactive oxygen species in MLTC-1 cells

To elucidate the underlying mechanisms by which steroidogenesis is affected by peroxisomal disturbances we analyzed the production of ROS after *Pex13* knockdown in MLTC-1 cells. It is well known that peroxisomes play an important role in both the generation and scavenging of ROS in the cell and increased oxidative stress has been linked to disrupted steroidogenesis in different studies (Diemer, et al. 2003; Zhou, et al. 2013).

4.10.1. Decrease of reduced glutathione levels in MLTC-1 cells with *Pex13* knock down

At first we measured cellular glutathione levels in control shRNA and *Pex13* shRNA transfected MLTC-1 cells. Glutathione (GSH) is an important endogenous antioxidant produced by the cells, which participates directly in the neutralization of free radicals and prevents damage to cells caused by reactive oxygen species. Glutathione exists mostly in the reduced state, which usually donates an electron to a reactive oxygen species to minimize or reduce them. After losing an electron glutathione is converted to its oxidized form, glutathione disulfide (GSSG). So, a decreased amount of reduced glutathione levels would indicate increased cellular ROS levels.

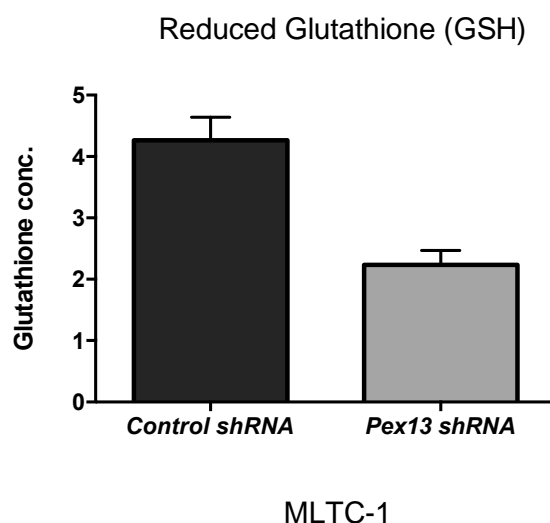


Figure 31. GSH-Glo™ Glutathione Assay in MLTC-1 cells with *Pex13* knockdown.

MLTC-1 cells transfected with *Pex13* shRNA and control shRNA were cultured in a 96-well plate. After 72 h of transfection, culture medium was removed from the plate and prepared GSH-Glo™ Reagent was added. Following 30min incubation

reconstituted Luciferin Detection Reagent was added to the plate. After a 15min incubation, the plate was read in a luminometer for quantitative determination of reduced GSH levels in cells.

As shown in figure 31 the amount of reduced GSH was significantly reduced in *Pex13* shRNA transfected cells indicating increased oxidative stress in these cells.

4.10.2. Detection of increased ROS production by DHE staining in MLTC-1 cells with *Pex13* knockdown

As an alternative approach increased ROS production was also determined by staining MLTC-1 cells with the fluorescent-dye, DHE as described in Materials and Methods (Chapter 2.8.). DHE is used in different studies to evaluate ROS production, particularly superoxide production in viable cells (Ahlemeyer, et al. 2012). DHE is dehydrogenated to ethidium upon reaction with superoxide anions and stains the nucleus.

Results show that the *Pex13* knockdown in MLTC-1 cells led to an increase in the staining intensity of DHE in the cytoplasm as well as in the nuclear region of some cells (Fig. 32). Especially the nucleus was brighter in *Pex13* shRNA transfected cells in comparison with MLTC-1 cells transfected with control shRNA. In short, this finding confirms the increased presence of ROS (mainly O_2^-), in MLTC-1 cells transfected with *Pex13* shRNA.

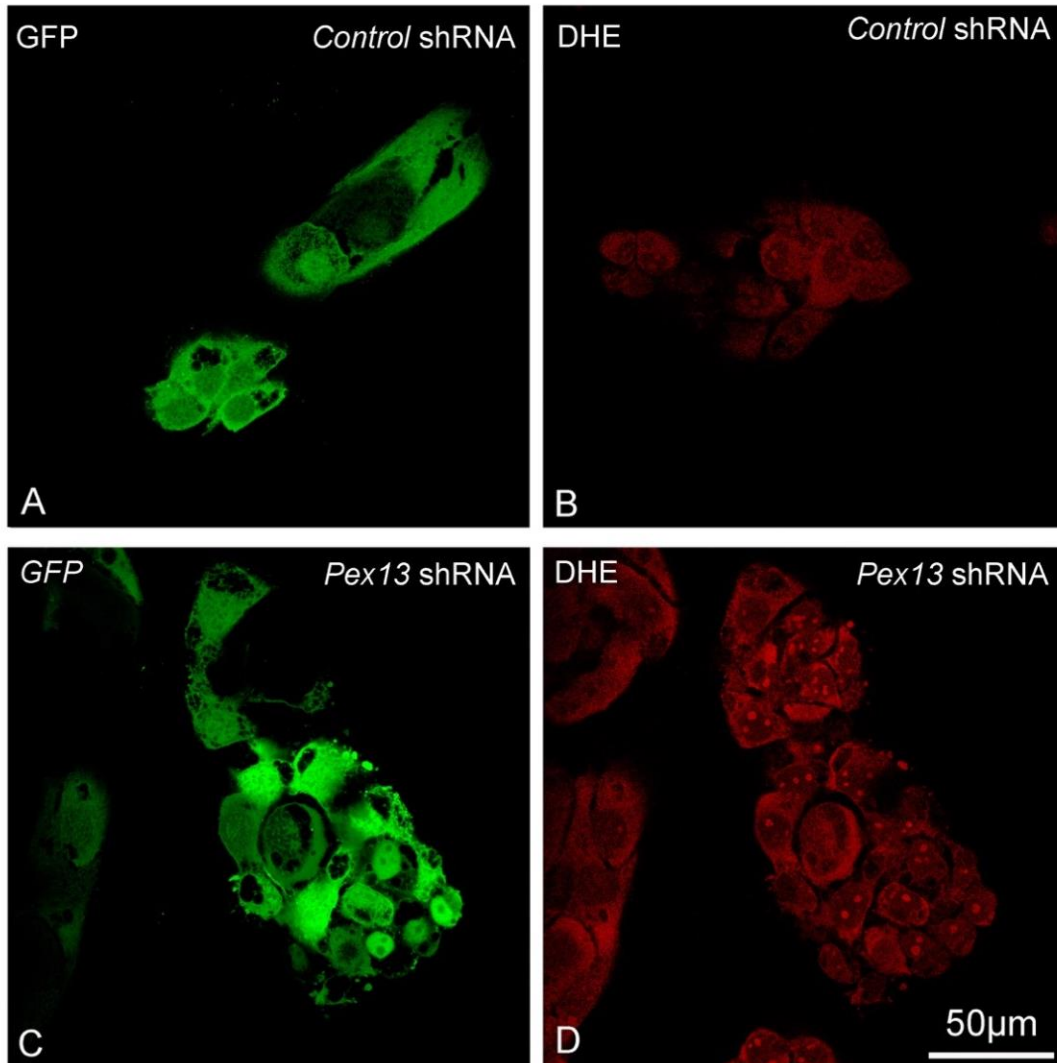


Figure 32. ROS detection by staining with DHE in MLTC-1 cells with *Pex13* knockdown.

MLTC-1 cells were transfected with *Pex13* shRNA and control shRNA. Following the shRNA transfection, the cells were stained with DHE for 30 min. Pictures were taken by confocal laser scanning microscopy (CLSM). Bars represent in A-D: 50µm. Representative pictures were obtained from 3 different experiments.

4.11. *Pex13* knockdown leads to alterations in antioxidative enzymes levels as well as catalase activity in MLTC-1 cells

Next, we hypothesized that the increased presence of ROS would alter the expression of antioxidative enzymes in *Pex13* shRNA transfected cells. To test this, we first analyzed the protein abundance of catalase, which is one of the most potent cellular antioxidative enzymes and is localized in the peroxisomes under normal conditions. Interestingly, the expression of catalase was drastically decreased in cells transfected with *Pex13* shRNA in comparison to control cells revealed by WB analysis (Fig. 33).

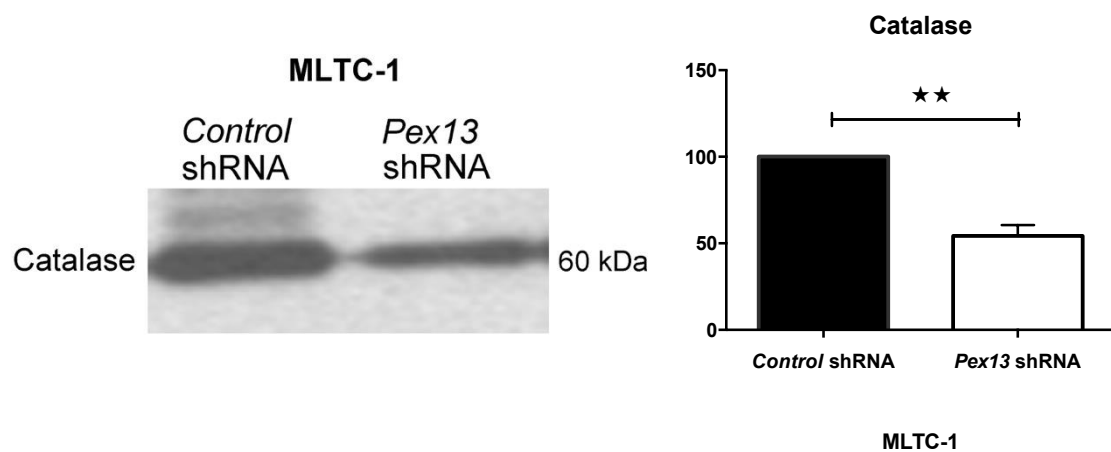


Figure 33. Western blot analysis for catalase in transfected MLTC-1 cells with *Pex13* shRNA and control shRNA. MLTC-1 cells were transfected with *Pex13*-shRNA and control shRNA. After 72 h of transfection, cells were lysed and twenty micrograms of proteins were loaded in each lane on 12.5% SDS gel. Data are representatives of similar results obtained from three independent experiments.

Next, to determine whether the observed protein reduction of catalase could reflect the enzymatic capacity we performed catalase activity assays.

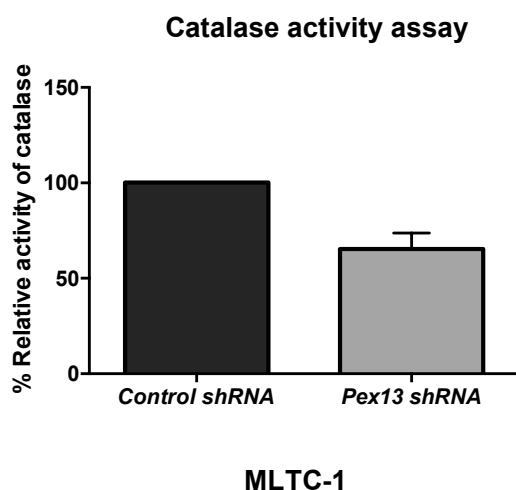


Figure 34. Catalase activity assay

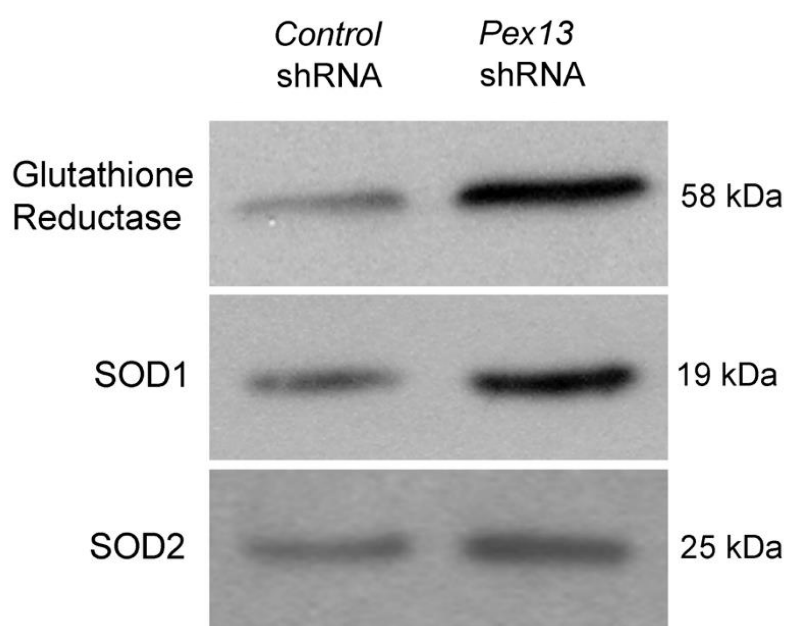
MLTC-1 cells after 72 h of transfection with *Pex13* and control shRNA were centrifuged at 2, 000 x for 10 min at 4 °C. Thereafter, cell pellet was homogenized on ice in 2 ml cold buffer containing 50 mM potassium phosphate, pH 7.0, containing 1 mM EDTA and then centrifuged at 10,000 x g for 15 minutes at 4°C. Supernatant was removed and stroed on ice for assay as described in Materials and Methods (Chapter 2.9.).

Catalase activity was measured according to the protocol (Catalase Assay Kit) using a plate reader with a 540 nm filter. In three independent experiments catalase activity was found to be reduced.

Results indicate that catalase activity was reduced in MLTC-1 cells with *Pex13* knockdown in comparison to control cells (Fig 34).

Finally, we also compared the expression of a series of other antioxidative enzymes such as cytoplasmic SOD-1, mitochondrial SOD-2 and the glutathione reductase, which were up-regulated in cells transfected with *Pex13* shRNA (Fig. 35).

A



B

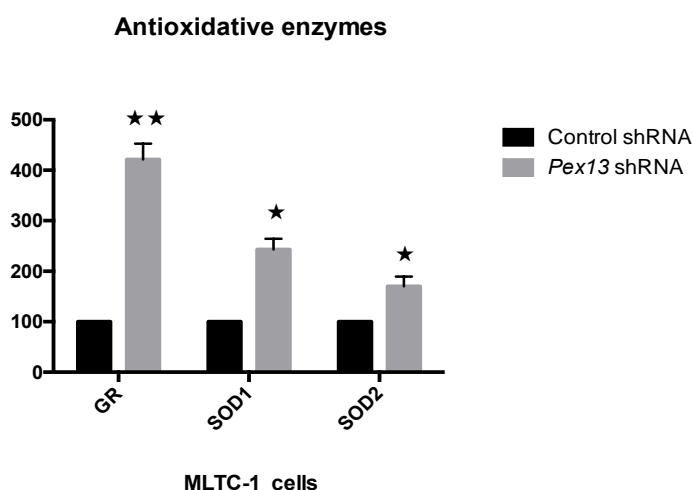


Figure 35. Western blot analyses for antioxidative enzymes in MLTC-1 cells transfected with *Pex13* shRNA and control shRNA.

MLTC-1 cells were transfected with *Pex13*-shRNA and control shRNA. After 72 h of transfection cells were lysed and twenty micrograms of proteins were loaded in each lane on 12.5% SDS gels. A. glutathione

reductase; superoxide dismutase 1(SOD1); superoxide dismutase 2 (SOD2). B. Quantification of the blots calculated from three independent experiments (ImageJ).

To summarize, the knockdown of *Pex13* in MLTC-1 cells leads to oxidative stress and causes an altered expression of antioxidative enzymes in *Pex13* shRNA transfected MLTC-1 cells.

4.12. Knockdown of *Pex13* induces mitochondrial dysfunction in MLTC-1 cells

Peroxisomes and mitochondria are closely linked organelles in several different metabolic pathways particularly in β -oxidation of specific fatty acids. It has been shown that peroxisomal knockouts often suffer from mitochondrial dysfunction (Baumgart et al. 2001). To test if *Pex13* knockdown leads to mitochondrial dysfunction in MLTC-1 cells, we performed assays to determine the mitochondrial membrane potential using the DePsipher™ Kit. This Kit uses a special cationic dye to detect the loss of the mitochondrial membrane potential. It can readily enter cells and form an orange-red fluorescent compound within healthy mitochondria. If the mitochondrial membrane potential is disturbed, the dye cannot reach the transmembrane space and remains in cytoplasm. Healthy mitochondria show red fluorescence, whereas when the mitochondrial membrane potential is disturbed the dye remains primarily green in its monomeric form.

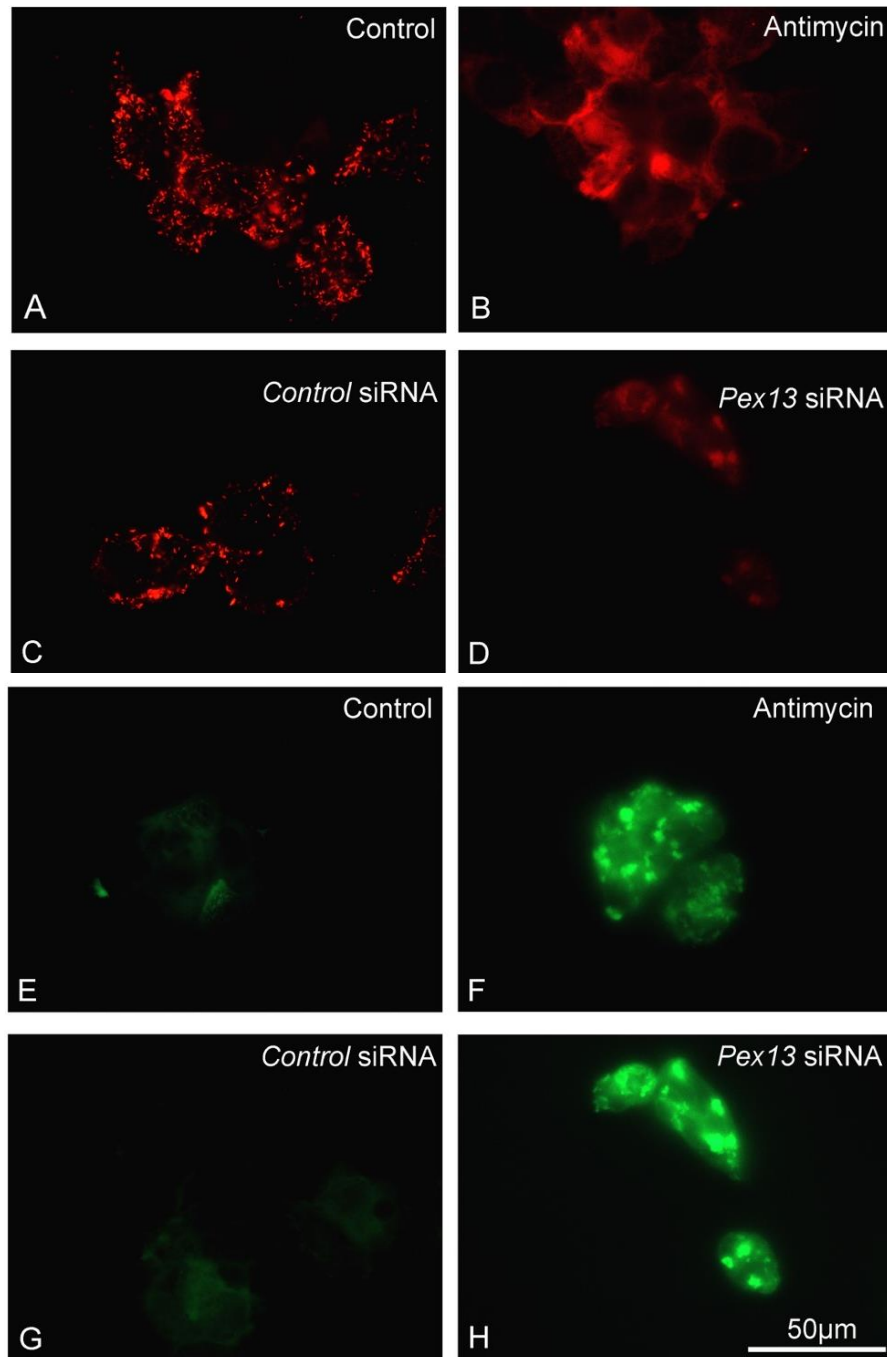


Figure 36. Mitochondrial membrane potential assay. A,E: Control MLTC-1 cells, B,F: MLTC-1 cells treated with Antimycin A. C,G: MLTC-1 cells transfected with control siRNA, D,H: MLTC-1 cells transfected with *Pex13* siRNA. Cells were incubated with medium containing DePsipher (25 µg/ml) for 30 min at 37 °C. Green fluorescence represents mitochondria with disturbed membrane potential. Bars represent in A-H: 50µm. Representative pictures were obtained from 3 different experiments.

The mitochondria of both control and *Pex13* knockdown MLTC-1 cells exhibited different patterns of red fluorescence signals. Untreated and unstimulated MLTC-1 cells taken as a control group showed a similar mitochondrial pattern as MLTC-1 cells transfected with control siRNA, indicating an intact mitochondrial potential in those cells (Fig 36 A,C,E,G). In contrast, cells with peroxisome deficiency due to the transfection with *Pex13* siRNA and cells treated with antimycin A exhibited an unspecific pattern, indicating the disturbance of mitochondrial membrane potential (Fig. 36 B,D,F,G). Antimycin A, a complex III inhibitor of the mitochondrial respiratory chain was used as a positive control to show the disturbed mitochondrial membrane potential. Moreover, an accumulation of green fluorescence signals was also noted in MLTC-1 cells with the *Pex13* knockdown and in cells treated with antimycin A indicating the increased presence of the monomeric form of the dye. In contrast, the untreated control group of MLTC-1 cells as well as MLTC-1 cells transfected with control shRNA showed only very weak green fluorescent signals (Fig. 36). This finding indicates that the mitochondrial membrane potential was reduced in MLTC-1 cells with peroxisome deficiency.

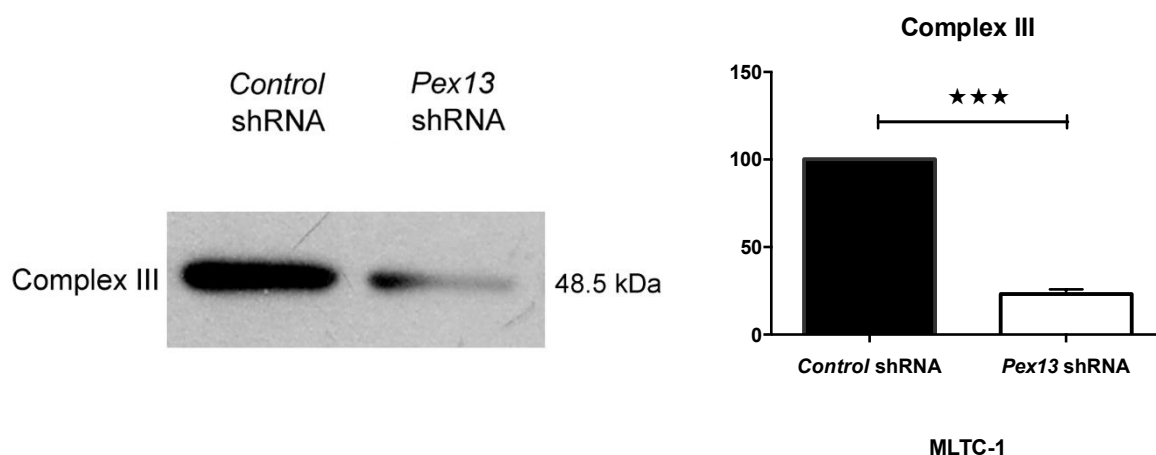


Figure 37. Western blot analysis for mitochondrial complex III of the respiratory chain in MLTC-1 cells transfected with *Pex13* shRNA and control shRNA.

Complex III: mitochondrial complex III of the respiratory chain. Cells were lysed and twenty micrograms of proteins were loaded in each lane on 12.5% SDS gels. Data are representative of similar results obtained from three independent experiments.

Further, we performed Western blot analyses for complex III of the mitochondrial respiratory chain and as shown in figure 37 the protein abundance of complex III was significantly reduced in MLTC-1 cells transfected with *Pex13* shRNA in comparison to cells transfected with control shRNA. To summarize, these results indicate the presence of mitochondrial dysfunction in *Pex13* shRNA transfected cells.

4.13. Mitochondrial dysfunction impairs hCG-induced as well as 22R-HC-mediated steroid synthesis in MLTC-1 cells.

Next, to test if mitochondrial dysfunction can lead to impaired steroid synthesis in Leydig cells we pretreated MLTC-1 cells with the complex III inhibitor antimycin A before stimulating with hCG and 22R-HC.

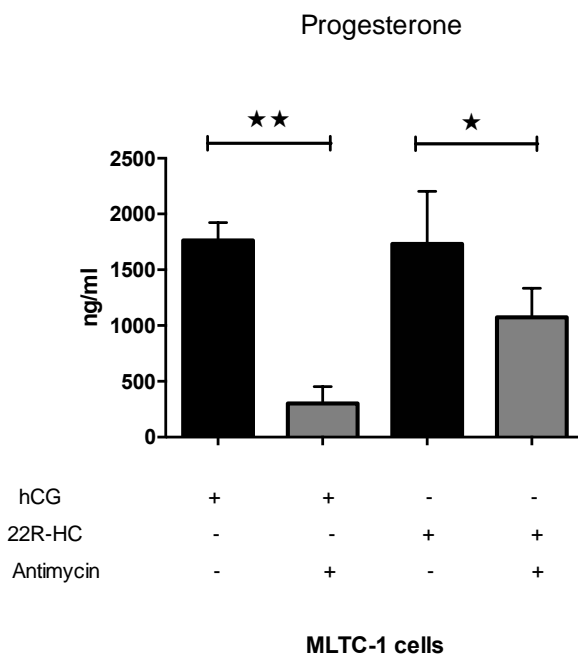


Figure 38. Effect of antimycin A in steroid synthesis in MLTC-1 cells after treatment with hCG and 22R-HC.

MLTC-1 cells were stimulated with hCG and 22R-HC in the presence and in the absence of the inhibitor antimycin A (5 μ M) for 1h. After 3h of stimulation progesterone production in the incubation medium was measured by ELISA and data are shown as progesterone concentration (ng/ml). The results are obtained from three independent experiments. *P \leq 0.05; **P \leq 0.01;

Progesterone measurements by ELISA revealed that hCG as well as 22R-HC-mediated progesterone production was decreased after antimycin-A treatment in MLTC-1 cells (Fig. 38). To summarize, these findings indicate that mitochondrial dysfunction in MLTC-1 cells may lead to disturbed steroid synthesis.

4.14. *Mfp2* siRNA transfection in primary Leydig cells

Different 17 β -HSDs participate in the process of steroid synthesis as well as inactivation, modulating the biological potency of estrogens and androgens by conversion at position 17. It has been shown earlier that the 17 β -HSD4 also known as peroxisomal multifunctional protein 2 (Mfp-2) is the only 17 β -HSD found in peroxisomes (Carstensen et al. 1996; Normand et al. 1995; Novikov et al. 1997). To further investigate the role of Mfp2 in steroidogenesis, we were interested to knockdown the expression of the *Mfp2* gene in primary Leydig cells. Therefore, primary Leydig cells were transfected with *Mfp2* siRNA and control siRNA as described in Materials and Methods (2.4.3., Fig. 10).

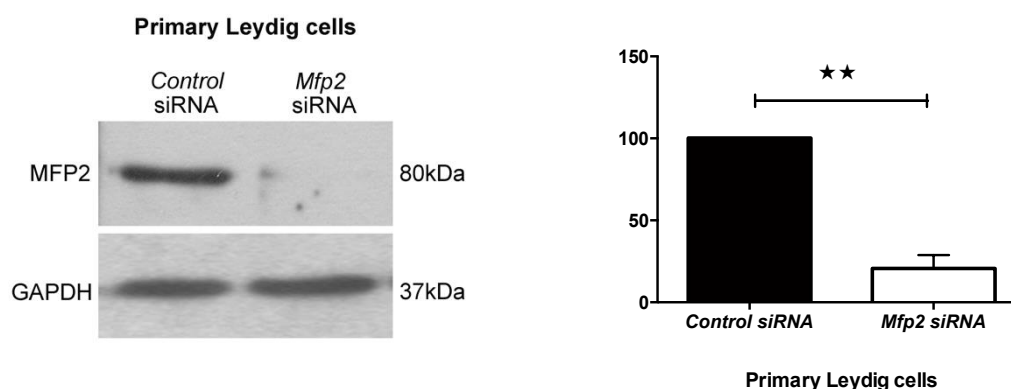


Figure 39. Western blot analysis for peroxisomal multifunctional protein 2 (MFP2) in mouse primary Leydig cells transfected with *Mfp2* siRNA. Primary Leydig cells were transfected with *Mfp2* siRNA and control siRNA. After 48 h of transfection total protein (15 μ g) from primary Leydig cells was subjected to subjected and loaded in each lane on 12.5% SDS gels. First the membrane was incubated with antibody against MFP2. The same blot was stripped and reprobbed for GAPDH the as an internal control. Chemiluminescent signals were visualized and quantified through ImageJ. Data are representative of similar results obtained from three independent experiments. (* $p \leq 0.05$, ** $p \leq 0.01$, **** $p \leq 0.001$) (N=3).

Western blot results show, that transfection with *MFP2* siRNA significantly reduced the expression of *MFP2* in primary Leydig cells in comparison to control siRNA transfected cells. The strongest knockdown of *MFP2* protein expression was found after 48 h of transfection (Fig. 39).

4.14.1. *Mfp2* knock down in Leydig cells leads to an inhibition of DHEA production.

The role of 17 β -HSD4 in different steps of steroidogenesis remains controversial. It has been shown earlier that isolated 17 β -HSD4 oxidized 5-androstene-3 β , 17 β -diol to DHEA in Leydig cells (Adamski et al., 2000). To evaluate the role of MFP2 in DHEA synthesis, primary Leydig cells were transfected with *Mfpsi* and control siRNA as described above and stimulated with hCG for 6 h. Thereafter, medium was subjected to DHEA level measurements via ELISA.

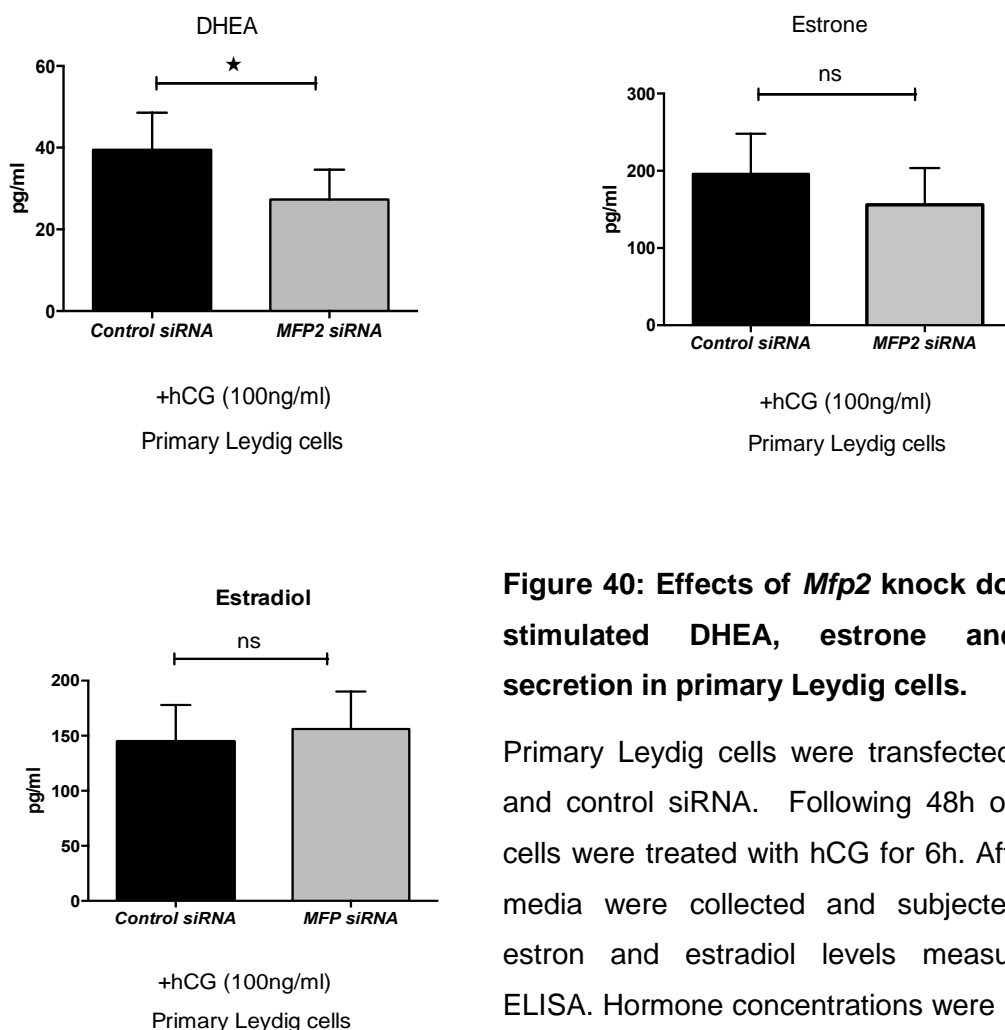


Figure 40: Effects of *Mfp2* knock down on hCG-stimulated DHEA, estrone and estradiol secretion in primary Leydig cells.

Primary Leydig cells were transfected with *Mfp2si* and control siRNA. Following 48h of transfection cells were treated with hCG for 6h. After treatment, media were collected and subjected to DHEA, estron and estradiol levels measurements via ELISA. Hormone concentrations were normalized to protein concentrations for each sample. Data are

representatives of similar results obtained from three independent experiments

Hormone measurement showed that down regulation of *MFP2* leads to the inhibition of DHEA secretion in Leydig cells. However, the estrone and estradiol levels were not affected by the *Mfp2* knockdown in primary Leydig cells (Fig. 40).

5. Discussion

Infertility is a global health issue, affecting approximately 10-15% of couples worldwide. Nature and exact proportion of the prevalent cause of the infertility is still controversial, however, the male partner is thought to be involved in 50% of cases. Even though the treatment of infertility has been largely improved, the genetic and molecular causes of male infertility are still elusive. The dysfunction of Leydig cells in testis is proposed to be a factor leading to infertility since Leydig cells are involved in steroid synthesis, particularly testosterone, which primary function is to maintain spermatogenesis.

Interestingly, human disorders with peroxisomal deficiency show a range of testicular pathologies leading to male infertility; the molecular pathogenesis of which is not yet understood (Aversa et al. 1998; Powers 1985; Powers and Schaumburg 1981). Previously we have characterized the peroxisomal protein composition in distinct cell types of mice and human testis, and have demonstrated that peroxisomes are abundant in both Leydig cells and Sertoli cells (Neniciu et al. 2007). Moreover, different studies have demonstrated that peroxisomes are essential for Sertoli cell functioning (Huyghe et al. 2006a; Neniciu 2010). However, till now only sparse information is available on the role of peroxisomes in Leydig cells. Mendis-Handagama and colleagues showed that LH/hCG treatment in Leydig cells increased the peroxisomal volume, intraperoxisomal SCP-2 content, whereas, LH deprivation resulted in a strong reduction in the number of these organelles (Mendis-Handagama 2000; Mendis-Handagama et al. 1992; Mendis-Handagama, et al. 1998; Mendis-Handagama et al. 1990a). In this thesis work we have extended these findings and we report that peroxisomes play a crucial role in steroidogenesis of murine Leydig cells. Furthermore, we demonstrate that peroxisomal dysfunction leads to an impaired regulation of the cholesterol transport protein StAR in mitochondria and leads to decreased production of hCG-stimulated testosterone.

5.1. Mouse Leydig tumor cells (MLTC-1 cells) produce steroids, including testosterone

Cell lines of various cell types are frequently used in literature for functional studies, and are a good research tool to perform multiple experiments. They can be expanded without limitation and are easy to culture. The mouse Leydig tumor cell lines MA-10 and MLTC-1 cells are derived from the transplantable and the hormonally responsive murine Leydig cell tumor designated as M5480, originating in a C57B1/6J mouse (Moyle and Ramachandran 1973; Neaves 1975). Two different subtypes of M5480 tumor were later identified: M5480A, which synthesize progesterone and androgens, and M5480P, which mainly produce progesterone. MA-10 (Ascoli 1981a, b; Ascoli and Puett 1978) and MLTC-1 cells (Rebois 1982) originate from M5480P and are the best characterized Leydig tumor cell lines so far.

Rebois et al. established the MLTC-1 cell line, where only hCG-stimulated progesterone production was measured. Measurements of other steroids were not done because of previous studies reporting minimal secretion of testosterone or androstenedione by M5480P cells, due to the loss of P450c17 (Cyp17) (Ascoli and Puett 1978; Lacroix, et al. 1979). It was also previously shown that originally M4580 cells were able to produce high levels of progesterone and androstenedione, but a low level of testosterone. Later with time these tumor cells started to synthesize mostly progesterone (Ascoli 1981a; Lacroix et al. 1979; Moyle and Ramachandran 1973). Later Panesar and colleagues showed that MLTC-1 cells produce progesterone as well as low concentration of androstenedione and testosterone (Panesar, et al. 2003). From the literature, it is known that both cell lines of MA-10 and MLTC-1 cells exhibit normal Leydig cell feature, but the expression of mRNA and activity of Cyp17, 17- β -HSDs and aromatase are insignificant. They produce large amount of progesterone and very small amounts of DHEA, testosterone, estradiol and estrone (Mellon and Vaisse 1989).

In our study, we demonstrated that MLTC-1 cells, purchased from ATCC (CRL-2065), express the key enzymes and important steroidogenic carrier proteins involved in steroid synthesis: Star, P450scc, 3 β -HSD, as well as Cyp17, 17 β -HSD4 and aromatase.

Previously it was reported that MA-10 cells don't express P450c17 and produce only progesterone (Mellon and Vaisse 1989). But our study indicates that under adequate cell culture conditions MA-10 cells express almost all steroidogenic enzymes, including the P450c17 gene. However, in contrast to MLTC-1 cells, MA-10 cells lacked the expression of aromatase. Moreover, MA-10 cells in culture formed clusters and their proliferation rate was low. In conclusion, these findings suggest that although MA-10 cells express P450c17, the MLTC-1 cell line is a better model to study steroidogenesis.

MLTC-1 cells have been extensively used in research to study the first steps of steroid synthesis because of their ability to respond to LH/hCG treatment and because they express the key genes of steroidogenesis: StAR, P450scc and 3 β -HSD (Manna, et al. 2004). Our findings are consistent with these reports, and state that MLTC-1 cells respond efficiently to hCG treatment. After hCG stimulation, the expression of StAR and P450scc was found to be up-regulated at the mRNA and protein levels. MLTC-1 cells also express high levels of LHr, which is the first target for LH/hCG to stimulate steroid synthesis. Our findings indicate that LHr mRNA expression is downregulated in response to hCG stimulation, which is in agreement with the previous report that the loss of steady-state levels of LHr mRNA in the hCG-induced state was due to a post transcriptional mechanism with increased degradation of the LHr mRNA (Menon, et al. 2004).

It is widely accepted that MLTC-1 cells produce mainly a high level of progesterone, because they do not contain the final two enzymes necessary for downstream steroid synthesis: P450c17 and 17 β -HSDs. But the results of this thesis indicate that MLTC-1 cells, besides producing high levels of progesterone, also have the capability to synthesize low levels of testosterone. Moreover, MLTC-1 cells produce high levels of androstenedione, as well as DHEA, upon hCG stimulation. Hence, we postulate that the conversion of progesterone and pregnenolone to downstream hormone synthesis is due to the expression of the P450c17 enzyme in MLTC-1 cells. However, RIA and ELISA analysis confirmed that the amount of progesterone produced by MLTC-1 cells was considerably higher (approximately 250-fold more) than that of the testosterone. Very low expression of 17 β HSD3 in MLTC-1 cells might explain the low level of testosterone converted from androstenedione. Finally, for the first time in this thesis it was reported that, besides progesterone and

androgens, MLTC-1 cells are capable of producing estrogens, estradiol and estrone, also confirming the expression and activity of aromatase, as well as different 17β HSDs genes. In summary, our study suggests that the Leydig tumor cell line MLTC-1 is also a suitable *in vitro* model to study the downstream steps of steroidogenesis in Leydig cells.

5.2. Primary Leydig cell culture

Compared to Leydig tumor cell lines, isolated Leydig cells in primary cells culture are a superior model, which is closer to the *in vivo* situation, and more importantly are considered to be better and more reliable than cell lines, as they maintain normal cell morphology and functions seen *in vivo*. In addition, experiments with primary Leydig cells are generally done to study the downstream steroid synthesis compared to Leydig tumor cell lines. Steroid synthesis in Leydig cells is regulated dominantly by LH/hCG produced by pituitary. Steroid synthesis can be modulated by different growth factors, steroids or cytokines through endocrine, autocrine and paracrine regulation or cell-cell interactions in the testis (Huleihel and Lunenfeld 2004; Matsumoto and Bremner 1989; Roser 2008; Sharpe, et al. 1990). In order to study the exact function of peroxisomes in Leydig cells it was necessary to establish a primary culture model, because in a whole body, for example in an animal model, such as mouse, it is difficult to observe whether the increased or decreased hormone production is due to the impaired steroid synthesis specifically in Leydig cells or because of other regulatory factors or disrupted function of other testicular cell types, which might have an influence on Leydig cell functioning.

After collagenase dissociation of decapsulated testis with some modifications of the method of Schumacher (Schumacher et al. 1978) we were able to obtain highly purified (80-90%) and viable populations of Leydig cells, using percoll gradient centrifugation. Following centrifugation, Leydig cells were isolated from the third band; it was crucial to wash cells three times to avoid further degenerative effect of collagenase on the cells. After isolation to stimulate their proliferation Leydig cells were directly cultured with serum supplemented medium for 24h, considering that Leydig cell proliferation, besides LH, is regulated by growth factors through endocrine, paracrine and autocrine mechanisms. LH, together with locally produced

growth factors, stimulates the proliferation and differentiation of Leydig cells, whereas LH alone exhibits a little effect (Khan, et al. 1992).

Thereafter, cells were incubated in special serum-free Leydig cell medium with daily change of the culture medium, as described in Materials and Methods (Chapter 2.1.2). In response to LH/hCG stimulation primary Leydig cells in the culture lose their ability to synthesize testosterone after a few days due to reduction of steroidogenic enzymes and LHr receptor activity (Chen et al. 2002; Hsueh 1980; Janszen et al. 1976; Klinefelter et al. 1987). After 3 days, the LHr mediated response of primary cultures of rat Leydig cells was described to be weak (Shiraishi und Ascoli 2007). In the present study, we were able to maintain mouse Leydig cells in primary culture with their ability to produce high levels of testosterone after 3d in culture without detecting any morphological changes. To culture primary Leydig cells for 3 days was necessary for the future experiments with *Pex13* siRNA transfection to observe the steroidogenesis in a condition of peroxisome deficiency. Our study indicates that primary mouse Leydig cells, after 3d of culture *in vitro*, were able to produce also other hormones: progesterone, DHEA, estrone and estradiol.

5.3. Comparison of MLTC-1 and primary mouse Leydig cells in their ability to produce steroid hormones

In this study, we have tried to draw a comparison between MLTC-1 cells and primary Leydig cells for their capacity to produce hormones. RIA and ELISA revealed that MLTC-1 cells produce two times more progesterone than primary Leydig cells. This observation is consistent with the current literature, that the activity of downstream enzymes of steroidogenesis is less in MLTC-1 cells compared to primary Leydig cells (Manna et al. 2006; Manna et al. 2004; Panesar et al. 2003).

RIA analysis showed that the concentration of testosterone produced from Leydig cells is 15 times more than in MLTC-1 cells (percentage 100% Leydig cells, 6% MLTC-1 cells). Free testosterone measurements via ELISA showed the same difference in testosterone production by MLTC-1 and primary Leydig cells.

Interestingly, DHEA production in MLTC-1 cells was much higher than in mouse primary Leydig cells. These findings indicate and confirm that MLTC-1 cells not only express P450c17 mRNA as mentioned above, but P450c17 is also enzymatically

active in these cells. These results lead to the hypothesis that the expression and activity of the multiple 17β -HSDs in MLTC-1 cells might be different, which are involved in the conversion of androgen precursors to testosterone, leading to their accumulation in medium.

Furthermore, ELISA-measurements showed that estrone secretion by MLTC-1 cells was higher in comparison to primary Leydig cells. It is known that estrone is synthesized through aromatase from androstenedione. This finding indicates that the aromatase gene is expressed and the protein is enzymatically active in MLTC-1 cells. Moreover, through increased levels of androstenedione produced by MLTC-1 cells, estrone conversion by aromatase is consequently elevated.

Interestingly, estradiol production by primary Leydig cells was increased compared to MLTC-1 cells. In Leydig cells estradiol is generated through two different enzymatic pathways. It can be converted from testosterone by aromatase. Additionally, as mentioned earlier, through action of aromatase androstenedione generates estrone, which then via 17β -HSDs is converted to its active form (estradiol). Taking into consideration that testosterone level secreted by primary Leydig cells was higher in comparison to MLTC-1 cells we postulate that estradiol is synthesized in primary Leydig cells through two defined pathways, whereas, in MLTC-1 cells estradiol is produced predominantly through estrone conversion by 17β -HSDs.

In summary, in primary cell culture isolated mouse Leydig cells showed high responsiveness to hCG treatment even after 3d of culture, by producing high level of hormones. In our model of MLTC-1 cells, all key enzymes necessary for steroid synthesis are expressed and their activity seems only slightly disturbed except for 17β -HSD3, which is the most important enzyme for the testosterone synthesis from androstenedione (Andersson 1995; Geissler et al. 1994; Sha et al. 1997). Thus, this thesis work provides an extended comparison of the steroidogenic capacity of MLTC-1 cells and primary Leydig cells and provides new information on the downstream steroidogenic activity of MLTC-1 cells.

5.4. Peroxisomal abundance in murine Leydig cells

In 1972, Reddy and Svoboda by cytochemistry observed peroxisomes through positive peroxidase staining of peroxisomal catalase in Leydig cells (Reddy and Svoboda 1972a), and showed that peroxisomes are highly abundant in mouse Leydig cells and are often closely associated with SER segments or with lipid droplets (Reddy and Svoboda 1972b; Reddy and Ohno 1981). They were the first to speculate that peroxisomes might play a role in steroid or cholesterol synthesis. This observation is consistent with our findings that catalase is highly abundant in Leydig cells. In addition, we found that almost all peroxisomal genes involved in peroxisomal biogenesis and metabolic functions are well expressed in Leydig cells. As described previously (Neniciu et al 2007), using antibodies against proteins of peroxisomal biogenesis, such as the peroxins 13 and 14 (PEX13 and PEX14), we were able to confirm additionally, that Leydig cells contain numerous peroxisomes.

5.4.1. Peroxisomal deficiency in Leydig cells and alteration of peroxisomal marker proteins

Patients with peroxisomal disorders show severe pathological alterations in different tissues and organs including reproductive system mostly with disturbed lipid metabolism. However, to date the pathogenesis of these organ defects is not completely understood.

Different mouse models have been developed with generalized inactivation of *Pex* genes involved in PTS1- and PTS2-dependant matrix protein import (*Pex2*-, *Pex5*- and *Pex13*-knockouts) to investigate the underlying pathogenesis of the most severe peroxisomal biogenesis disorder: Zellweger syndrome (Baes et al. 1997; Faust and Hatten 1997; Liu et al. 1999). All knockout models demonstrated different organ impairments typical for ZS, including disturbed neocortex neuronal migration and development, as well as hypotonia. Due to their early postnatal mortality, it is not possible to investigate the role of peroxisomes in adult tissues of *Pex*-knockout mice. As a result, they lose their usefulness as models for investigation of postnatal disease pathogenesis. Particularly, these *Pex*-KO mice are not suitable to study testicular pathologies observed in patients with Zellweger syndrome, since the testis are not mature at birth, and in mice the spermatogenesis starts only at postnatal day

20. However, in the last decade, through advanced Cre-loxP technology, it became possible to conditionally inactivate genes in specific cell types. Conditional knockout of *Pex13* and *Pex5* specifically in Sertoli cells were generated to study the functional importance of peroxisomes in these cells. Both knockouts showed severely impaired spermatogenesis, with lipid accumulation in Sertoli cells leading to the arrest of spermatogenesis (Huyghe et al. 2006b; Nenicu et al. 2007). In Sertoli cell-specific *Pex13*-KO mice the proliferation of Leydig cells with hormonal alterations was observed, which is considered to be a compensatory alteration in response to the loss of Sertoli cells. Therefore, to achieve an in vitro model with peroxisomal deficiency in Leydig cells, we chose to target the peroxisomal biogenesis protein *Pex13*. The *Pex13* gene encodes a protein that is localized in the membrane docking complex, essential for the import of PTS1- and PTS2-dependent matrix proteins into the peroxisome. The *Pex13* protein was described to interact not only with the PTS1-receptor *Pex5p*, but also with PTS2-receptor *Pex7p* (Stein et al. 2002). Deletion of *Pex13* leads to a loss of import of both, PTS1 and PTS2, proteins. If the import of matrix proteins is defective, this results in a complete disruption of peroxisomal metabolism (Gould et al. 1996). In the *Pex13*^{-/-} mouse, morphologically detectable peroxisomes were absent in the liver and peroxisomal ghosts in cultured fibroblast were detected with peroxisomal metabolic deficiency (Maxwell et al. 2003). Similarly, in our in vitro model the knockdown of *Pex13* gene, as well as the reduced levels of PEX13 protein was verified in Leydig cells, independently by semi-quantitative RT-PCR and Western blot analyses respectively. In addition, IF staining revealed the mistargeting of catalase into the cytoplasm, which is common phenomenon observed in patients with peroxisomal deficiency (Baumgart, et al. 2003). For example, in vitro in skin fibroblasts obtained from patients with Zellweger-like clinical features or embryonic fibroblasts of appropriate *Pex* gene knockout models catalase was mislocalized to the cytosol (Baes et al. 1997; Sheikh et al. 1998).

5.5. Disturbed ROS homeostasis and disturbed mitochondrial function in *Pex13* knockdown Leydig cells

Reactive oxygen species are a double-edged sword; on one hand they are vital for cellular signaling and on the other hand they are detrimental in excess amounts, leading to lipid peroxidation and cell death. The fine balance or homeostasis is provided by multiple enzymes involved in production as well as scavenging of ROS. Peroxisomes contain multiple enzymes involved in different peroxisomal metabolic pathways that generate reactive oxygen species as metabolic by-products (Antonenkova, et al. 2010; Dansen and Wirtz 2001; Schrader and Fahimi 2006; Van Veldhoven 2010). Peroxisomes also contain various antioxidant enzymes, including catalase, Cu/Zn-superoxide dismutase (SOD1), glutathione peroxidase and peroxiredoxin1,5 (PRDX1,5) (Antonenkova et al. 2010; Immenschuh et al. 2003). It was shown that catalase, as a peroxisomal antioxidant, is responsible for the metabolism of H₂O₂ generated in peroxisomes and elsewhere in the human cells (Koepke, et al. 2007; Koepke, et al. 2008). Several studies show that the loss of catalase and increased peroxisomal reactive oxygen species can affect the peroxisomal metabolism (Sheikh et al. 1998; Titorenko and Terlecky 2011). It is well accepted, that peroxisomes play an important role in both the generation and scavenging of ROS in the cell, in particular hydrogen peroxide.

In addition, peroxisomes and catalase activity are highly reduced in different pathological conditions in the body, including tumors of the liver and other organs, as well as after ischemia-reperfusion injury, inflammation (Canonico, et al. 1975; Khan, et al. 2000; Lauer, et al. 1999; Litwin, et al. 1999). Similarly, in Leydig cells, deficiency of functional peroxisomes induced by *Pex13* knockdown leads to the reduction in the amount, as well as activity, of the peroxisomal antioxidant enzyme catalase due to the mistargeting and partial degradation of the enzyme in the cytoplasm (see Western blot analysis and catalase activity assay).

Indications suggestive of a disturbed ROS homeostasis in *Pex13* knockdown Leydig cells include increased levels of the cytoplasmic antioxidant enzyme SOD1 and glutathione reductase, and a decrease in the reduced-form of glutathione.

Furthermore, the mitochondrial anti-oxidant enzyme SOD2 was found to be up-regulated in *Pex13* knockdown Leydig cells. SOD2 converts superoxide anions

(O₂⁻), generated from mitochondrial electron transport chain (Chance et al. 1979; Hansford et al. 1997), into hydrogen peroxide (H₂O₂), which are usually reduced to H₂O by mitochondrial peroxiredoxins, GPX1 or catalase. It is known that in conditions of oxidative stress, the mitochondria harbor increased amounts of SOD2. Increased oxidative stress with elevated levels of SOD2 is also observed in different organs including liver, heart, kidney, adrenal cortex of *Pex5* knockout mice (Baumgart et al. 2003; Baumgart et al. 2001; Schrader and Fahimi 2004). Finally, the observation that in a *Pex13* knockdown Leydig cell the intensity of DHE staining was increased, supports the conclusion that peroxisome dysfunction leads to oxidative stress in Leydig cells.

The changes of antioxidant enzymes in different subcellular compartments suggest that in *Pex13* knockdown Leydig cells there is an effect on the general redox balance. Even though almost all antioxidant enzymes are up-regulated, this increase is not sufficient to compensate the oxidative stress shown by DHE staining and reduced GSH levels. One of the reasons could be the observed reduction of mitochondrial complex III of respiratory chain in *Pex13* knockdown Leydig cells leading to the release of mitochondrial ROS.

5.6. Functional significance of peroxisomes in steroid synthesis in Leydig cells

Importantly, patients with peroxisomal disorders surviving to adolescence exhibit different testicular pathologies including impaired spermatogenesis, testicular atrophy, degeneration of Leydig cells and hormonal dysfunction. Interestingly, in our study, *Pex13* knockdown in Leydig cells led to a decrease in the hCG-induced up-regulation of the intramitochondrial form of StAR protein, which is crucial for cholesterol transport into the mitochondria, where the first step of steroidogenesis takes place.

Following hormonal (LH/hCG) stimulation, StAR is synthesized as a 37-kDa precursor in the cytoplasm and translocates to the outer mitochondrial membrane, where it gets activated via phosphorylation by PKA (Arakane 1997, Phosphorylation, Dyson 2008 mitochondrial A-Kinase). It is then imported and processed within the mitochondria to a 30 kDa intramitochondrial form by cleavage of an N-terminal mitochondrial import sequence (King and Stocco 1996). In our study, there was no

significant decrease in protein level of the 37 kDa precursor form of StAR in *Pex13* knockdown Leydig cells, indicating that the synthesis and expression of StAR protein is not affected. However, the cleaved 30 kDa form of StAR was remarkably down-regulated in *Pex13* knockdown Leydig cells in comparison to control shRNA or siRNA transfected Leydig cells. Since in our study we also observed mitochondrial dysfunction in *Pex13*-knockdown Leydig cells, it is feasible that this leads to the impaired StAR processing. Because of the disrupted StAR processing there was reduced production of the immediate downstream hormone pregnenolone, which is produced in the mitochondria by the enzyme P450_{scc}. However, the observed reduction of hCG-stimulated pregnenolone was completely reversed when the cells were treated with 22R-HC instead of hCG under simultaneous inhibition of P450_{c17} and 3 β -HSD, suggesting that the *Pex13* knockdown in Leydig cells did not inhibit the P450_{scc} enzyme activity, but that the impaired cholesterol transport due to the defective processing of StAR led to the reduced levels of pregnenolone in hCG-stimulated *Pex13* knockdown cells. In contrast, treatment with hCG as well as 22R-HC led to a decrease in progesterone synthesis in Leydig cells with *Pex13* knockdown, indicating that the activity of 3 β -HSD is affected independent of the StAR protein function. This finding is consistent with earlier reports, that defective StAR processing leads to a reduction in steroidogenesis (Allen, et al. 2006; Midzak, et al. 2011; Stocco 2001).

Finally, *Pex13* knockdown in Leydig cells also leads to a strong reduction of hCG-stimulated testosterone synthesis. After treating with 22R-HC, the testosterone synthesis was still significantly reduced, confirming that the activity of steroidogenic enzymes downstream of StAR activity, such as P450_{c17} and 17 β -HSDs, might be altered. Noteworthy, and may be related to our findings, is the observation that patients with the peroxisomal disorders X-ALD/AMN exhibit testicular endocrine dysfunction with low testosterone and compensatory elevated LH levels in serum. The mean testosterone/LH ratio is strongly reduced in these patients indicating an impairment of the Leydig cells whereas FSH was elevated in response to impaired spermatogenesis (Brennemann et al. 1997).

The hCG-stimulated production of other androgens such as DHEA was also decreased in Leydig cells with peroxisomal deficiency after hCG as well as 22R-HC stimulation. DHEA is a metabolic intermediate in the testosterone and estrogen

synthesis and it is considered to be a relatively weak androgen (Bazin, et al. 2007). It has been shown, that in X-ALD patients with a single transporter peroxisomal disorder, DHEA levels are low (Assies et al. 1998), which corroborates our findings. To summarize, the collective data indicates that *Pex13* knockdown inhibits not only the up-regulation of intramitochondrial *Star*, but also 3 β -HSD and possibly other steroidogenic enzymes downstream of the mitochondria activity: such as P450c17 and 17 β -HSD, whereas, P450scc enzyme activity was not affected, thus, leading to a strong reduction in steroid synthesis.

5.7. Functional peroxisomes and mitochondria are required for steroidogenesis in Leydig cells

Peroxisomes and mitochondria are functionally interconnected (Demarquoy and Le Borgne 2015; Lismont, et al. 2015; Schrader, et al. 2015). In Leydig cells with *Pex13* knockdown, the reduction in mitochondrial membrane potential and the decrease in the protein levels of complex III of the mitochondrial respiratory chain were noted. These findings corroborate with the existing literature that *Pex5* knockout mice had severe mitochondrial abnormalities (Baumgart et al. 2001) in the liver and many other tissues or that the absence of peroxisomes caused mitochondrial alterations in isolated hepatocytes (Janssen, et al. 2003). Here in we speculate on two different possibilities for the cause of mitochondrial dysfunction. Firstly, the down-regulation of peroxisomal metabolism in *Pex13* knockdown Leydig cells might lead to a condition where the lipid metabolites are solely dependent on mitochondria for metabolism. This can overwhelm the mitochondrial capacity and thus lead to a breakdown of mitochondrial functions. Alternatively, mitochondrial dysfunction could also arise from the increased oxidative stress derived in *Pex13* knockdown Leydig cells, where mistargeting, reduction and dysfunction of catalase were noted. In line with this notion is the finding from Ivashenko et al that in catalase-deficient mammalian cells the loss of mitochondrial redox balance was observed (Ivashchenko, et al. 2011). However, the source of ROS generation needs to be identified to consider ROS as the reason for mitochondrial dysfunction since it can be generated in various cellular compartments such as by NADPH oxidases, in the plasma membrane or ER, in the cytoplasm or in mitochondria itself.

One of the key findings of this thesis work is that the knockdown of *Pex13* in MLTC-1 cells leads to the inhibition of the 30kDa StAR protein. It is plausible that the mitochondrial dysfunction caused by peroxisome deficiency in Leydig cells resulted in the inhibition of StAR transport into the mitochondria. Regardless of the controversial debate whether 30 or 37kDa StAR is responsible for cholesterol transfer and how StAR acts, it is conclusive that functional mitochondria are required for StAR activity and normal cholesterol transfer for steroid synthesis. This notion is supported by findings that intact mitochondrial proton pump is required for proper StAR activity, and disturbed mitochondrial function leads to the inefficiency in cholesterol transport and impaired steroid synthesis (Allen, et al. 2004; Allen et al. 2006; Diemer et al. 2003; King, et al. 1999; Midzak et al. 2011; Midzak, et al. 2007).

Scheme summarizing an alteration in Leydig cells after *Pex13* knockdown

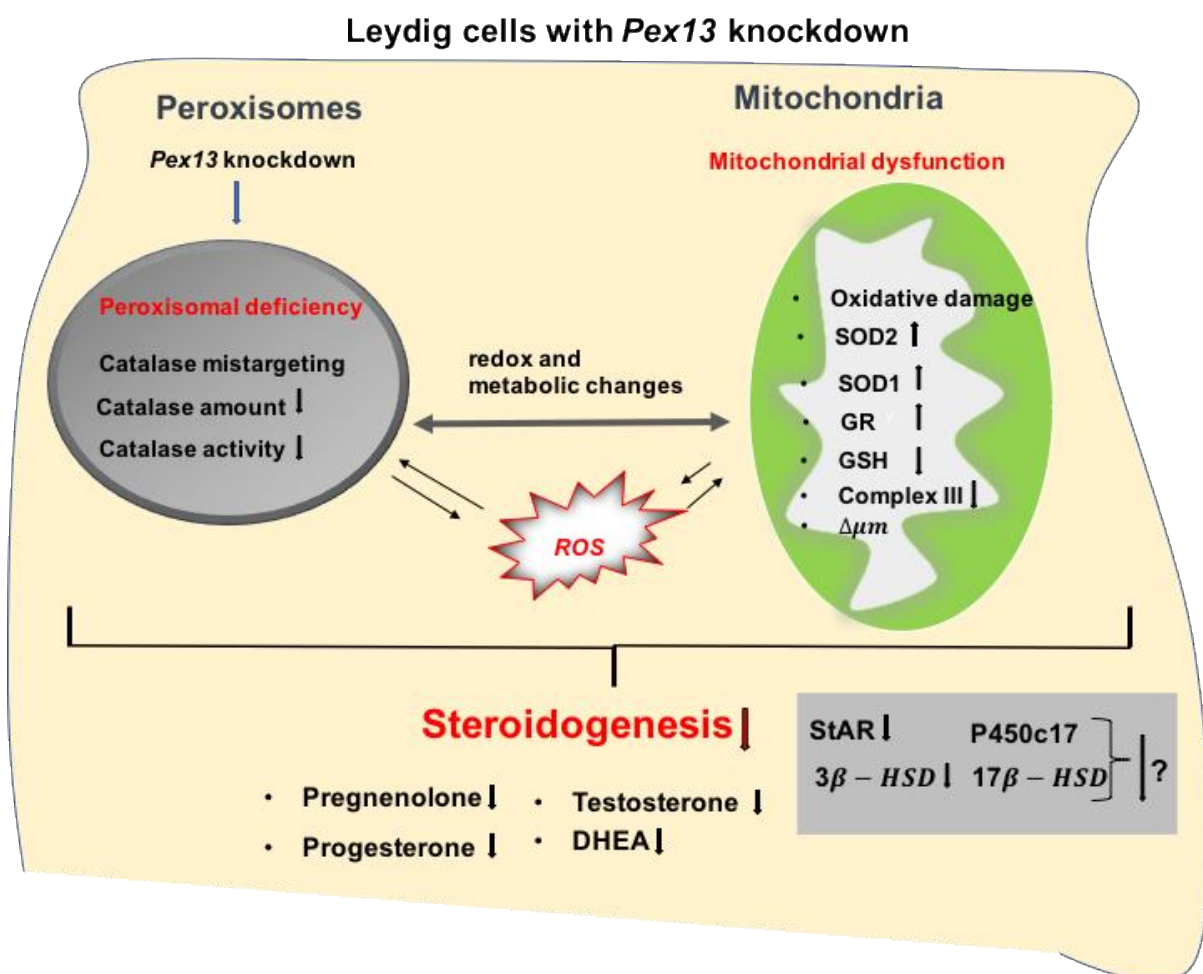


Figure 41. Deficiency of *Pex13* gene in Leydig cells induces a peroxisome biogenesis defect leading to defective matrix protein import and catalase mistargeting, which is a common phenomenon observed in conditions of peroxisomal deficiency. Furthermore, peroxisomal deficiency induces mitochondrial disturbance and oxidative stress in Leydig cells. The hCG-mediated induction of the intramitochondrial 30 kDa form of StAR protein was significantly reduced in Leydig cells with *Pex13* knockdown. Moreover, 3 β -HSD and possibly also other steroidogenic enzymes activity downstream of the mitochondrial enzymes such as cytochrome P450c17 and 17 β -HSD may be decreased in Leydig cells with peroxisome deficiency. Thus, peroxisome dysfunction and secondary disturbance of mitochondria together in *Pex13* knockdown Leydig cells lead to impaired steroidogenesis with significant reduction in the production of progesterone, testosterone and DHEA.

The inhibition of intramitochondrial StAR was found to be partially responsible for the impaired steroidogenesis in this study. The reason explaining the inhibition of androgen synthesis through decreased activity of above mentioned steroidogenic enzymes in Leydig cell with peroxisomal deficiency needs to be explored further. It seems unlikely that the inhibition of steroidogenesis is only due to the decreased total cholesterol amount, because treatment with 22R-HC also resulted in the inhibition of steroid synthesis. However, it needs to be pointed out that in comparison to 22R-HC stimulation hCG-mediated steroid synthesis is reduced more in MLTC-1 and in primary Leydig cells, which may be due to the additional step of disrupted cholesterol transport via reduced StAR activity.

In conclusion, our findings indicate that peroxisomal deficiency induces mitochondrial disturbance in Leydig cells. These two organelles show a significant functional interplay involving ROS balance, oxidative metabolism of fatty acids and probably other not yet identified functional interactions, one of which might be steroid synthesis. An interesting hypothesis in this context is that some steps of steroid synthesis could take place in peroxisomes and therefore peroxisomal deficiency might result in the inhibition of androgen synthesis. However, at present we do not have enough evidence to support this notion. Further studies need to be done to address peroxisomal alterations after disturbing the mitochondrial potential by antimycin-A to understand if the inter-play between the organelles is uni-directional or bi-directional.

5.8. Biological potency of androgens and estrogens in Leydig cells with *Mfp2* knockdown.

Patients with X-ALD, besides exhibiting infertility and impaired spermatogenesis also show hormonal dysfunction including the inhibition of DHEA synthesis (Assies et al. 1998). Similarly, in our study the peroxisome deficiency in Leydig cells with *Pex13* knockdown leads to reduction of hCG as well as 22R-HC mediated DHEA production. DHEA is produced by the adrenal cortex and gonads in humans, whereas in laboratory animals sex steroids are secreted mostly in the gonads. It is also produced in adipose tissue, brain and skin. DHEA, together with its sulfate version (DHEAS), which is generated in liver, are the most abundant endogenous steroids in men and women. DHEA, an endogenous precursor to more potent androgens such as testosterone and DHT, is produced in its highest amount at ages 20-30 in human. The secretion of DHEA and DHEAS decrease profoundly with increasing age (Belanger, et al. 1994; Orentreich, et al. 1992; Yen and Laughlin 1998), which has generated a great clinical interest since this decline is associated with impairment of health and age-related diseases including cardiovascular diseases, metabolic diseases, cancers, immune and neurological disorders. Interestingly, there are many studies revealing the importance of peroxisomal metabolism in aging and age-related diseases (Fransen, et al. 2013). Aging is linked with decreased activities of peroxisomal β -oxidation enzymes and catalase in aging rat liver (Terlecky, et al. 2006).

The peroxisomal enzyme *Mfp2* also known as D-bifunctional protein or 17 β -HSD4 is involved in steroid synthesis altering the activity of androgens and estrogens. 17 β -HSD4 is expressed the most in liver, followed by heart, prostate, testis and also other organs. Generally, 17 β -HSDs are modulating the biological potency of androgens and estrogens by conversion at position C17. 17 β -HSD4 is the only 17 β -HSD found in peroxisomes (Markus et al. 1995) and it was suggested that DHEA is metabolized by this enzyme (Prough, et al. 1994). According to several studies, androstenediol is catalyzed by 17 β -HSD4 and 2 to DHEA (Adamski et al. 1995; Labrie et al. 2000; Peltoketo et al. 1999) and estradiol is converted to inactive estrone by 17 β -HSD2, 4, 8, 10 (Fomitcheva et al. 1998; Labrie et al. 2000). It has

been also shown, that 17 β -HSD4 catalyzes the oxidation of estradiol to estrone and oxidizes androstenediol to DHEA more efficiently than the reverse reaction.

Patients with *Mfp-2/17 β -HSD4* deficiency show severe developmental abnormalities and early postnatal death (Wanders et al. 2001b). *Mfp-2*-knockout mice did not exhibit severe developmental alterations and in contrast to human disease their survival into adulthood was a good possibility to investigate the role of *Mfp2/17 β -HSD4* in testis and other organs (Huyghe et al. 2006a). Knocking out *Mfp-2* resulted in severe male infertility with neutral lipid accumulation in Sertoli cells and at later stages to complete fatty degeneration of seminiferous tubules and testis atrophy (Huyghe et al. 2006b). The morphology of Leydig cells was not altered until 12 weeks after which the number of Leydig cells was difficult to estimate due to disintegrating seminiferous epithelium. However, in this study DHEA levels were not determined. Our observations indicate that after knockdown of *Mfp2* in primary Leydig cells, the secretion of DHEA was decreased. Considering the peroxisomal localization of *Mfp2/17 β -HSD4*, this finding suggested that peroxisomes could be involved in oxidation of DHEA. Testosterone production was not changed in Leydig cells with *Mfp2* knockdown, which is in agreement with results from *Mfp2* knockout mice (reference). Moreover, *Mfp2* knock-down in primary Leydig cells also leads to slightly reduction in estrone synthesis.

Collectively, this thesis work demonstrates that in Leydig cells the peroxisomal deficiency with *Pex13* knockdown and knockdown of *Mfp2* result in the inhibition of DHEA production, indicating that peroxisomes could play an important role in oxidation of steroids. Pathological effects of peroxisomal deficiency on cells can be mediated not only through known mechanisms such as disturbed lipid oxidation or redox balance but also through disturbed steroid oxidation which can lead to the development of pathological conditions or diseases.

6. Summary

Infertility is a global health issue, affecting approximately 10-15% of couples worldwide. Male patients with peroxisomal diseases exhibit depending on the phenotype severity either cryptorchidism or a range of testicular pathologies leading in final consequence also to male infertility. Peroxisomes are ubiquitous organelles, which besides other metabolic pathways are involved in ROS-metabolism, cholesterol synthesis and in beta-oxidation of a variety of bioactive lipid derivatives. In this dissertation, the possible role of peroxisomes in Leydig cell steroid metabolism was investigated.

The mouse tumor Leydig cell line MLTC-1 and mouse primary Leydig cells were used to knockdown the *Pex13* gene by transfection using a *Pex13* shRNA plasmid and microporation or *Pex13* siRNA and lipofection. The resulting phenotype was characterized by immunofluorescence, Western blots, RT-PCR, Radioimmunoassays, ELISAs and different assays, analyzing ROS metabolism and mitochondrial dysfunction in cells.

Our results show that the mouse Leydig tumor cell line MLTC-1 is a good model system to analyze the peroxisomal compartment and steroid synthesis. These cells exhibited, by using the correct cell culture conditions, a strong hCG-mediated increase of steroid synthesis, a typical feature for Leydig cells. We established *Pex13* knockdown model in MLTC-1 cells and in primary Leydig cells (*Pex13* KD) to study the consequences of peroxisomal dysfunction on steroid synthesis. Western blot and RT-PCR analyses revealed a strong reduction of the *Pex13* gene as well as the PEX13 protein in more than 70% of these cells. Moreover, *Pex13* KD led to mistargeting of catalase into the cytoplasm in Leydig cells, which is a common phenomenon observed in condition of peroxisomal deficiency.

Furthermore, the hCG-mediated induction of the intramitochondrial 30 kDa form of StAR protein (steroidogenic acute regulatory protein) was decreased in Leydig cells with peroxisome deficiency. We also showed that a peroxisomal knockdown leads to significantly reduced levels of progesterone, testosterone and dehydroepiandrosterone (DHEA) synthesis in these cells after stimulation with hCG as well as with 22(R)-Hydroxycholesterol (22R-HC). In contrast, 22R-HC-mediated pregnenolone production was not changed in Leydig cells with peroxisome

deficiency. This data indicates that besides StAR, the *Pex13* knockdown inhibits 3-hydroxysteroid dehydrogenase (3 β -HSD), and possibly also other steroidogenic enzymes activity downstream of the mitochondrial enzymes such as cytochrome P450c17 (P450c17) and 17 β -hydroxysteroid dehydrogenase (17 β -HSD), whereas, cytochrome P450 side-chain cleavage enzyme (P450scc) activity was not affected, thus, leading to a strong reduction in steroid synthesis. The molecular mechanism explaining the inhibition of androgen synthesis through decreased activity of the above mentioned enzymes in Leydig cell with peroxisome deficiency needs to be further explored.

The results of this thesis indicate that peroxisomal deficiency induces mitochondrial disturbance and oxidative stress in Leydig cells. These two organelles exhibit an important functional interplay involving ROS balance, oxidative metabolism of fatty acids and probably other not yet identified functional interactions, one of which might be steroid synthesis.

Additionally, knockdown of *Mfp2/17 β -Hsd4* resulted in the inhibition of DHEA production, indicating that peroxisomes could play an important role in the metabolism of steroids.

In conclusion, our observations support the conclusion that *Pex13* knockdown in MLTC-1 cells and in primary Leydig cells inhibits steroid synthesis due to functional disturbance of peroxisomes and secondary dysfunction of mitochondria.

7. Zusammenfassung

Unfruchtbarkeit ist ein globales Gesundheitsproblem, das etwa 10-15% der Paare weltweit betrifft. Männliche Patienten mit peroxisomalen Erkrankungen zeigen je nach Phänotypschwere entweder Kryptorchismus oder eine Reihe von Hodenpathologien, die in letzter Konsequenz auch zur männlichen Unfruchtbarkeit führen. Peroxisomen sind ubiquitäre Zellorganellen, die neben anderen Stoffwechselwegen am ROS-Metabolismus, der Cholesterinsynthese und bei der β -Oxidation einer Vielzahl von bioaktiven Lipidderivaten beteiligt sind. In dieser Doktorarbeit wurde die mögliche Rolle von Peroxisomen im Steroid-Metabolismus von Leydig-Zellen untersucht.

Die Maus-Leydig-Tumorzelllinie MLTC-1 und primäre Leydig-Zellen der Maus wurden verwendet, um das *Pex13*-Gen durch Transfektion eines *Pex13* shRNA Plasmids mittels Mikroporation oder durch Transfektion von *Pex13* siRNA mittels Lipofektion herunterzuregulieren (*Pex13* Knockdown). Der resultierende Phänotyp wurde durch Immunfluoreszenz, Western-Blots, RT-PCR, Radioimmunoassays/ELISAs und verschiedenen Assays, die den ROS-Metabolismus und die mitochondriale Dysfunktion in den Zellen analysierten, charakterisiert.

Die Ergebnisse dieser Dissertation erbrachten, dass die MLTC-1 Zellen ein gutes Modellsystem darstellen, um das peroxisomale Kompartiment und die Steroidsynthese zu analysieren. Tatsächlich konnte in dieser Doktorarbeit gezeigt werden, dass die MLTC-1 Zellen unter den richtigen Zellkulturbedingungen eine hCG-induzierte Steigerung der Steroidsynthese aufwiesen, ein typisches Merkmal primären Leydig-Zellen. Daraufhin wurde ein gutes *Pex13* Knockdown-Modell (*Pex13* KD) in MLTC-1-Zellen und in primären Leydig-Zellen etabliert, um die Konsequenzen einer peroxisomalen Dysfunktion auf die Steroidsynthese zu untersuchen. Western-Blot- und RT-PCR-Analysen zeigten eine starke Reduktion des *Pex13*-Gens sowie des PEX13-Proteins in mehr als 70% dieser Zellen. Der *Pex13* KD führte zu der Mislokalisierung der Katalase in das Zytoplasma in Leydig-Zellen, was ein typisches Phänomen bei peroxisomalen Biogenesestörungen darstellt.

Die hCG-vermittelte Induktion der intramitochondrialen 30 kDa Form des StAR-Proteins (steroidogenic acute regulatory protein) war in Leydig-Zellen mit Peroxisomenmangel herunterreguliert. Es wurde weiterhin nachgewiesen, dass der peroxisomale Knockdown in diesen Zellen nach Stimulation mit hCG sowie mit 22(R)-Hydroxycholesterin (22R-HC) zu signifikant reduzierten Progesteron-, Testosteron- und Dehydroepiandrosteron (DHEA)-Synthesen führt.

Im Gegensatz dazu war die 22R-HC-vermittelte Pregnenolon-Produktion in Leydig-Zellen mit Peroxisom-Mangel unverändert. Diese Daten zeigen, dass neben StAR durch den *Pex13*-Knockdown auch 3 β -Hydroxysteroid-Dehydrogenase (3 β -HSD) und vermutlich auch andere steroidogene Enzymaktivitäten abwärts der mitochondrialen Enzyme wie z.B. Cytochrom P450c17 (P450c17) und 17 β -Hydroxysteroid-Dehydrogenasen (17 β -HSDs) beeinträchtigt wurden, so dass eine starke Reduktion in Steroidsynthese daraus resultierte. Der molekulare Mechanismus, der zu der Hemmung der Androgensynthese durch eine verminderte Aktivität der oben erwähnten Enzyme in Leydig-Zellen mit peroxisomaler Biogenese Störung führt, muss in weiterführenden Studien noch geklärt werden.

Die Ergebnisse dieser Dissertation zeigen auch, dass peroxisomale Biogenese Störungen sekundäre mitochondriale Dysfunktion und oxidativen Stress in Leydig-Zellen induzierten. Diese Biogenese Störungen beider Zellorganellen zeigen ein wichtiges funktionelles Zusammenspiel in der Regulierung der ROS-Balance, dem oxidativen Metabolismus von Fettsäuren und vermutlich auch anderen, noch nicht identifizierten, funktionellen Interaktionen, von denen eine die Steroidsynthese sein könnte.

Darüber hinaus führte der Knockdown von *Mfp2/ 17 β -Hsd4* zu einer Hemmung der DHEA-Produktion, was darauf hinweist, dass Peroxisomen eine wichtige Rolle im Metabolismus von Steroiden spielen.

Die in der Dissertation gemachten Beobachtungen unterstützen die Schlussfolgerung, dass der *Pex13*-Knockdown in MLTC-1-Zellen und in primären Leydig-Zellen die Steroidsynthese aufgrund einer funktionellen Störung von Peroxisomen und daraus resultierender sekundären Dysfunktion von Mitochondrien hemmt.

8. References

- Adamski J & Jakob FJ 2001 A guide to 17 β -hydroxysteroid dehydrogenases. *Mol Cell Endocrinol* **171** 1-4.
- Adamski J, Normand T, Leenders F, Monte D, Begue A, Stehelin D, Jungblut PW & de Launoit Y 1995 Molecular cloning of a novel widely expressed human 80 kDa 17 β -hydroxysteroid dehydrogenase IV. *Biochem J* **311** (Pt 2) 437-443.
- Alberta JA, Epstein LF, Pon LA & Orme-Johnson NR 1989 Mitochondrial localization of a phosphoprotein that rapidly accumulates in adrenal cortex cells exposed to adrenocorticotrophic hormone or to cAMP. *J Biol Chem* **264** 2368-2372.
- Allen JA, Diemer T, Janus P, Hales KH & Hales DB 2004 Bacterial endotoxin lipopolysaccharide and reactive oxygen species inhibit Leydig cell steroidogenesis via perturbation of mitochondria. *Endocrine* **25** 265-275.
- Allen JA, Shankara T, Janus P, Buck S, Diemer T, Hales KH & Hales DB 2006 Energized, polarized, and actively respiring mitochondria are required for acute Leydig cell steroidogenesis. *Endocrinology* **147** 3924-3935.
- Andersson S 1995 Molecular genetics of androgenic 17 β -hydroxysteroid dehydrogenases. *J Steroid Biochem Mol Biol* **55** 533-534.
- Antonenkova VD, Grunau S, Ohlmeier S & Hiltunen JK 2010 Peroxisomes are oxidative organelles. *Antioxid Redox Signal* **13** 525-537.
- Arakane F, Sugawara T, Nishino H, Liu Z, Holt JA, Pain D, Stocco DM, Miller WL & Strauss JF, 3rd 1996 Steroidogenic acute regulatory protein (StAR) retains activity in the absence of its mitochondrial import sequence: implications for the mechanism of StAR action. *Proc Natl Acad Sci U S A* **93** 13731-13736.
- Ascoli M 1981a Characterization of several clonal lines of cultured Leydig tumor cells: gonadotropin receptors and steroidogenic responses. *Endocrinology* **108** 88-95.
- Ascoli M 1981b Regulation of gonadotropin receptors and gonadotropin responses in a clonal strain of Leydig tumor cells by epidermal growth factor. *J Biol Chem* **256** 179-183.
- Ascoli M, Fanelli F & Segaloff DL 2002 The lutropin/choriogonadotropin receptor, a 2002 perspective. *Endocr Rev* **23** 141-174.
- Ascoli M & Puett D 1978 Gonadotropin binding and stimulation of steroidogenesis in Leydig tumor cells. *Proc Natl Acad Sci U S A* **75** 99-102.
- Assies J, van Geel B & Barth P 1998 Low dehydroepiandrosterone sulphate (DHEAS) levels in X-linked adrenoleukodystrophy. *Clin Endocrinol (Oxf)* **49** 691-692.
- Aversa A, Palleschi S, Cruccu G, Silvestroni L, Isidori A & Fabbri A 1998 Rapid decline of fertility in a case of adrenoleukodystrophy. *Hum Reprod* **13** 2474-2479.
- Baes M, Gressens P, Baumgart E, Carmeliet P, Casteels M, Franssen M, Evrard P, Fahimi D, Declercq PE, Collen D, et al. 1997 A mouse model for Zellweger syndrome. *Nat Genet* **17** 49-57.
- Baker BY, Yaworsky DC & Miller WL 2005 A pH-dependent molten globule transition is required for activity of the steroidogenic acute regulatory protein, StAR. *J Biol Chem* **280** 41753-41760.
- Balaban RS, Nemoto S & Finkel T 2005 Mitochondria, oxidants, and aging. *Cell* **120** 483-495.

Baumgart E 1997 Application of in situ hybridization, cytochemical and immunocytochemical techniques for the investigation of peroxisomes. A review including novel data. Robert Feulgen Prize Lecture 1997. *Histochem Cell Biol* **108** 185-210.

Baumgart E, Fahimi HD, Steininger H & Grabenbauer M 2003 A review of morphological techniques for detection of peroxisomal (and mitochondrial) proteins and their corresponding mRNAs during ontogenesis in mice: application to the PEX5-knockout mouse with Zellweger syndrome. *Microsc Res Tech* **61** 121-138.

Baumgart E, Schad A, Volkl A & Fahimi HD 1997 Detection of mRNAs encoding peroxisomal proteins by non-radioactive in situ hybridization with digoxigenin-labelled cRNAs. *Histochem Cell Biol* **108** 371-379.

Baumgart E, Vanhooren JC, Fransen M, Mannaerts GP & Van Veldhoven PP 1996a Mammalian peroxisomal acyl-CoA oxidases. III. Molecular characterization of human branched chain fatty acyl-CoA oxidase. *Ann N Y Acad Sci* **804** 678-679.

Baumgart E, Vanhooren JC, Fransen M, Marynen P, Puype M, Vandekerckhove J, Leunissen JA, Fahimi HD, Mannaerts GP & van Veldhoven PP 1996b Molecular characterization of the human peroxisomal branched-chain acyl-CoA oxidase: cDNA cloning, chromosomal assignment, tissue distribution, and evidence for the absence of the protein in Zellweger syndrome. *Proc Natl Acad Sci U S A* **93** 13748-13753.

Baumgart E, Vanhorebeek I, Grabenbauer M, Borgers M, Declercq PE, Fahimi HD & Baes M 2001 Mitochondrial alterations caused by defective peroxisomal biogenesis in a mouse model for Zellweger syndrome (PEX5 knockout mouse). *Am J Pathol* **159** 1477-1494.

Baumgart E, Volkl A, Hashimoto T & Fahimi HD 1989 Biogenesis of peroxisomes: immunocytochemical investigation of peroxisomal membrane proteins in proliferating rat liver peroxisomes and in catalase-negative membrane loops. *J Cell Biol* **108** 2221-2231.

Bazin MA, Travert C, Carreau S, Rault S & El Kihel L 2007 First synthesis of 7alpha- and 7beta-amino-DHEA, dehydroepiandrosterone (DHEA) analogues and preliminary evaluation of their cytotoxicity on Leydig cells and TM4 Sertoli cells. *Bioorg Med Chem* **15** 3152-3160.

Belanger A, Candas B, Dupont A, Cusan L, Diamond P, Gomez JL & Labrie F 1994 Changes in serum concentrations of conjugated and unconjugated steroids in 40- to 80-year-old men. *J Clin Endocrinol Metab* **79** 1086-1090.

Biardi L & Krisans SK 1996 Compartmentalization of cholesterol biosynthesis. Conversion of mevalonate to farnesyl diphosphate occurs in the peroxisomes. *J Biol Chem* **271** 1784-1788.

Biardi L, Sreedhar A, Zokaei A, Vartak NB, Bozeat RL, Shackelford JE, Keller GA & Krisans SK 1994 Mevalonate kinase is predominantly localized in peroxisomes and is defective in patients with peroxisome deficiency disorders. *J Biol Chem* **269** 1197-1205.

Bonekamp NA, Grille S, Cardoso MJ, Almeida M, Aroso M, Gomes S, Magalhaes AC, Ribeiro D, Islinger M & Schrader M 2013 Self-interaction of human Pex11pbeta during peroxisomal growth and division. *PLoS One* **8** e53424.

Bose HS, Lingappa VR & Miller WL 2002 Rapid regulation of steroidogenesis by mitochondrial protein import. *Nature* **417** 87-91.

Bose HS, Whittall RM, Baldwin MA & Miller WL 1999 The active form of the steroidogenic acute regulatory protein, StAR, appears to be a molten globule. *Proc Natl Acad Sci U S A* **96** 7250-7255.

Bose HS, Whittall RM, Bose M & Debnath D 2009a Hydrophobic core of the steroidogenic acute regulatory protein for cholesterol transport. *Biochemistry* **48** 1198-1209.

Bose HS, Whittall RM, Debnath D & Bose M 2009b Steroidogenic acute regulatory protein has a more open conformation than the independently folded smaller subdomains. *Biochemistry* **48** 11630-11639.

- Bose M, Whittal RM, Miller WL & Bose HS 2008 Steroidogenic activity of StAR requires contact with mitochondrial VDAC1 and phosphate carrier protein. *J Biol Chem* **283** 8837-8845.
- Boveris A 1984 Determination of the production of superoxide radicals and hydrogen peroxide in mitochondria. *Methods Enzymol* **105** 429-435.
- Brennemann W, Kohler W, Zierz S & Klingmuller D 1997 Testicular dysfunction in adrenomyeloneuropathy. *Eur J Endocrinol* **137** 34-39.
- Buzzard JJ, Wreford NG & Morrison JR 2003 Thyroid hormone, retinoic acid, and testosterone suppress proliferation and induce markers of differentiation in cultured rat sertoli cells. *Endocrinology* **144** 3722-3731.
- Campo ML, Kinnally KW & Tedeschi H 1992 The effect of antimycin A on mouse liver inner mitochondrial membrane channel activity. *J Biol Chem* **267** 8123-8127.
- Canonica PG, White JD & Powanda MC 1975 Peroxisome depletion in rat liver during pneumococcal sepsis. *Lab Invest* **33** 147-150.
- Carreau S, Bourguiba S, Lambard S & Galeraud-Denis I 2002a [Testicular aromatase]. *J Soc Biol* **196** 241-244.
- Carreau S, Bourguiba S, Lambard S, Galeraud-Denis I, Genissel C & Levallet J 2002b Reproductive system: aromatase and estrogens. *Mol Cell Endocrinol* **193** 137-143.
- Carreau S, Genissel C, Bilinska B & Levallet J 1999 Sources of oestrogen in the testis and reproductive tract of the male. *Int J Androl* **22** 211-223.
- Carstensen JF, Tesdorpf JG, Kaufmann M, Markus MM, Husen B, Leenders F, Jakob F, de Launoit Y & Adamski J 1996 Characterization of 17 beta-hydroxysteroid dehydrogenase IV. *J Endocrinol* **150 Suppl** S3-12.
- Chance B, Sies H & Boveris A 1979 Hydroperoxide metabolism in mammalian organs. *Physiol Rev* **59** 527-605.
- Chang C, Chen YT, Yeh SD, Xu Q, Wang RS, Guillou F, Lardy H & Yeh S 2004 Infertility with defective spermatogenesis and hypotestosteronemia in male mice lacking the androgen receptor in Sertoli cells. *Proc Natl Acad Sci U S A* **101** 6876-6881.
- Chapple IL 1997 Reactive oxygen species and antioxidants in inflammatory diseases. *J Clin Periodontol* **24** 287-296.
- Chase RA** 2007 *The Bassett Atlas of Human Anatomy*. Benjamin Cummings.
- Chen H, Hardy MP & Zirkin BR 2002 Age-related decreases in Leydig cell testosterone production are not restored by exposure to LH in vitro. *Endocrinology* **143** 1637-1642.
- Christensen AK 1965 The Fine Structure of Testicular Interstitial Cells in Guinea Pigs. *J Cell Biol* **26** 911-935.
- Christensen AK & Fawcett DW 1966 The fine structure of testicular interstitial cells in mice. *Am J Anat* **118** 551-571.
- Clark BJ, Combs R, Hales KH, Hales DB & Stocco DM 1997 Inhibition of transcription affects synthesis of steroidogenic acute regulatory protein and steroidogenesis in MA-10 mouse Leydig tumor cells. *Endocrinology* **138** 4893-4901.
- Clark BJ, Wells J, King SR & Stocco DM 1994 The purification, cloning, and expression of a novel luteinizing hormone-induced mitochondrial protein in MA-10 mouse Leydig tumor cells. Characterization of the steroidogenic acute regulatory protein (StAR). *J Biol Chem* **269** 28314-28322.
- Cooke BA 1999 Signal transduction involving cyclic AMP-dependent and cyclic AMP-independent mechanisms in the control of steroidogenesis. *Mol Cell Endocrinol* **151** 25-35.

- Cooke BA, Choi MC, Dirami G, Lopez-Ruiz MP & West AP 1992 Control of steroidogenesis in Leydig cells. *J Steroid Biochem Mol Biol* **43** 445-449.
- Cross AR & Jones OT 1991 Enzymic mechanisms of superoxide production. *Biochim Biophys Acta* **1057** 281-298.
- Dansen TB & Wirtz KW 2001 The peroxisome in oxidative stress. *IUBMB Life* **51** 223-230.
- Davidoff MS, Middendorff R, Kofuncu E, Muller D, Jezek D & Holstein AF 2002 Leydig cells of the human testis possess astrocyte and oligodendrocyte marker molecules. *Acta Histochem* **104** 39-49.
- Davidoff MS, Middendorff R, Muller D & Holstein AF 2009 The neuroendocrine Leydig cells and their stem cell progenitors, the pericytes. *Adv Anat Embryol Cell Biol* **205** 1-107.
- De Duve C & Baudhuin P 1966 Peroxisomes (microbodies and related particles). *Physiol Rev* **46** 323-357.
- De Gendt K, Swinnen JV, Saunders PT, Schoonjans L, Dewerchin M, Devos A, Tan K, Atanassova N, Claessens F, Lecureuil C, et al. 2004 A Sertoli cell-selective knockout of the androgen receptor causes spermatogenic arrest in meiosis. *Proc Natl Acad Sci U S A* **101** 1327-1332.
- Demarquoy J & Le Borgne F 2015 Crosstalk between mitochondria and peroxisomes. *World J Biol Chem* **6** 301-309.
- Dhaunsi GS, Gulati S, Singh AK, Orak JK, Asayama K & Singh I 1992 Demonstration of Cu-Zn superoxide dismutase in rat liver peroxisomes. Biochemical and immunochemical evidence. *J Biol Chem* **267** 6870-6873.
- Diemer T, Allen JA, Hales KH & Hales DB 2003 Reactive oxygen disrupts mitochondria in MA-10 tumor Leydig cells and inhibits steroidogenic acute regulatory (StAR) protein and steroidogenesis. *Endocrinology* **144** 2882-2891.
- Distel B, Erdmann R, Gould SJ, Blobel G, Crane DI, Cregg JM, Dodt G, Fujiki Y, Goodman JM, Just WW, et al. 1996 A unified nomenclature for peroxisome biogenesis factors. *J Cell Biol* **135** 1-3.
- Dufau ML 1988 Endocrine regulation and communicating functions of the Leydig cell. *Annu Rev Physiol* **50** 483-508.
- Dunkel L, Siimes MA & Bremner WJ 1993 Reduced inhibin and elevated gonadotropin levels in early pubertal boys with testicular defects. *Pediatr Res* **33** 514-518.
- Ellis GB, Desjardins C & Fraser HM 1983 Control of pulsatile LH release in male rats. *Neuroendocrinology* **37** 177-183.
- Engfelt WH, Shackelford JE, Aboushadi N, Jessani N, Masuda K, Paton VG, Keller GA & Krisans SK 1997 Characterization of UT2 cells. The induction of peroxisomal 3-hydroxy-3-methylglutaryl-coenzyme A reductase. *J Biol Chem* **272** 24579-24587.
- Epstein LF & Orme-Johnson NR 1991a Acute action of luteinizing hormone on mouse Leydig cells: accumulation of mitochondrial phosphoproteins and stimulation of testosterone synthesis. *Mol Cell Endocrinol* **81** 113-126.
- Epstein LF & Orme-Johnson NR 1991b Regulation of steroid hormone biosynthesis. Identification of precursors of a phosphoprotein targeted to the mitochondrion in stimulated rat adrenal cortex cells. *J Biol Chem* **266** 19739-19745.
- Fan CY, Pan J, Chu R, Lee D, Kluckman KD, Usuda N, Singh I, Yeldandi AV, Rao MS, Maeda N, et al. 1996a Hepatocellular and hepatic peroxisomal alterations in mice with a disrupted peroxisomal fatty acyl-coenzyme A oxidase gene. *J Biol Chem* **271** 24698-24710.

- Fan CY, Pan J, Chu R, Lee D, Kluckman KD, Usuda N, Singh I, Yeldandi AV, Rao MS, Maeda N, et al. 1996b Targeted disruption of the peroxisomal fatty acyl-CoA oxidase gene: generation of a mouse model of pseudoneonatal adrenoleukodystrophy. *Ann N Y Acad Sci* **804** 530-541.
- Fan YS, Sasi R, Lee C, Winter JS, Waterman MR & Lin CC 1992 Localization of the human CYP17 gene (cytochrome P450(17 alpha)) to 10q24.3 by fluorescence in situ hybridization and simultaneous chromosome banding. *Genomics* **14** 1110-1111.
- Faust PL & Hatten ME 1997 Targeted deletion of the PEX2 peroxisome assembly gene in mice provides a model for Zellweger syndrome, a human neuronal migration disorder. *J Cell Biol* **139** 1293-1305.
- Feuilloley M & Vaudry H 1996 Role of the cytoskeleton in adrenocortical cells. *Endocr Rev* **17** 269-288.
- Fialkow L, Wang Y & Downey GP 2007 Reactive oxygen and nitrogen species as signaling molecules regulating neutrophil function. *Free Radic Biol Med* **42** 153-164.
- Fleury A, Mathieu AP, Ducharme L, Hales DB & LeHoux JG 2004 Phosphorylation and function of the hamster adrenal steroidogenic acute regulatory protein (StAR). *J Steroid Biochem Mol Biol* **91** 259-271.
- Fomitcheva J, Baker ME, Anderson E, Lee GY & Aziz N 1998 Characterization of Ke 6, a new 17beta-hydroxysteroid dehydrogenase, and its expression in gonadal tissues. *J Biol Chem* **273** 22664-22671.
- Foresta C, Zuccarello D, Garolla A & Ferlin A 2008 Role of hormones, genes, and environment in human cryptorchidism. *Endocr Rev* **29** 560-580.
- Fransen M, Nordgren M, Wang B, Apanasets O & Van Veldhoven PP 2013 Aging, age-related diseases and peroxisomes. *Subcell Biochem* **69** 45-65.
- Frolov A, Cho TH, Billheimer JT & Schroeder F 1996 Sterol carrier protein-2, a new fatty acyl coenzyme A-binding protein. *J Biol Chem* **271** 31878-31884.
- Fujiki Y 2016 Peroxisome biogenesis and human peroxisome-deficiency disorders. *Proc Jpn Acad Ser B Phys Biol Sci* **92** 463-477.
- Fujiki Y, Fowler S, Shio H, Hubbard AL & Lazarow PB 1982 Polypeptide and phospholipid composition of the membrane of rat liver peroxisomes: comparison with endoplasmic reticulum and mitochondrial membranes. *J Cell Biol* **93** 103-110.
- Gallegos AM, Atshaves BP, Storey SM, Starodub O, Petrescu AD, Huang H, McIntosh AL, Martin GG, Chao H, Kier AB, et al. 2001 Gene structure, intracellular localization, and functional roles of sterol carrier protein-2. *Prog Lipid Res* **40** 498-563.
- Geissler WM, Davis DL, Wu L, Bradshaw KD, Patel S, Mendonca BB, Elliston KO, Wilson JD, Russell DW & Andersson S 1994 Male pseudohermaphroditism caused by mutations of testicular 17 beta-hydroxysteroid dehydrogenase 3. *Nat Genet* **7** 34-39.
- Goldfischer S, Moore CL, Johnson AB, Spiro AJ, Valsamis MP, Wisniewski HK, Ritch RH, Norton WT, Rapin I & Gartner LM 1973 Peroxisomal and mitochondrial defects in the cerebro-hepato-renal syndrome. *Science* **182** 62-64.
- Goldstein JL & Brown MS 1990 Regulation of the mevalonate pathway. *Nature* **343** 425-430.
- Gould SJ, Kalish JE, Morrell JC, Bjorkman J, Urquhart AJ & Crane DI 1996 Pex13p is an SH3 protein of the peroxisome membrane and a docking factor for the predominantly cytoplasmic PTs1 receptor. *J Cell Biol* **135** 85-95.
- Govaerts L, Monnens L, Tegelaers W, Trijbels F & van Raay-Selten A 1982 Cerebro-hepato-renal syndrome of Zellweger: clinical symptoms and relevant laboratory findings in 16 patients. *Eur J Pediatr* **139** 125-128.

- Haider SG 2004 Cell biology of Leydig cells in the testis. *Int Rev Cytol* **233** 181-241.
- Haider SG, Laue D, Schwochau G & Hilscher B 1995 Morphological studies on the origin of adult-type Leydig cells in rat testis. *Ital J Anat Embryol* **100 Suppl 1** 535-541.
- Hansford RG, Hogue BA & Mildaziene V 1997 Dependence of H₂O₂ formation by rat heart mitochondria on substrate availability and donor age. *J Bioenerg Biomembr* **29** 89-95.
- Hess RA 2003 Estrogen in the adult male reproductive tract: a review. *Reprod Biol Endocrinol* **1** 52.
- Hoffmann B, Kyrein HJ & Ender ML 1973 An efficient procedure for the determination of progesterone by radioimmunoassay applied to bovine peripheral plasma. *Horm Res* **4** 302-310.
- hReddy J & Svoboda D 1972 Microbodies in Leydig cell tumors of rat testis. *J Histochem Cytochem* **20** 793-803.
- Hsueh AJ 1980 Gonadotropin stimulation of testosterone production in primary culture of adult rat testis cells. *Biochem Biophys Res Commun* **97** 506-512.
- Huleihel M & Lunenfeld E 2004 Regulation of spermatogenesis by paracrine/autocrine testicular factors. *Asian J Androl* **6** 259-268.
- Huyghe S, Mannaerts GP, Baes M & Van Veldhoven PP 2006a Peroxisomal multifunctional protein-2: the enzyme, the patients and the knockout mouse model. *Biochim Biophys Acta* **1761** 973-994.
- Huyghe S, Schmalbruch H, De Gendt K, Verhoeven G, Guillou F, Van Veldhoven PP & Baes M 2006b Peroxisomal multifunctional protein 2 is essential for lipid homeostasis in Sertoli cells and male fertility in mice. *Endocrinology* **147** 2228-2236.
- Immenschuh S, Baumgart-Vogt E, Tan M, Iwahara S, Ramadori G & Fahimi HD 2003 Differential cellular and subcellular localization of heme-binding protein 23/peroxiredoxin I and heme oxygenase-1 in rat liver. *J Histochem Cytochem* **51** 1621-1631.
- Ivashchenko O, Van Veldhoven PP, Brees C, Ho YS, Terlecky SR & Fransen M 2011 Intraperoxisomal redox balance in mammalian cells: oxidative stress and interorganellar cross-talk. *Mol Biol Cell* **22** 1440-1451.
- Janssen A, Gressens P, Grabenbauer M, Baumgart E, Schad A, Vanhorebeek I, Brouwers A, Declercq PE, Fahimi D, Evrard P, et al. 2003 Neuronal migration depends on intact peroxisomal function in brain and in extraneuronal tissues. *J Neurosci* **23** 9732-9741.
- Janszen FH, Cooke BA, Van Driel MJ & Van Der Molen HJ 1976 The effect of calcium ions on testosterone production in Leydig cells from rat testis. *Biochem J* **160** 433-437.
- Jefcoate CR, McNamara BC, Artemenko I & Yamazaki T 1992 Regulation of cholesterol movement to mitochondrial cytochrome P450_{scc} in steroid hormone synthesis. *J Steroid Biochem Mol Biol* **43** 751-767.
- Karnati S, Luers G, Pfreimer S & Baumgart-Vogt E 2013 Mammalian SOD2 is exclusively located in mitochondria and not present in peroxisomes. *Histochem Cell Biol* **140** 105-117.
- Keller GA, Barton MC, Shapiro DJ & Singer SJ 1985 3-Hydroxy-3-methylglutaryl-coenzyme A reductase is present in peroxisomes in normal rat liver cells. *Proc Natl Acad Sci U S A* **82** 770-774.
- Keller GA, Warner TG, Steimer KS & Hallewell RA 1991 Cu,Zn superoxide dismutase is a peroxisomal enzyme in human fibroblasts and hepatoma cells. *Proc Natl Acad Sci U S A* **88** 7381-7385.

- Kemp S & Wanders RJ 2007 X-linked adrenoleukodystrophy: very long-chain fatty acid metabolism, ABC half-transporters and the complicated route to treatment. *Mol Genet Metab* **90** 268-276.
- Kerr JB & Knell CM 1988 The fate of fetal Leydig cells during the development of the fetal and postnatal rat testis. *Development* **103** 535-544.
- Khan M, Contreras M & Singh I 2000 Endotoxin-induced alterations of lipid and fatty acid compositions in rat liver peroxisomes. *J Endotoxin Res* **6** 41-50.
- Khan S, Teerds K & Dorrington J 1992 Growth factor requirements for DNA synthesis by Leydig cells from the immature rat. *Biol Reprod* **46** 335-341.
- King SR, Liu Z, Soh J, Eimerl S, Orly J & Stocco DM 1999 Effects of disruption of the mitochondrial electrochemical gradient on steroidogenesis and the Steroidogenic Acute Regulatory (StAR) protein. *J Steroid Biochem Mol Biol* **69** 143-154.
- King SR & Stocco DM 1996 ATP and a mitochondrial electrochemical gradient are required for functional activity of the steroidogenic acute regulatory (StAR) protein in isolated mitochondria. *Endocr Res* **22** 505-514.
- Klinefelter GR, Hall PF & Ewing LL 1987 Effect of luteinizing hormone deprivation in situ on steroidogenesis of rat Leydig cells purified by a multistep procedure. *Biol Reprod* **36** 769-783.
- Koepke JI, Nakrieko KA, Wood CS, Boucher KK, Terlecky LJ, Walton PA & Terlecky SR 2007 Restoration of peroxisomal catalase import in a model of human cellular aging. *Traffic* **8** 1590-1600.
- Koepke JI, Wood CS, Terlecky LJ, Walton PA & Terlecky SR 2008 Progeric effects of catalase inactivation in human cells. *Toxicol Appl Pharmacol* **232** 99-108.
- Kovacs WJ, Faust PL, Keller GA & Krisans SK 2001 Purification of brain peroxisomes and localization of 3-hydroxy-3-methylglutaryl coenzyme A reductase. *Eur J Biochem* **268** 4850-4859.
- Kovacs WJ, Olivier LM & Krisans SK 2002 Central role of peroxisomes in isoprenoid biosynthesis. *Prog Lipid Res* **41** 369-391.
- Krisans SK 1992 The role of peroxisomes in cholesterol metabolism. *Am J Respir Cell Mol Biol* **7** 358-364.
- Krisans SK, Ericsson J, Edwards PA & Keller GA 1994 Farnesyl-diphosphate synthase is localized in peroxisomes. *J Biol Chem* **269** 14165-14169.
- Krueger RJ & Orme-Johnson NR 1983 Acute adrenocorticotrophic hormone stimulation of adrenal corticosteroidogenesis. Discovery of a rapidly induced protein. *J Biol Chem* **258** 10159-10167.
- Kuopio T, Tapanainen J, Pelliniemi LJ & Huhtaniemi I 1989 Developmental stages of fetal-type Leydig cells in prepubertal rats. *Development* **107** 213-220.
- Labrie F, Luu-The V, Lin SX, Simard J, Labrie C, El-Alfy M, Pelletier G & Belanger A 2000 Intracrinology: role of the family of 17 beta-hydroxysteroid dehydrogenases in human physiology and disease. *J Mol Endocrinol* **25** 1-16.
- Lacroix A, Ascoli M, Puett D & McKenna TJ 1979 Steroidogenesis in HCG-responsive Leydig cell tumor variants. *J Steroid Biochem* **10** 669-675.
- Lambard S, Galeraud-Denis I, Bouraima H, Bourguiba S, Chocat A & Carreau S 2003 Expression of aromatase in human ejaculated spermatozoa: a putative marker of motility. *Mol Hum Reprod* **9** 117-124.

- Lauer C, Volkl A, Riedl S, Fahimi HD & Beier K 1999 Impairment of peroxisomal biogenesis in human colon carcinoma. *Carcinogenesis* **20** 985-989.
- Lazarow PB & Fujiki Y 1985 Biogenesis of peroxisomes. *Annu Rev Cell Biol* **1** 489-530.
- Lejeune H, Habert R & Saez JM 1998 Origin, proliferation and differentiation of Leydig cells. *J Mol Endocrinol* **20** 1-25.
- Leydig F 1850 Zur Anatomie der maennlichen Geschlechtsorgane und Alndruesen der Saeugethiere. *Z Wiss. Zool.* **2:1-57**.
- Lin D, Sugawara T, Strauss JF, 3rd, Clark BJ, Stocco DM, Saenger P, Rogol A & Miller WL 1995 Role of steroidogenic acute regulatory protein in adrenal and gonadal steroidogenesis. *Science* **267** 1828-1831.
- Lismont C, Nordgren M, Van Veldhoven PP & Fransen M 2015 Redox interplay between mitochondria and peroxisomes. *Front Cell Dev Biol* **3** 35.
- Litwin JA, Beier K, Volkl A, Hofmann WJ & Fahimi HD 1999 Immunocytochemical investigation of catalase and peroxisomal lipid beta-oxidation enzymes in human hepatocellular tumors and liver cirrhosis. *Virchows Arch* **435** 486-495.
- Liu J, Rone MB & Papadopoulos V 2006 Protein-protein interactions mediate mitochondrial cholesterol transport and steroid biosynthesis. *J Biol Chem* **281** 38879-38893.
- Liu Y, Bjorkman J, Urquhart A, Wanders RJ, Crane DI & Gould SJ 1999 PEX13 is mutated in complementation group 13 of the peroxisome-biogenesis disorders. *Am J Hum Genet* **65** 621-634.
- Lording DW & De Kretser DM 1972 Comparative ultrastructural and histochemical studies of the interstitial cells of the rat testis during fetal and postnatal development. *J Reprod Fertil* **29** 261-269.
- Lorence MC, Murry BA, Trant JM & Mason JI 1990 Human 3 beta-hydroxysteroid dehydrogenase/delta 5----4isomerase from placenta: expression in nonsteroidogenic cells of a protein that catalyzes the dehydrogenation/isomerization of C21 and C19 steroids. *Endocrinology* **126** 2493-2498.
- Luers GH, Schad A, Fahimi HD, Volkl A & Seitz J 2003 Expression of peroxisomal proteins provides clear evidence for the presence of peroxisomes in the male germ cell line GC1spg. *Cytogenet Genome Res* **103** 360-365.
- Luers GH, Thiele S, Schad A, Volkl A, Yokota S & Seitz J 2006 Peroxisomes are present in murine spermatogonia and disappear during the course of spermatogenesis. *Histochem Cell Biol* **125** 693-703.
- Madamanchi NR, Vendrov A & Runge MS 2005 Oxidative stress and vascular disease. *Arterioscler Thromb Vasc Biol* **25** 29-38.
- Mammucari C & Rizzuto R Signaling pathways in mitochondrial dysfunction and aging. *Mech Ageing Dev* **131** 536-543.
- Mammucari C & Rizzuto R 2010 Signaling pathways in mitochondrial dysfunction and aging. *Mech Ageing Dev* **131** 536-543.
- Manna PR, Chandrala SP, Jo Y & Stocco DM 2006 cAMP-independent signaling regulates steroidogenesis in mouse Leydig cells in the absence of StAR phosphorylation. *J Mol Endocrinol* **37** 81-95.
- Manna PR, Huhtaniemi IT & Stocco DM 2004 Detection of hCG Responsive Expression of the Steroidogenic Acute Regulatory Protein in Mouse Leydig Cells. *Biol Proced Online* **6** 83-93.

- Manna PR, Kero J, Tena-Sempere M, Pakarinen P, Stocco DM & Huhtaniemi IT 2001 Assessment of mechanisms of thyroid hormone action in mouse Leydig cells: regulation of the steroidogenic acute regulatory protein, steroidogenesis, and luteinizing hormone receptor function. *Endocrinology* **142** 319-331.
- Mannaerts GP, Van Veldhoven PP & Casteels M 2000 Peroxisomal lipid degradation via beta- and alpha-oxidation in mammals. *Cell Biochem Biophys* **32 Spring** 73-87.
- Markus M, Husen B, Leenders F, Jungblut PW, Hall PF & Adamski J 1995 The organelles containing porcine 17 beta-estradiol dehydrogenase are peroxisomes. *Eur J Cell Biol* **68** 263-267.
- Martin LA, Kennedy BE & Karten B 2016 Mitochondrial cholesterol: mechanisms of import and effects on mitochondrial function. *J Bioenerg Biomembr* **48** 137-151.
- Matsumoto AM & Bremner WJ 1987 Endocrinology of the hypothalamic-pituitary-testicular axis with particular reference to the hormonal control of spermatogenesis. *Baillieres Clin Endocrinol Metab* **1** 71-87.
- Matsumoto AM & Bremner WJ 1989 Endocrine control of human spermatogenesis. *J Steroid Biochem* **33** 789-790.
- Matthiesson KL, McLachlan RI, O'Donnell L, Frydenberg M, Robertson DM, Stanton PG & Meachem SJ 2006 The relative roles of follicle-stimulating hormone and luteinizing hormone in maintaining spermatogonial maturation and spermiation in normal men. *J Clin Endocrinol Metab* **91** 3962-3969.
- Maxwell M, Bjorkman J, Nguyen T, Sharp P, Finnie J, Paterson C, Tonks I, Paton BC, Kay GF & Crane DI 2003 Pex13 inactivation in the mouse disrupts peroxisome biogenesis and leads to a Zellweger syndrome phenotype. *Mol Cell Biol* **23** 5947-5957.
- McLachlan RI, O'Donnell L, Meachem SJ, Stanton PG, de K, Pratis K & Robertson DM 2002 Hormonal regulation of spermatogenesis in primates and man: insights for development of the male hormonal contraceptive. *J Androl* **23** 149-162.
- Mellon SH & Vaisse C 1989 cAMP regulates P450scc gene expression by a cycloheximide-insensitive mechanism in cultured mouse Leydig MA-10 cells. *Proc Natl Acad Sci U S A* **86** 7775-7779.
- Mendis-Handagama SM 1997 Luteinizing hormone on Leydig cell structure and function. *Histol Histopathol* **12** 869-882.
- Mendis-Handagama SM 2000 Peroxisomes and intracellular cholesterol trafficking in adult rat Leydig cells following Luteinizing hormone stimulation. *Tissue Cell* **32** 102-106.
- Mendis-Handagama SM, Watkins PA, Gelber SJ & Scallen TJ 1992 Leydig cell peroxisomes and sterol carrier protein-2 in luteinizing hormone-deprived rats. *Endocrinology* **131** 2839-2845.
- Mendis-Handagama SM, Watkins PA, Gelber SJ & Scallen TJ 1998 The effect of chronic luteinizing hormone treatment on adult rat Leydig cells. *Tissue Cell* **30** 64-73.
- Mendis-Handagama SM, Watkins PA, Gelber SJ, Scallen TJ, Zirkin BR & Ewing LL 1990a Luteinizing hormone causes rapid and transient changes in rat Leydig cell peroxisome volume and intraperoxisomal sterol carrier protein-2 content. *Endocrinology* **127** 2947-2954.
- Mendis-Handagama SM, Zirkin BR, Scallen TJ & Ewing LL 1990b Studies on peroxisomes of the adult rat Leydig cell. *J Androl* **11** 270-278.
- Menon KM, Munshi UM, Clouser CL & Nair AK 2004 Regulation of luteinizing hormone/human chorionic gonadotropin receptor expression: a perspective. *Biol Reprod* **70** 861-866.

- Midzak AS, Chen H, Aon MA, Papadopoulos V & Zirkin BR 2011 ATP synthesis, mitochondrial function, and steroid biosynthesis in rodent primary and tumor Leydig cells. *Biol Reprod* **84** 976-985.
- Midzak AS, Liu J, Zirkin BR & Chen H 2007 Effect of myxothiazol on Leydig cell steroidogenesis: inhibition of luteinizing hormone-mediated testosterone synthesis but stimulation of basal steroidogenesis. *Endocrinology* **148** 2583-2590.
- Miller WL 1997 Congenital lipoid adrenal hyperplasia: the human gene knockout for the steroidogenic acute regulatory protein. *J Mol Endocrinol* **19** 227-240.
- Miller WL 2008 Steroidogenic enzymes. *Endocr Dev* **13** 1-18.
- Miller WL 2013 Steroid hormone synthesis in mitochondria. *Mol Cell Endocrinol* **379** 62-73.
- Miller WL & Bose HS 2011 Early steps in steroidogenesis: intracellular cholesterol trafficking. *J Lipid Res* **52** 2111-2135.
- Moyle WR & Ramachandran J 1973 Effect of LH on steroidogenesis and cyclic AMP accumulation in rat Leydig cell preparations and mouse tumor Leydig cells. *Endocrinology* **93** 127-134.
- Murphy EJ 1998 Sterol carrier protein-2 expression increases NBD-stearate uptake and cytoplasmic diffusion in L cells. *Am J Physiol* **275** G237-243.
- Neaves WB 1975 Growth and composition of a transplantable murine Leydig cell tumor. *J Natl Cancer Inst* **55** 623-631.
- Nenicu 2010 Influence of peroxisomes on development, maturation and adult functions of the testis.
- Nenicu A, Luers GH, Kovacs W, David M, Zimmer A, Bergmann M & Baumgart-Vogt E 2007 Peroxisomes in human and mouse testis: differential expression of peroxisomal proteins in germ cells and distinct somatic cell types of the testis. *Biol Reprod* **77** 1060-1072.
- Nordgren M & Fransen M 2014 Peroxisomal metabolism and oxidative stress. *Biochimie* **98** 56-62.
- Normand T, Husen B, Leenders F, Pelczar H, Baert JL, Begue A, Flourens AC, Adamski J & de Launoit Y 1995 Molecular characterization of mouse 17 beta-hydroxysteroid dehydrogenase IV. *J Steroid Biochem Mol Biol* **55** 541-548.
- Novikov D, Dieuaide-Noubhani M, Vermeesch JR, Fournier B, Mannaerts GP & Van Veldhoven PP 1997 The human peroxisomal multifunctional protein involved in bile acid synthesis: activity measurement, deficiency in Zellweger syndrome and chromosome mapping. *Biochim Biophys Acta* **1360** 229-240.
- O'Donnell L, Robertson KM, Jones ME & Simpson ER 2001 Estrogen and spermatogenesis. *Endocr Rev* **22** 289-318.
- O'Shaughnessy PJ, Baker PJ & Johnston H 2005 Neuroendocrine regulation of Leydig cell development. *Ann N Y Acad Sci* **1061** 109-119.
- Orentreich N, Brind JL, Vogelmann JH, Andres R & Baldwin H 1992 Long-term longitudinal measurements of plasma dehydroepiandrosterone sulfate in normal men. *J Clin Endocrinol Metab* **75** 1002-1004.
- Ortiz de Montellano PR 1995 The 1994 Bernard B. Brodie Award Lecture. Structure, mechanism, and inhibition of cytochrome P450. *Drug Metab Dispos* **23** 1181-1187.
- Oshino N, Chance B, Sies H & Bucher T 1973 The role of H₂O₂ generation in perfused rat liver and the reaction of catalase compound I and hydrogen donors. *Arch Biochem Biophys* **154** 117-131.

Panesar NS, Chan KW & Ho CS 2003 Mouse Leydig tumor cells produce C-19 steroids, including testosterone. *Steroids* **68** 245-251.

Papadopoulos V & Miller WL 2012 Role of mitochondria in steroidogenesis. *Best Pract Res Clin Endocrinol Metab* **26** 771-790.

Peltoketo H, Luu-The V, Simard J & Adamski J 1999 17 β -hydroxysteroid dehydrogenase (HSD)/17-ketosteroid reductase (KSR) family; nomenclature and main characteristics of the 17HSD/KSR enzymes. *J Mol Endocrinol* **23** 1-11.

Pentikainen V, Erkkila K, Suomalainen L, Parvinen M & Dunkel L 2000 Estradiol acts as a germ cell survival factor in the human testis in vitro. *J Clin Endocrinol Metab* **85** 2057-2067.

Pham NA, Robinson BH & Hedley DW 2000 Simultaneous detection of mitochondrial respiratory chain activity and reactive oxygen in digitonin-permeabilized cells using flow cytometry. *Cytometry* **41** 245-251.

Polyakov VY, Soukhomlinova MY & Fais D 2003 Fusion, fragmentation, and fission of mitochondria. *Biochemistry (Mosc)* **68** 838-849.

Pon LA, Epstein LF & Orme-Johnson NR 1986 Acute cAMP stimulation in Leydig cells: rapid accumulation of a protein similar to that detected in adrenal cortex and corpus luteum. *Endocr Res* **12** 429-446.

Powers JM 1985 Adreno-leukodystrophy (adreno-testiculo-leukomyelo-neuropathic-complex). *Clin Neuropathol* **4** 181-199.

Powers JM & Schaumburg HH 1981 The testis in adreno-leukodystrophy. *Am J Pathol* **102** 90-98.

Prinz W 2002 Cholesterol trafficking in the secretory and endocytic systems. *Semin Cell Dev Biol* **13** 197-203.

Prough RA, Webb SJ, Wu HQ, Lapenson DP & Waxman DJ 1994 Induction of microsomal and peroxisomal enzymes by dehydroepiandrosterone and its reduced metabolite in rats. *Cancer Res* **54** 2878-2886.

Puett D, Li Y, DeMars G, Angelova K & Fanelli F 2007 A functional transmembrane complex: the luteinizing hormone receptor with bound ligand and G protein. *Mol Cell Endocrinol* **260-262** 126-136.

Raha S & Robinson BH 2000 Mitochondria, oxygen free radicals, disease and ageing. *Trends Biochem Sci* **25** 502-508.

Rebois RV 1982 Establishment of gonadotropin-responsive murine leydig tumor cell line. *J Cell Biol* **94** 70-76.

Reddy J & Svoboda D 1972a Microbodies (peroxisomes) identification in interstitial cells of the testis. *J Histochem Cytochem* **20** 140-142.

Reddy J & Svoboda D 1972b Microbodies (peroxisomes) in the interstitial cells of rodent testes. *Lab Invest* **26** 657-665.

Reddy JK & Ohno S 1981 Testicular feminization of the mouse: paucity of peroxisomes in Leydig cell of the testis. *Am J Pathol* **103** 96-104.

Reisse S, Rothardt G, Volkl A & Beier K 2001 Peroxisomes and ether lipid biosynthesis in rat testis and epididymis. *Biol Reprod* **64** 1689-1694.

Rhodin A, Gronbladh A, Ginya H, Nilsson KW, Rosenblad A, Zhou Q, Enlund M, Hallberg M, Gordh T & Nyberg F 1954 Combined analysis of circulating beta-endorphin with gene polymorphisms in OPRM1, CACNAD2 and ABCB1 reveals correlation with pain, opioid sensitivity and opioid-related side effects. *Mol Brain* **6** 8.

Rodemer C, Thai TP, Brugger B, Kaercher T, Werner H, Nave KA, Wieland F, Gorgas K & Just WW 2003 Inactivation of ether lipid biosynthesis causes male infertility, defects in eye development and optic nerve hypoplasia in mice. *Hum Mol Genet* **12** 1881-1895.

Rone MB, Fan J & Papadopoulos V 2009 Cholesterol transport in steroid biosynthesis: role of protein-protein interactions and implications in disease states. *Biochim Biophys Acta* **1791** 646-658.

Rone MB, Midzak AS, Issop L, Rammouz G, Jagannathan S, Fan J, Ye X, Blonder J, Veenstra T & Papadopoulos V Identification of a dynamic mitochondrial protein complex driving cholesterol import, trafficking, and metabolism to steroid hormones. *Mol Endocrinol* **26** 1868-1882.

Rone MB, Midzak AS, Issop L, Rammouz G, Jagannathan S, Fan J, Ye X, Blonder J, Veenstra T & Papadopoulos V 2012 Identification of a dynamic mitochondrial protein complex driving cholesterol import, trafficking, and metabolism to steroid hormones. *Mol Endocrinol* **26** 1868-1882.

Roser JF 2008 Regulation of testicular function in the stallion: an intricate network of endocrine, paracrine and autocrine systems. *Anim Reprod Sci* **107** 179-196.

Russel L & Burguet S 1977 Ultrastructure of leydig cells as revealed by secondary tissue treatment with a ferrocyanide-osmium mixture. *Tissue Cell* **9** 751-766.

Saez JM 1994 Leydig cells: endocrine, paracrine, and autocrine regulation. *Endocr Rev* **15** 574-626.

Schrader M, Bonekamp NA & Islinger M 2012 Fission and proliferation of peroxisomes. *Biochim Biophys Acta* **1822** 1343-1357.

Schrader M, Costello J, Godinho LF & Islinger M 2015 Peroxisome-mitochondria interplay and disease. *J Inherit Metab Dis* **38** 681-702.

Schrader M & Fahimi HD 2004 Mammalian peroxisomes and reactive oxygen species. *Histochem Cell Biol* **122** 383-393.

Schrader M & Fahimi HD 2006 Peroxisomes and oxidative stress. *Biochim Biophys Acta* **1763** 1755-1766.

Schulze C 1984 Sertoli cells and Leydig cells in man. *Adv Anat Embryol Cell Biol* **88** 1-104.

Schumacher M, Schafer G, Holstein AF & Hilz H 1978 Rapid isolation of mouse Leydig cells by centrifugation in Percoll density gradients with complete retention of morphological and biochemical integrity. *FEBS Lett* **91** 333-338.

Sha JA, Dudley K, Rajapaksha WR & O'Shaughnessy PJ 1997 Sequence of mouse 17 β -hydroxysteroid dehydrogenase type 3 cDNA and tissue distribution of the type 1 and type 3 isoform mRNAs. *J Steroid Biochem Mol Biol* **60** 19-24.

Sharpe RM 1990 Intratesticular control of steroidogenesis. *Clin Endocrinol (Oxf)* **33** 787-807.

Sharpe RM, Maddocks S & Kerr JB 1990 Cell-cell interactions in the control of spermatogenesis as studied using Leydig cell destruction and testosterone replacement. *Am J Anat* **188** 3-20.

Sharpe RM, McKinnell C, Kivlin C & Fisher JS 2003 Proliferation and functional maturation of Sertoli cells, and their relevance to disorders of testis function in adulthood. *Reproduction* **125** 769-784.

Sheikh FG, Pahan K, Khan M, Barbosa E & Singh I 1998 Abnormality in catalase import into peroxisomes leads to severe neurological disorder. *Proc Natl Acad Sci U S A* **95** 2961-2966.

- Shimomura Y, Nishikimi M & Ozawa T 1985 Novel purification of cytochrome c1 from mitochondrial Complex III. Reconstitution of antimycin-insensitive electron transfer with the iron-sulfur protein and cytochrome c1. *J Biol Chem* **260** 15075-15080.
- Shimozawa N, Suzuki Y, Zhang Z, Imamura A, Toyama R, Mukai S, Fujiki Y, Tsukamoto T, Osumi T, Oritani T, et al. 1999 Nonsense and temperature-sensitive mutations in PEX13 are the cause of complementation group H of peroxisome biogenesis disorders. *Hum Mol Genet* **8** 1077-1083.
- Sies H 1974 Biochemistry of the peroxisome in the liver cell. *Angew Chem Int Ed Engl* **13** 706-718.
- Silva FR, Leite LD & Wassermann GF 2002 Rapid signal transduction in Sertoli cells. *Eur J Endocrinol* **147** 425-433.
- Simpson ER, Mahendroo MS, Means GD, Kilgore MW, Hinshelwood MM, Graham-Lorence S, Amarneh B, Ito Y, Fisher CR, Michael MD, et al. 1994 Aromatase cytochrome P450, the enzyme responsible for estrogen biosynthesis. *Endocr Rev* **15** 342-355.
- Singh AK, Dhaunsi GS, Gupta MP, Orak JK, Asayama K & Singh I 1994 Demonstration of glutathione peroxidase in rat liver peroxisomes and its intraorganellar distribution. *Arch Biochem Biophys* **315** 331-338.
- Singh I 1996 Mammalian peroxisomes: metabolism of oxygen and reactive oxygen species. *Ann N Y Acad Sci* **804** 612-627.
- Singh J, O'Neill C & Handelsman DJ 1995 Induction of spermatogenesis by androgens in gonadotropin-deficient (hpg) mice. *Endocrinology* **136** 5311-5321.
- Siril Ariyaratne HB, Chamindrani Mendis-Handagama S, Buchanan Hales D & Ian Mason J 2000 Studies on the onset of Leydig precursor cell differentiation in the prepubertal rat testis. *Biol Reprod* **63** 165-171.
- Skinner MK, Norton JN, Mullaney BP, Rosselli M, Whaley PD & Anthony CT 1991 Cell-cell interactions and the regulation of testis function. *Ann N Y Acad Sci* **637** 354-363.
- Song M, Shao H, Mujeeb A, James TL & Miller WL 2001 Molten-globule structure and membrane binding of the N-terminal protease-resistant domain (63-193) of the steroidogenic acute regulatory protein (StAR). *Biochem J* **356** 151-158.
- Song XQ, Fukao T, Yamaguchi S, Miyazawa S, Hashimoto T & Oritani T 1994 Molecular cloning and nucleotide sequence of complementary DNA for human hepatic cytosolic acetoacetyl-coenzyme A thiolase. *Biochem Biophys Res Commun* **201** 478-485.
- Spiteri-Grech J & Nieschlag E 1993 Paracrine factors relevant to the regulation of spermatogenesis--a review. *J Reprod Fertil* **98** 1-14.
- Stein K, Schell-Stephen A, Erdmann R & Rottensteiner H 2002 Interactions of Pex7p and Pex18p/Pex21p with the peroxisomal docking machinery: implications for the first steps in PTS2 protein import. *Mol Cell Biol* **22** 6056-6069.
- Steinberg SJ, Dodt G, Raymond GV, Braverman NE, Moser AB & Moser HW 2006 Peroxisome biogenesis disorders. *Biochim Biophys Acta* **1763** 1733-1748.
- Stocco DM 1999a The steroidogenic acute regulatory (StAR) protein. *Medicina (B Aires)* **59** 538-539.
- Stocco DM 1999b An update on the mechanism of action of the Steroidogenic Acute Regulatory (StAR) protein. *Exp Clin Endocrinol Diabetes* **107** 229-235.
- Stocco DM 2000 Intramitochondrial cholesterol transfer. *Biochim Biophys Acta* **1486** 184-197.

- Stocco DM 2001 StAR protein and the regulation of steroid hormone biosynthesis. *Annu Rev Physiol* **63** 193-213.
- Stocco DM & Clark BJ 1996a Regulation of the acute production of steroids in steroidogenic cells. *Endocr Rev* **17** 221-244.
- Stocco DM & Clark BJ 1996b Role of the steroidogenic acute regulatory protein (StAR) in steroidogenesis. *Biochem Pharmacol* **51** 197-205.
- Stocco DM & Sodeman TC 1991 The 30-kDa mitochondrial proteins induced by hormone stimulation in MA-10 mouse Leydig tumor cells are processed from larger precursors. *J Biol Chem* **266** 19731-19738.
- Stocco DM, Wang X, Jo Y & Manna PR 2005 Multiple signaling pathways regulating steroidogenesis and steroidogenic acute regulatory protein expression: more complicated than we thought. *Mol Endocrinol* **19** 2647-2659.
- Stocco DM, Wells J & Clark BJ 1993 The effects of hydrogen peroxide on steroidogenesis in mouse Leydig tumor cells. *Endocrinology* **133** 2827-2832.
- Stolowich NJ, Frolov A, Atshaves B, Murphy EJ, Jolly CA, Billheimer JT, Scott AI & Schroeder F 1997 The sterol carrier protein-2 fatty acid binding site: an NMR, circular dichroic, and fluorescence spectroscopic determination. *Biochemistry* **36** 1719-1729.
- Subramani S 1993 Protein import into peroxisomes and biogenesis of the organelle. *Annu Rev Cell Biol* **9** 445-478.
- Sugawara T, Holt JA, Driscoll D, Strauss JF, 3rd, Lin D, Miller WL, Patterson D, Clancy KP, Hart IM, Clark BJ, et al. 1995 Human steroidogenic acute regulatory protein: functional activity in COS-1 cells, tissue-specific expression, and mapping of the structural gene to 8p11.2 and a pseudogene to chromosome 13. *Proc Natl Acad Sci U S A* **92** 4778-4782.
- Terlecky SR, Koepke JI & Walton PA 2006 Peroxisomes and aging. *Biochim Biophys Acta* **1763** 1749-1754.
- Titorenko VI & Terlecky SR 2011 Peroxisome metabolism and cellular aging. *Traffic* **12** 252-259.
- Tsai SC, Lu CC, Lin CS & Wang PS 2003 Antisteroidogenic actions of hydrogen peroxide on rat Leydig cells. *J Cell Biochem* **90** 1276-1286.
- Tsujishita Y & Hurley JH 2000 Structure and lipid transport mechanism of a StAR-related domain. *Nat Struct Biol* **7** 408-414.
- Van Veldhoven PP 2010 Biochemistry and genetics of inherited disorders of peroxisomal fatty acid metabolism. *J Lipid Res* **51** 2863-2895.
- Wanders RJ 2004 Peroxisomes, lipid metabolism, and peroxisomal disorders. *Mol Genet Metab* **83** 16-27.
- Wanders RJ, Jansen GA & Skjeldal OH 2001a Refsum disease, peroxisomes and phytanic acid oxidation: a review. *J Neuropathol Exp Neurol* **60** 1021-1031.
- Wanders RJ & Tager JM 1998 Lipid metabolism in peroxisomes in relation to human disease. *Mol Aspects Med* **19** 69-154.
- Wanders RJ, Vreken P, Ferdinandusse S, Jansen GA, Waterham HR, van Roermund CW & Van Grunsven EG 2001b Peroxisomal fatty acid alpha- and beta-oxidation in humans: enzymology, peroxisomal metabolite transporters and peroxisomal diseases. *Biochem Soc Trans* **29** 250-267.
- Wanders RJ & Waterham HR 2005 Peroxisomal disorders I: biochemistry and genetics of peroxisome biogenesis disorders. *Clin Genet* **67** 107-133.

Wanders RJ & Waterham HR 2006 Peroxisomal disorders: the single peroxisomal enzyme deficiencies. *Biochim Biophys Acta* **1763** 1707-1720.

Yen SS & Laughlin GA 1998 Aging and the adrenal cortex. *Exp Gerontol* **33** 897-910.

Zhou L, Beattie MC, Lin CY, Liu J, Traore K, Papadopoulos V, Zirkin BR & Chen H 2013 Oxidative stress and phthalate-induced down-regulation of steroidogenesis in MA-10 Leydig cells. *Reprod Toxicol* **42** 95-101.

Zini A & Schlegel PN 1996 Catalase mRNA expression in the male rat reproductive tract. *J Androl* **17** 473-480.

Zuber MX, Simpson ER & Waterman MR 1986 Expression of bovine 17 alpha-hydroxylase cytochrome P-450 cDNA in nonsteroidogenic (COS 1) cells. *Science* **234** 1258-1261.

9. List of Abbreviations

ABCD	ATP-binding cassette family of transporters group D
ACOX	Acyl-CoA oxidase
cAMP	cyclic adenosine 3',5'-monophosphate
APS	Ammonium persulfate
BSA	Bovine serum albumin
cDNA	Complementary deoxyribonucleic acid
P450arom	Cytochrome P450 aromatase
P450scc	Cytochrome P450 side-chain cleavage enzyme
P450c17	Cytochrome P450 17 α -hydroxylase/C17 - 20 lyase
cAMP	Cyclic adenosine 3',5'-cyclic monophosphate
4-A	androstenedione
5-A	androstanediol
DHEA	Dehydroepiandrosterone
DHT	Dihydrotestosterone
DMSO	Dimethyl sulfoxide
DNA	Deoxyribonucleic acid
DTT	1,4-dithio-DL-threitol
EDTA	Ethylene-diamine tetraacetate
ER	Endoplasmic reticulum
FSH	Follicle-stimulating hormone
GnRH	Gonadotropin-releasing hormone
GFP	Green fluorescent protein
GSH	Glutathione
GSSG	Glutathione disulfide
hCG	Human chorionic gonadotropin
22R-HC	22(R)-hydroxycholesterol
3 β -HSD	3 -hydroxysteroid dehydrogenase
17 β -HSD	17 -hydroxysteroid dehydrogenase
HPT	Hypothalamic–pituitary–testis axis
HSD	Hydroxysteroid dehydrogenase
IF	Immunofluorescence
IGF-1	insulin-like growth factor 1
IHC	Immunohistochemistry
IMM	Inner mitochondrial membrane
INSL3	Insulin like peptide 3
KH ₂ PO ₄	Potassium dihydrogen phosphate
LCFA	Long-chain fatty acid
LDL	Low-density lipoproteins
LH	Luteinizing hormone
MFP-2	Multifunctional protein-2

MLTC-1	Mouse Leydig tumor cells
Na ₂ HPO ₄	Disodium hydrogen phosphate
NaOH	Sodium hydroxide
OMM	Outer mitochondrial membrane
17OH-P	17-hydroxypregnenolone
PBD	Peroxisome biogenesis disorder
PBS	Phosphate-buffered saline
PBST	Phosphate-buffered saline with Tween
PCR	Polymerase chain reaction
Pex	Gene encoding a peroxin (peroxisome biogenesis protein)
PGE	Prostaglandin
PFA	Paraformaldehyde
PKA	Proteinkinase A
PMP	Peroxisomal membrane protein
PPAR	Peroxisome proliferator activated receptor
17OH-Pre	17-hydroxyprogesterone
PTS	Peroxisomal targeting signal
PUFA	Polyunsaturated fatty acids
RIA	Radioimmunoassay
RNA	Ribonucleic acid
ROS	Reactive oxygen species
RXR	Retinoic X receptor
SDS-PAGE	Sodium dodecyl sulfate polyacrylamide gel electrophoresis
sER	Smooth endoplasmic reticulum
shRNA	Short hairpin RNA
siRNA	Small interfering RNA
SOD	Superoxide dismutase
SR-B1	Scavenger receptor B1
StAR	Steroidogenic acute regulator protein
T	Testosterone
TAE	Tris acetate EDTA buffer
TEMED	N, N, N, N-tetramethylethylenediamine
TGF α and β	Transforming growth factor α and β
THIOLASE	peroxisomal 3-ketoacyl-CoA thiolase
Tris	Tris (hydroxymethyl) aminomethane
VLCFA	Very long-chain fatty acid
WB	Western blot
X-ALD	X-linked adrenoleukodystrophy
ZS	Zellweger syndrome

Acknowledgment

Firstly, I would like to express my sincere gratitude and special appreciation to my supervisor Prof. Eveline Baumgart-Vogt who established the subject of the thesis and guided my study with the working group. From the very first day she helped me to learn a lot about cell biology, cell metabolism and develop the scientific way of thinking. I am very grateful for her motivation, patience and continuous support. I would like to thank her for encouraging my research, for the fruitful lengthy discussions, for helping me writing the thesis and for allowing me to grow as a research scientist. I also appreciate a lot that she encouraged me to express my ideas and to have the freedom to work as a researcher. Her advice on both research as well as on my career have been priceless. Besides my supervisor, I would like to thank Dr. Vijith Vijayan for his excellent, continued guidance and support. I feel lucky for having the opportunity to work with him. His intelligence, creativity in science and constructive remarks helped me a lot during this PhD study.

During my PhD study a lot of people have helped me with their discussions and technical assistance. Special thanks to my friends in the lab Dr. Claudia Colasante and Rocio Bonilla-Martinez for their support and assistance throughout my research work. I really appreciate and will always remember those warm, happy and funny days we spent together. Special gratitude to Andrea Textor, Petra Hahn-Kohlberger, Gabriele Thiele, Bianca Pfeiffer, Susanne Pfreimer, Elke Rodenberg-Frank and all colleagues in our lab for their excellent technical assistance, for creating a warm, kind and wonderful atmosphere, which I miss so much. Vielen, lieben Dank to Frau Silvia Heller, who was always so helpful and kind to me. I also thank PD Dr. Barbara Ahlemeyer, Dr. Srikanth Karnati, Dr. Dr. Klaus Peter Valerius and Dr. Wieland Stöckmann for their kind support at all times without hesitation. Thanks a lot to Natalia El-Merhi for giving me helpful tips while writing the thesis as well as for her warm and friendly nature. I would like also to thank Dr. Anca Nenicu, whose previous research work in this lab helped me a lot during my PhD study especially with the isolation and culture of mouse primary Leydig cells. I also thank Prof. Dr. Schuler laboratory for performing radioimmunological assays.

I would like to acknowledge the people who always believed in me, never stopped motivating me and make me happy: my family and my friends. Thanks to my

dearest, best friend Christine Ordyan for her love and emotional support, for being there whenever I needed a friend, who always took the time to listen, even when I was just complaining. Thanks to my beautiful cousin Lilit Vardanyan for her care and encouragement, for the lengthy conversations over the phone, short visits and lovely moments we had together. Finally, I am very grateful to my family- Serzh Kamalyan (Dad), Alvina Mkrtchyan (mom), Lusine Tarakjian (sister), Saqo Tarakjian (brother) and my lovely, sweet niece Maria Tarakjian. I am so blessed and lucky to have my grandparents Leonard Mkrtchyan and Goar Mkrtchyan in my life. I love you all. I dedicate this thesis to my dearest niece Maria Tarakjian.

Thank you, Jesus for always being there for me.



édition scientifique
VVB LAUFERSWEILER VERLAG

VVB LAUFERSWEILER VERLAG
STAUFENBERGRING 15
D-35396 GIESSEN

Tel: 0641-5599888 Fax: -5599890
redaktion@doktorverlag.de
www.doktorverlag.de

ISBN: 978-3-8359-6683-3



9 78 3 8359 6683 3